IEEEP NEW HORIZONS

[ISSN: 2226-3659]
Volume 101, Nos. 1-2, January-December, 2019

IEEEP

Journal of The Institution of Electrical and Electronics Engineers Pakistan

BOARD OF PUBLICATIONS

EDITORIAL BOARD

CONTENTS

VOLUME 101 NOS. 1-2 JANUARY-DECEMBER, 2019

Published by: IEEEP Head Quarters, 4-Lawrence Road, Lahore Pakistan
Ph:(042) 36305289 Fax: (042) 36360287
Email:ieeep1969@gmail.com Website:www.ieeep.org.pk

ACKNOWLEDGMENT

The Board of Publications "New Horizons (Journal of the Institution of Electrical and Electronics Engineers Pakistan)", extremely grateful the Natinal and International Referees/Experts for their valuable technical comments/suggestions on research papers to improve the quality of journal, published in the Bio-Annually New Horizons IEEEP, Volume 101, Numbers 1-2, January-December, 2019 issue

NATIONAL REFEREES/EXPERTS

Dr. Rabia Noor Enam
Associate Professor
Department of Computer Engineering
Sir Syed University of Engineering & Technology
Karachi, Pakistan
E-Mail: afaq_rabia@yahoo.com

Dr. Rehan Inam Qureshi
Associate Professor
Department of Computer Engineering
Sir Syed University of Engineering & Technology
Karachi, Pakistan
E-Mail: riqureshi@ssuet.edu.pk

Dr. Imtiaz Hussain
Associate Professor
Department of Electrical Engineering
DHA Suffa University Karachi, Pakistan
E-Mail: imtiaz.hussain@dsu.edu.pk,
Imtiaz.kalwar@gmail.com

Dr. Umar Shami
Associate Professor
Department of Electrical Engineering
University of Engineering & Technology Lahore, Pakistan
E-Mail: ushami@ymail.com

Dr. Muhammad Ibrar-ul-Haque
Associate Professor
Department of Electrical Engineering
Sir Syed University of Engineering & Technology
Karachi, Pakistan
E-Mail: mihaque@ssuet.edu.pk

Dr. Atif Jamil
Assistant Professor
Department of Electronic Engineering
Dawood University of Engineering & Technology
Karachi, Pakistan
E-Mail: atif.jamil@duet.edu.pk, atishaikh@gmail.com

Dr. Abdul Rehman Abbasi
Associate Professor
Karachi Institute of Power Engineering Karachi, Pakistan
E-Mail: arehman.abbasi@paec.gov.pk

Prof. Dr. Khalid Khan
Director
College of Computing & Information Sciences
PAF-Karachi Institute of Economics & Technology
Karachi, Pakistan
E-Mail: khalid.khan@pafkiet.edu.pk

Dr. Bhagwan Das
Associate Professor
Department of Electronic Engineering
Quaid-e-Awam University of Engineering,
Science & Technology Nawabshah, Pakistan
E-Mail: engr.bhagwandas@hotmail.com

INTERNATIONAL REFEREES/EXPERTS

Engr. Dr. Zain Anwar Ali
Senior Researcher
Beijing Normal University
Zhuhai, Guangdong China
E-Mail: zainanwar86@hotmail.com,
zainanwar86@nuaa.edu.cn,
11132019631@bnu.edu.cn

Dr. Noramalina Abdullah
Senior Lecturer
School of Electrical & Electronic Engineering
Universiti Sains Malaysia
Malaysia
E-Mail: eenora@usm.my

Dr. Nawab Muhammad Faseeh Qureshi
Assistant Professor
Department of Computer Education
Sungkyunkwan University Seoul, South Korea
E-Mail: faseeh@skku.edu

Dr. Tariq Masood
University of Bath UK
E-Mail: t.masood.dr@bath.edu

Dr. Muhammad Shafi
Associate Professor
Faculty of Computing & Information Technology
Sohar University Oman
E-Mail: mshafi@su.edu.om

Dr. Hazlee Illias
Associate Professor
Department of Electrical Engineering
University of Malaya Kuala Lumpur, Malaysia
E-Mail: h.illias@um.edu.my

Dr. Bishwajeet Pandey
Gyancity Research Lab. Center of Energy Excellence
Gran Sasso Science Institute Italy
E-Mail: bishwajeet.pandey@gssi.it,
gyancity@gyancity.com

Dr. Dil Muhammad Akbar Hussain
Associate Professor
Department of Energy Technology
Section for Power Electronics Systems
Aalborg University Denmark
E-Mail: akh@et.aau.dk

Dr. Li Huan
Associate Professor,
Tsinghua University China
E-Mail: li.huan@sz.tsinghua.edu.cn

Use of Internet of Things to Improve Educational Environment

Salma Jamali*, Akhtar Hussain Jalbani*, Rafia Naz Memon*, Mudasar Ahmed Soomro*, and Fiza Siyal*

* Department of Information Technology, Quaid-e-Awam University of Engineering, Science & Technology, Nawabshah, Pakistan

salma.jamali@quest.edu.pk, jalbaniakhtar@gmail.com, rafia@quest.edu.pk, engr_fizza2001@quest.edu.pk, mudasar1717@gmail.com

ABSTRACT

IoT (Internet of Things) is being used in different contexts, there are so many applications used for different purpose such as the education, medical, homes, cities, industry and global environment and so on, but this study focused on IoT in education. IoT is a part of information technology in which various types of objects and methods communicate with each other to exchange information. The main purpose of IoT is to transform the objects of real world into virtual objects. From the literature review, it is observed that researchers still report a lot of problems faced by students and teachers in education. So the purpose of this research is to find problems in school education and then solve with the help of IoT technology. In this study to identify problems of education and limitation is this study only in Nawabshah schools through focus group discussions from students, teachers and administration staff. After investigation of identified problems an IoT base framework is proposed which solves different problems of education through IoT tools. In this framework an IoT end device placed in campus which done all works automatically without human intervention. This device consists of some online system tools, camera system an GPS (Global Positioning System). It is concluded from this study that technology is very important tool for all the sectors of society, no any sector gives best performance without the help of technology. From education perspective IoT gives a lot of benefits to the educational organization, it helps in increasing performance of education institutions; enhance quality of education, saving time and budget and so on.

Key Words: Internet of Things, Role of IoT in Education, Technology Enhanced Learning

1. INTRODUCTION

In smart technology the things are connected with each other anywhere and anytime through internet. These connected devices communicate and then share information for further processing. This entire concept is known as IoT. In 1999 Kevin Ashton is the first person who used this term, then many researchers defined the term of IoT is different ways like: Internet of people, Internet of data, Internet of anything, Internet of everything, Internet of sign [1-12].

According to Cisco, IoT is the network in which physical objects are connected and also used the term Internet of everything for both physical and virtual objects. For making network connection more valuable IoT brings together the people, process, data and things, which create new opportunities, capabilities and good experience for businesses, education and medical and so on [13].

IoT play a vital role in the improvement of education. It is also known as a technological solution. Educational system is incomplete without the help of IoT technology because this technology gives a lot of benefits to the education system like: paperless environment, providing a helping aid to teachers and students, enhancing the performance of students, enhance the professional development of teachers, enhances the architecture of the educational organization, improve the quality of education, create a secure environment, brought changing in the standard teaching execution from school to university level, save time and budget of the school and so on [13].

It also allows the teachers and students to communicate with each other and share information just like: test result, annual examination result, checking upcoming events and so on. IoT also provide a secure network in which students save your specific ideas with full confidence without any worrying. Before coming of IoT the system of education is directionless. IoT gives a shape and particular direction to the education system and removes all the barriers in the field of education system which create difficulties for students and staff members [14].

2. RELATED STUDIES

Meola [15] provides a report about IoT education. According to author IoT has improved the quality of education it plays important role for educational up gradation and improvement from schools to university level. It facilitates the educational infrastructure in such a way that through this technology the process of teaching and learning become more enhanced. IoT is not only helps students, teachers but also changes the complete infrastructure of educational sector. Hence now education is far from the area of our lives that the IoT will transform. In the coming years not only the education but energy, medical transportation, homes, medical etc will all feel the touch of the IoT.

Augur [16] provides a daydream idea about IoT in education that in what way improved the education through IoT, which resources, ways and road maps provides by IoT for enhancing the teaching and learning. In what way it facilitate the parents to check status of students by viewing the class website what their child is

working on, they communication with teachers via email, and even they might evaluate child's attendance and grades via online systems and how IoT will be successfully integrated into the education system.

Peters [17] provides a report in which demonstrated the scope of IoT in education and how they fulfillment the requirements of student regarding learning, also described that the use of IoT in education is expected to increase due to the growth of online and blended educational programs as well as in traditional class rooms that increasingly use technology as a teaching tool.

Zeinab and Elmustafa [18] provide a review of many IoT applications and future possibilities for new related technologies in addition to the challenges that facing the implementation of the IoT. According to him, with the help of IoT technology the world will becomes smart in every aspects, every institute becomes smart. Just like: IoT will provide smart cities, smart healthcare, smart homes and building, smart education and so on.

Gul et. al. [19] provides the applications and usefulness of IoT in the field of education. Moreover, it tries to present the recent research works, challenges and impact of IoT in future education. Research is being conducted in designing IoT based teaching platforms including smart classrooms, smart labs and entire smart campuses. Studies have also been doing to investigate the usefulness of IoT based smart learning applications and still much more is left to study regarding IoT in education. Though there are various advantages of IoT in education but may have to compromise privacy and security. In the future new techniques may be introduced that can resolve all these issues.

3. PROBLEM STATEMENT

From literature review, it have been found in different studies still report a lot of problems faced by students in education such as taking attendance, security, checking behavior of students in classroom. Teachers and administrative staff are facing many problems present in the classrooms as well as in the school environment. So, in this situation it has been decided to explore the real issues in school education and to propose a solution to cope with the issues.

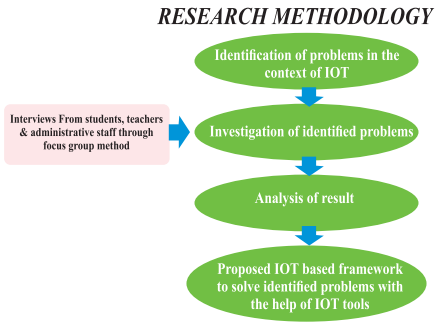

FIG. 1. IDENTIFICATION OF PROBLEMS IN THE CONTEXT OF IOT

4. METHOD

This study is aim to find the problems of school education and then solve these problems with the help of IoT technology as shown in Fig.1. These set of steps representing the methodology of the research that are going to be undertaken.

Problems of education are identified form the four phase in the context of IoT. There are so many problems in the school education which are faced by students, teachers and administration staff. From which some of them are mention in this paper and trying to solve through technology. These types of problems have been source of attraction for the researchers around the world for many years in the field of education.

Then Problems of education are investigated through focus group discussions from students, teachers and administration staff of Nawabshah schools. During government schools visit, meeting with headmistress and other staff members are arranged; main problems of the schools were discussed and informed the advantages of IoT technology. They were informed that the combination of IoT technology and education makes learning process faster and simpler, removes all the barriers in education such as physical location, languages and so on. Along with this technology improve the quality of education, save time and budget of the school and improve professional development of teachers and so on.

After investigation of identified problems an IoT base framework is proposed which solves different problems of school education with the help of IoT tools.

5. EFFECT OF IOT ON SCHOOL SYSTEMS

IoT is an excellent technology for all educational institutions because through this all school works done automatically within the seconds without human intervention. So this technology is also very necessary for all the government schools. Following Government Schools are visited.

(1) Government Girls High School Afzal Shah, Nawabshah.
(2) Government Girls High School Ghareeb Abad, Nawabshah.
(3) Government High School Taj-e-Azam Colony, Nawabshah.
(4) Government Boys Elementary School Awami Colony, Nawabshah.

During IoT base schools visit, meeting with principle, vice principle and other staff members are arranged; main problems of the school were discussed and ask them the advantages of IoT technology. Staff say that IoT is very good thing for the educational institutions because there are many benefits of this device in the school, through this

device not only enhance the quality of education but also improve the professional development of teachers hence students take interest in their studies and so on. Hence the facility of this technology is very necessary for all government and private schools as well.

Following IoT Base schools are visited

(i) Kazi Jameel Public School, Nawabshah

(ii) Fauji Foundation Model School, Nawabshah

Existing Problems of Teachers: Fig. 2(a-b**)** shows nine problems of school education. Section (a) consists of five problems and section (b) consists of four problems as under.

Section (a): According to survey Problem-1 "lack of quality education" has 50% frequency in government schools while IoT based schools have only 10%. Problem-2 "lack of professional development of teachers" has 65% frequency in government schools while IoT based schools have only 5%. Problem-3 "lack of teacher's innovation" has 70% frequency in government schools while IoT based schools have only 5%. Problem-4 "untrained teachers" has 55% frequency in government schools while IoT based schools have only 5%. Problem-5 "Lack of uniformity" has 70% frequency in government schools while IoT based schools have only 5%.

Section (b): Problem-6 "lack of teacher's dedication, motivation and interest in their profession" has 70% frequency in government schools while IoT based schools have only 5%. Problem-7 "overcrowded classrooms" has 95% frequency in government schools while IoT based schools is 5%. Problem-8 "education without direction" has 80% frequency in government schools while IoT based schools have only 0%. Problem-9 "smart interactive white board" has 90% in government schools while IoT based schools have only 50%.

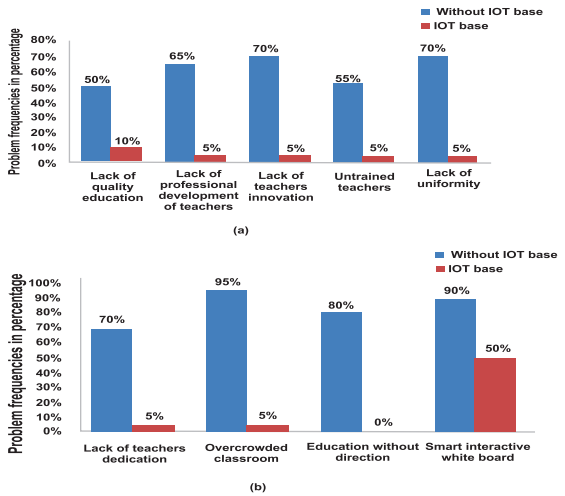

FIG. 2. EXISTING PROBLEMS OF TEACHERS IN SCHOOL EDUCATION

So the result shows that the minimum problem frequency in government schools was 50% in "lack of quality education" and the maximum problem frequency in government schools was 95% in "overcrowded classroom" while the minimum problem frequency in IoT based schools was 0% in "education without direction" and the maximum problem frequency in IoT based schools was 50% in "smart interactive white board" which faced by teachers.

Existing Problems of Administration: Fig. 3 shows six problems of school education. According to survey Problem-1 "Lack of funds" has 90% frequency in government schools while IoT based schools have only 10%. Problem-2 "Lack of resources" has 85% frequency in government schools while IoT based schools have only 5%. Problem-3 "Lack of proper" has 80% frequency in government schools while IoT based schools have only 5%. Problem-4 "uplifting administration" has 75% frequency in government schools while IoT based schools have only 5%. Problem-5 "Lack of physical facilities" has 60% in government schools while IoT based schools have only 10%. Problem-6 "High cost of education" has 55% frequency in government schools while IoT base schools have only 10%.

So the result shows that the minimum problem frequency in government schools was 55% in "high cost of education" and the maximum problem frequency in government schools was 90% in "lack of funds" while the minimum problem frequency in IoT based schools was 0% in "lack of proper planning" and the maximum problem frequency in IoT based schools was 15% in "lack of funds" which faced by administration.

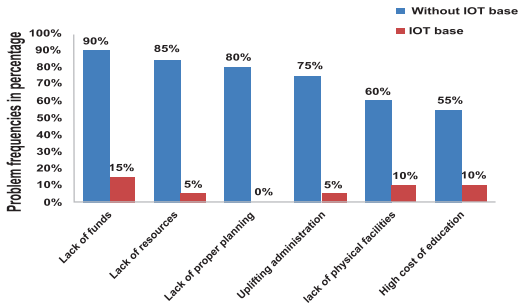

FIG. 3. EXISTING PROBLEMS OF ADMINISTRATION IN SCHOOL EDUCATION

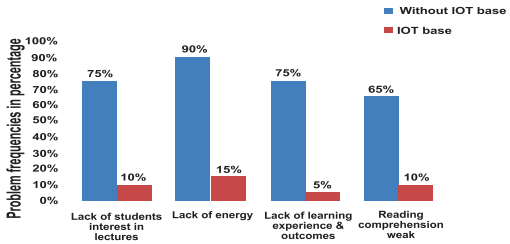

FIG. 4. EXISTING PROBLEMS OF STUDENTS IN SCHOOL EDUCATION

Existing Problems of Students: Fig. 4 shows Problem-1 "Lack students interest in lectures" has 75% frequency in government schools while IoT based schools have only 10%. Problem-2 "lack of energy" has 90% frequency in government schools while IoT based schools have only 15%. Problem-3 "lack of learning experience and outcomes" has 75% frequency in government schools while IoT based schools have only 5%. Problem-4 "Reading comprehension weak" has 65% frequency in government schools while IoT based schools have only 10%.

Study result shows that the minimum problem frequency in government schools was 65% in "reading comprehension weak" and the maximum problem frequency in government schools was 90% in "lack of energy". While the minimum problem frequency in IoT based schools was 5% in " Lack of learning experience and outcomes " and the maximum problem frequency in IoT based schools was 15% in " Lack of energy" which faced by students.

Existing Security Problems: Fig. 5 shows two problems of school education. According to survey Problem-1 "Access door control mechanism" has 90% frequency in government schools while IoT based schools have only 10%. Problem-2 "war on terror" has 95% frequency in government schools while IoT based schools have only 10%.

So the result shows that the minimum problem frequency in government schools was 90% in "Access door lock control mechanism" and the maximum problem frequency in government schools was 95% in "war on terror" while the minimum problem frequency in IoT based schools was 5% in "Access door lock control mechanism" and the maximum problem frequency in IoT based schools was 10% in "war on terror" which faced by security staff.

6. ROLE OF IOT IN EDUCATION

IoT technology has an important impact on the field of education. IoT technology is playing a likely role for the improvement of education at all levels including school, college and university teaching. From student to teacher, classroom to campus, everything can get benefitted with this technology. It has greater importance for the education to make the learning experience smart and enhanced for the students. Thus IoT is making the transforming the education sector and providing the safe and sound learning environment for the students. The IoT has the potential to impact every aspect of student learning. It also helps in decision making, automatic execution and providing security features.

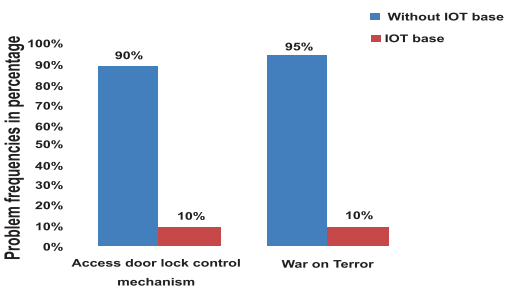

FIG. 5. EXISTING SECURITY ISSUES IN SCHOOL EDUCATION

7. CONCLUSION

It was concluded from this study that IoT is very necessary for all the sectors of society but here in education perspective IoT helps to increase performance of the education system, enhance quality of education, helps in saving budget and time of the school. Additionally students, teachers, administrators and parents may see a range of other benefits which coming soon arising from this technology.

8. FUTURE WORK

In this paper, the importance of IoT has been explored in school education. In future, the similar study can be performed to explore the problems of students and teachers in universities and colleges education as well.

ACKNOWLEDGEMENT

Authors are thankful to the Quaid-e-Awam University of Engineering, Science & Technology, Nawabshah, Pakistan, for providing facilities to conduct this research paper.

REFERENCES

[1] McRae, L., Ellis, K., and Kent, M., "Internet of Things (IoT): Education and Technology: The Relationship between Education and Technology for Students with Disabilities", Curtin University of Technology, School of Media, pp. 1-37, 2018.

[2] Temkar, R., Gupte, M., and Kalgaonkar, S., "Internet of Things for Smart Classrooms", International Research Journal of Engineering and Technology, Volume 3, No. 7, pp. 203-207, 2016.

[3] Bude, C., and Kervefors, B., A., "Internet of Things: Exploring and Securing a Future Concept", Cristian Bude Andreas Kervefors Bergstrand, 2015.

[4] Mahakam, S., Ramaswamy, R., and Tripathi, S., "Internet of Things (IoT): A Literature Review", Journal of Computer and Communications, Volume 3, No. 5, pp. 164-173, 2015.

[5] Cajide. J., "The Connected School: How IoT Could Impact Education", Multipotentialite at the Intersection of Product, Marketing and Finance, 2015.

[6] Technologies Zebra, "How the Internet of Things is Transforming Education", Motorola Solution's Enterprises Business, 2014.

[7] Shanmugasundaram, M., "The Role of IoT in Providing Security, Efficiency and Accessibility in Education", Happiest Minds Technologies Bangalore, India, 2014.

[8] Suchitra, C., "Internet of Things and Security Issues", International Journal of Computer Science and Mobile Computing, Volume 5, No. 1, pp. 133-139, 2016.

[9] Clarity Innovation, "Internet of Things", pp. 1-18, 2016.

[10] Rose, K., Eldridge, S., and Chapin, L., "The Internet of Things: An Overview", The Internet Society, pp. 1-75, 2015.

[11] GSMA Association, "Understanding the Internet of Things (IoT)", A Report, pp. 1-13, 2014.

[12] Gubbi, J., Buyya, R., Marusic, S., and Palaniswami, M., "Internet of Things (IoT): A Vision, Architectural Elements, and Future Directions", Future Generation Computer Systems, Volume 29, No.7, pp. 1-28, 2013.

[13] Tan, P., Wu, H., Li, P., and Xu, H., "Teaching Management System with Applications of RFID and IoT Technology", Education Sciences, Volume 8, No. 26, pp. 1-13. 2018.

[14] Mathew, A., and Nitha, K.P., "Smart Academy an IoT Approach a Survey on IOT in Education", International Journal of Advanced Research Trends in Engineering and Technology, Volume 3, No. 2, pp. 1-41, 2016.

[15] Meola, A., "How IoT in Education is Changing the Way We Learn", Business Insider Intelligence, New York, USA, 2016.

[16] Augur, H., "IoT in Education: The Internet of School Things", IBM Technology Berlin, Germany, 2016.

[17] Peters, J., "The Internet of Things in Education is Expected to Increase Dramatically", Innovation News, 2016.

[18] Zeinab, K.A.M., and Elmustafa, S.A.A., "Internet of Things Applications Challenges and Related Future Technologies", World Scientific News, Volume 67, No. 2, pp. 126-148, 2017.

[19] Gul, S., Asif, M., Ahmad, S., Yasir, M., Majid, M., and Arshad, M.S, "A Survey on Role of Internet of Things in Education", International Journal of Computer Science and Network Security, Volume 17, No. 5, pp. 159-165, 2017.

Active DDoS Attack Mitigation and Secure Threat Intelligence Sharing

Khuda Bux*, Akhtar Hussain Jalbani, Ghulam Hussain Jalbani**, Saima Siraj Soomro**, and Salma Jamali****

*Riphah Institute of Systems Engineering, Riphah International University, Islamabad, Pakistan.

**Department of Information Technology, Quaid-e-Awam University of Engineering, Science &Technology, Nawabshah, Pakistan.

bux.khuda@gmail.com, jalbaniakhtar@quest.edu.pk, ghjalbani@gmail.com, saimasiraj@quest.edu.pk, salma.jamali@quest.edu.pk

ABSTRACT

The DDoS (Distributed Denial of Service) attacks are increasing by each passing day on networks. There is a need to mitigate or prevent the networks from these types of attacks. To mitigate the DDoS active attack there are too many entities involved for sending signals and messages securely.This incident information is shared with the help of DoSTS (Denial of Service Open Threat Signaling). The DOTS framework provides a separate path along with DOTS clients and DOTS server for the process of information-sharing regarding active DDoS attack on attack target. For detection and mitigation of DDoS attack or any other malicious traffic on the network there is a need for continuous monitoring and automate all this process. Security Automation and Continuous Monitoring is deployed, with this, the incident threat information will be shared securely. The detection of active DDoS attacks, tracing of source, and mitigation is processed with the help of Managed Incident Lightweight Exchange. These incident messages are shared with the modified XML (Extensible Markup Language) or JSON (JavaScript Object Notation) function for security and privacy of network information on the attack target. With the help of a service provider or a third party, the active DDoS attack will be mitigated. These three frameworks are proposed by the standard body IETF (Internet Engineering Task Force). In this paper, we have proposed to combine these three frameworks for good results. Due to these frameworks, the existing devices and protocol are used to share the threat information and mitigate the active DDoS attack also. Due to this, the action against the malicious traffic on the network will be taken timely for detection and mitigation. And also, the services of attack targets for their customers will remain offline for a short period of time.

Key Words: DDoS Attacks, Mitigation, Targeted Network, Network Security, Security Events, Information Sharing, Attack Targets.

1. INTRODUCTION

The DDoS attacks area big risk to real-time service providers or to a computer network. Such as online taxi services, ISPs (Internet Service Providers), smart houses, and online banking services, etc. A DDoS attack is described by attempting to block the services for legitimate users [1]. The objective of a DDoS attack is to cut off clients from a server or system asset by overloading it with requests for services. While a straightforward DoS includes one "attack" system and one unfortunate casualty, conveyed DoS depend on the number of infected or "bot" systems ready to do tasks at the same time. The impact of DDoS attacks in this way loses clients, money, time and reputation of the company. It all depends on the attack density, the services will not be available for several hours or too many numbers of days. Due to this attack, the services of any organization has been denied for the real user. It will consume a huge amount of bandwidth on the network. As these attacks are carried out on the targeted network consumes less bandwidth. Due to this functionality of attack, it is hard to differentiate the real traffic and malicious traffic on the network.

To send a signal for mitigating the active DDoS attack on the targeted network the standard body suggested DDoS (DOTS) [2]. DOTS characterizes a strategy for planning cautious measures between willing peers to mitigate the attack quickly and proficiently. Activating hybrid attack response locally or near to the target of a functioning attack, or anyplace in-way between attack sources and target. How these security event signals will be communicated and monitored automatically another method has been proposed by the standard body is SACM (Security Automation and Continuous Monitoring) [3]. The SACM main focus on by what means to gather and share this data subject to utilize cases that incorporate demonstration examination of clients/servers. Versatile also feasible accumulation, articulation, then assessment of clients/servers information are central to SACM's objective [4]. This should most likely decide, offer, and utilize this data in a protected, advantageous, unsurprising, and with an auto, approach to perform client/server present assessments. To communicate with each other in the ecosystem – each player of this communication is known as SACM components. These SACM components may play one or more roles in this ecosystem.

After the communication of security event signals regarding DDoS active attack on the targeted network. How to mitigate it, the standard body proposed a method known as MILE (Management Incident Lightweight Exchange) [5]. Incident handling the care includes the detection, revealing, distinguishing proof and mitigation of the incident. For example, it very well may be a configuration of issue, IT (Information Technology) issue, an infraction to a SLA (Service Level Agreement),

framework bargain, socially structured phishing assault, or a DoS assaults, and so on. At the point when an incident is identified, the reaction may incorporate just recording information, warning to the source of the incident. A mitigation solicitation to a SP (Service Provider) or a solicitation to discover the source of the assault. The RID (Real-Time Inter-Arrange Defense) utilized as a dynamic between organizing correspondence for sharing incidents taking care of data by coordinating with existing location, following, source recognizable proof, and mitigation framework for a total occurrence taking care of solution. These security groups are not limited to only DDoS attack events, but these can handle any type of security incidents. In early work for the mitigation or detection of DDoS attack SDN (Software-Defined Network) is used. This is divided into two methods mostly, one is the signal controller and the second is data. The SDN is deployed only for the DDoS attack mitigation or detection. All this is based on the threshold of routers on a network for all applications running on the attack target. To overcome all shortcomings of existing work, we have proposed to combine the three standard body security groups (DOTS, SACM, and MILE) frameworks to mitigate or detect the DDoS attack or another malicious traffic on the network.

The rest of this paper is sorted as follows: Section-2 gives an overview of standard body security groups. Section-3 describes related work for DDoS mitigation and threat information sharing. In section-4, we have proposed a combined methodology of standard body security groups. Section-5, the tools and incident information sharing method are discussed. Last, section-6, the conclusion of the paper is given.

2. OVERVIEW OF STANDARD BODY SECURITY GROUPS FOR DDOS MITIGATION

Standard body SA (Security Area) has defined a few mechanisms for the mitigation of DDoS active attack on the targeted network. First SG (Security Group) all the parties involved coordinating for a defensive response to a DDoS active attack. They must define a common understanding of mechanisms and roles for signaling. The DDoS Open Threat Signaling has been introduced by the standard body for the signaling layer and supplementary messaging. Second SACM and SG have developed a method that defines how to continuously monitor and automate security events information sharing. Third SG has defined methods on how to mitigate active DDoS attacks and send security events by using JSON, XML or UML (Unified Modeling Language). It is known as MILE. To share threat information between peers of detection or mitigate the malicious traffic on the network. The secure method of XML or JSON has been defined in the MILE framework for sharing security incidents.

2.1 DOTS Signaling and Data Sharing Architecture

To mitigate the active DDoS attacks there be situated to share information regarding that attack. To meet this need the DDoS open threat signaling has been introduced with its own DOTS client and DOTS server as shown in Fig. 1.

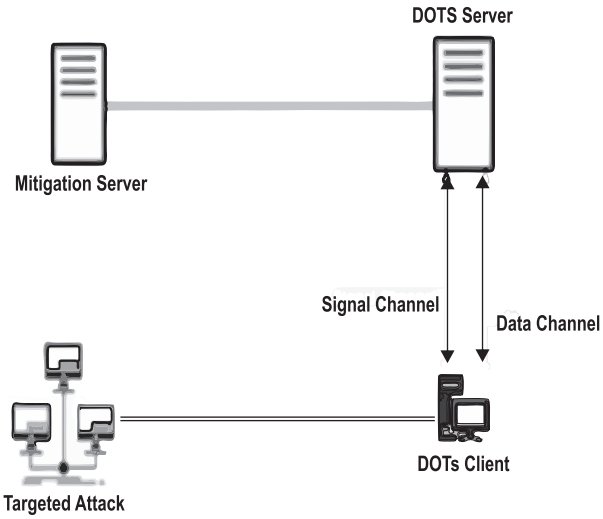

FIG. 1. DDOS OPEN THREAT SIGNALING ARCHITECTURE

In the above architecture, the signaling channel is used for communication between DOTS clients and servers. As the DOTS server receives signals from DOTS client it may change the path of destined traffic for the attack targets. The organization takes a DOTS user, which gets information regarding the DDoS attack and sends a signal to the DOTS server for assistance to mitigating the attack. The DOTS server thus activates at least one mitigator, which is entrusted with mitigating the real DDoS attack. By this to decrease the malicious traffic and allow the legitimate traffic to be accessible on attack target. The main function of DOTS is to provide the signaling channel and data channel for information sharing. The communication process of information is not secure among the DOTS user and DOTS server.

2.2 SACM Architecture

To mitigate or detect the DDoS attack on attack target a continuous monitoring and security event information sharing system need to deploy. The SACM will assess and compare data models from the collected information, check the interfaces and protocols are being used in communication. The SACM architecture comprises of a number of SACM Components, and named components are planned to encapsulate at least one explicit capabilities. Communicating with these abilities will require at least two degrees of interface determination. The first is a logical interface determination, and the

second is at least one binding to an explicit transfer system, as shown in Fig. 2. This will be further elaborated in section 5.

2.3 MILE Tracing and Mitigation

The managed incident lightweight exchange is used for the mitigation of active DDoS attacks and secure incident information sharing on the attack targets. The network used for the correspondence should comprise of out-of-band or secured passages or else encoded passages devoted to vehicle RID communications. The correspondence connections should be immediate associations (virtual or physical) among companions who have settled upon utilizing and misuse approaches via a consortium. The security, setup, and assurance scoring plans regarding RID informing peers and should be consulted with peers. This communication should meet some criteria general prerequisites for a completely associated system (Web, government, training, and so forth.) through the peering and additionally a consortium-based understanding. The incident information will be shared by RID and the active DDoS attack will be mitigated by a service provider or a third party as shown in Fig. 3.

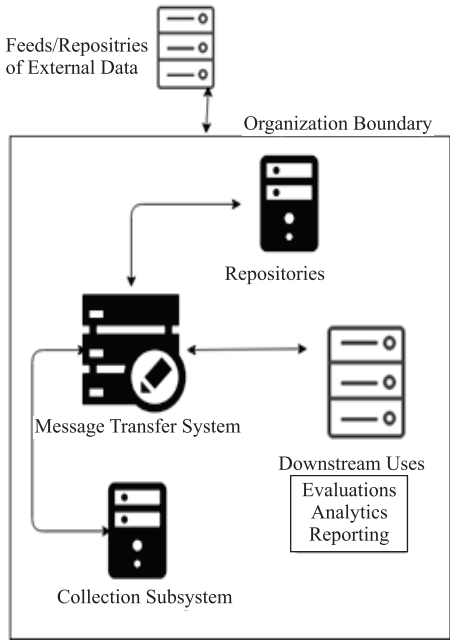

FIG. 2. AN OVERVIEW OF SCAM INFORMATION SHARING

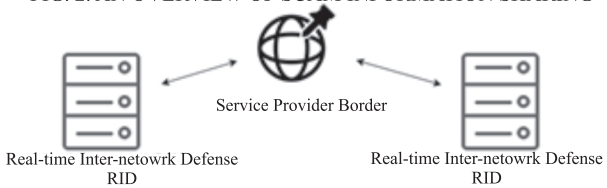

FIG. 3. MILE MITIGATION PEERS

3. RELATED WORK AND THEIR LIMITATIONS

For the mitigation of active DDoS attacks on the attack target, there are few important components. These components are used for information sharing, tracing of attack source, detection, and mitigation of DDoS attack. The FLEX (Flow-Based Event Exchange Format) has been used for the communication process. It will support to achieve the awareness of the current threat, its expertise, and resources used by this attack on the attack target [6]. A multi-level DDoS mitigation system for the IoT (Internet of Things) that incorporates an edge computing level, a fog computing level, and a cloud computing level. The edge computing level uses an SDN-based IoT gateway to oversee and secure the IoT perception layer. An IMCU (Internet Management Control Unit) is comprised of fog computing. To identify and check DDoS attacks by utilizing the IMCU bunch with the SDN controllers and it is applications [7]. The SDN framework is also implemented to mitigate the DDoS attack. Verizon's apparent SDN framework has been utilized as a contextual investigation by researchers. The SDN architecture divides the network into two planes control and data. Due to this separation of the network traffic will be operated and managed dynamically as per customer need. For the defense of DDoS attacks, the central control and functionality of the SDN feature are also in use plus malicious traffic on attack targets [8].The machine learning method has been used by researchers for the detection of DDoS attacks. They have used public repositories of intrusion detection datasets for covering DDoS attack evaluation to create the machine learning models. The specific dataset has been taken for the test of legitimate traffic and malicious DDoS attack traffic [9].To control DDoS attack traffic the data model of PT-DCTL+TS (Progressive Transfer Deep Coordinated Team Learning with Team Structure) has been used. The router throttling is used to deal with DDoS attacks by three proposed methods. The first with, they have utilized profound system as opposed to the tile coding for this DDoS issue with deep learning strategies. Second, they add group structure information to the state so pros with the heterogeneous gathering structure can even now share on deep systems. Third, their dynamic trade learning can show signs of improvement approach with less time usage [10]. The SDN has been divided into three layers: application, control and data processing. The processing starts as a packet reaches the data layer which contains the packet handles and, if there is a need, it will be forwarded to the control layer. In last the control layer may need different types of applications with multiple functionalities. The SDN has useful capabilities for the DDoS attack defense, which makes it more useful for protecting too many types of network topologies [11]. The researchers have proposed the ProDefense, it can be configured for each application as per the need of network

traffic threshold. By implementing this custom configuration will be used for the detection of DDoS attacks. The distributed controller framework used by deploying load balancing and this will decrease the probability of controller failure. As per the researcher, ProDefense can be used in different types of networks which may include cyber-physical systems, smart grid, and e-governance [12]. Another method has been proposed to mitigate the DDoS attack with lightweight information sharing, efficient, and easy to deploy SDN. The researcher has been designed a secure protocol known as C-to-C communication for SDN-controllers in between multiple AS (Autonomous Systems). By effective communication between the SDN controller and with the neighboring domains controllers about the active DDoS attack. Due to this, SDN-controller will be able to do these two tasks. First, block the malicious traffic on the attack target. Second, send information signals regarding the active attack to neighboring domains or networks [13]. The sFlow [14] framework has been used for the SDN-controller to improve accuracy and timeliness. The entropy-based technique has been used for checking the network feature changes, and a machine learning method used to detect network anomalies automatically. The DDoS attack can be detected at an early stage by using this mentioned method. As the controller-based, sFlow-based data gathering technique, entropy-based feature extraction technique, and SVM (Support Vector Machine)-based classification should be deployed to improve the accuracy and timeliness of active DDoS attack detection [15]. For the detection of a DDoS attack, the deep belief network feature of extraction has been used along with LSTM (Long Short-Term Memory) method. The deep belief network is used for the extraction of IP (Internet Protocol) packet details. After that network, the traffic pattern has been taken by using LSTM. This proposed model by a researcher is suitable for DDoS attack detection only [16]. The TAXII (Trusted Automated Exchange of Indicator Information) is network-driven exertion, these defines ideas, protocols, and message trades to share cyber threat data for detection, counteractive action, what's more, relief between confided in accomplices. The improvement of TAXII is composed of Miter. The TAXII data traded is spoken for the XML STIX (Structured Threat Data Expression) program [17]. Firecol et. al. [18] is a cooperative framework that identifies flooding DDoS attacks at the ISP level and gives an administration to which clients can subscribe. This membership structure disseminated engineering of numerous IPSs that figures furthermore trade conviction scores on potential attacks. On the off chance, that Firecol identifies an attack, the attack is hindered as close as conceivable to its source(s). Further, the IPS that identifies the attack advises its upstream IPSs, which thus likewise performs moderation strategies.

3.1 Related Work: State-of-the-Art

For the protection against the DDoS attacks, researchers have made a suggestion. Like as particular blackholing updates ISPs with information for (DDoS) assaults. The technique effectively expels contorted parcels from the system, limiting the potential harm that could be caused [19]. To speak to and investigate the stream tablespace of a switch, the author has given a lining hypothesis-based scientific model to speak to the stream table-space of a switch. From that point forward, the researcher has displayed a novel stream table sharing a way to deal with increment the obstruction of the SDN-based cloud during stream table over-loading DDoS assaults. The focal point of their commitment is to viably share the unused stream table-space of different switches with a switch right now enduring an onslaught with negligible inclusion of the controller [20]. The researcher has seen that danger insight (TI) has numerous points of interest around there. Finding clandestine digital assaults and new malware, giving early admonitions, and specifically conveying TI information is only a portion of these favorable circumstances. They have given a clear meaning of danger insight and how writing subdivides it. By researcher concentrated on specialized danger insight (TTI) and the serious issues identified with it [21].

Most of the tools and techniques proposed by the researchers are depends on SDNs. The SDN provides two channels for control and messaging on the same path. And it depends on the same threshold of the router for all the applications which are used within a domain network. In these tools and techniques, the functionality of mitigation or detection or threat information sharing is provided. However, no tool provides all services for DDoS attacks by them currently. Another major drawback of security and privacy during threat information sharing is less consideration from these tools.

4. PROPOSED SOLUTION AND METHODOLOGY

Insecurity incidents, there may be network compromises, viruses, worms, phishing attacks, and denial of service attacks. By these few mentioned attacks on any attack, the target may lose critical data, services to its customers, and maybe loss human and system resources. To handle this security incident, the service provider and CSIRT (Computer Security Incident Response Team) need to be fully ready and prepared with tools to help in tracing security incidents and communicate before any event of an attack. To achieve this, we have proposed standard body security group DOTS, SACM, and MILE frameworks should be combined to get good results. The DOTS will provide an alternate path on the attack target. The DOTS client and DOTS server will communicate on two channels signaling and data, these channels are used for information sharing. The SACM is used for the automated processes of information sharing and continuous monitoring of the network. The main

functionality of SACM how the information will be collected and shared regarding security events on the attack target [22]. Third, the MILE is used for detection of security event or DDoS attacks, it will trace the source of attack also. The MILE will mitigate the DDoS attack with the help of a service provider or third party support. The security event messages are shared securely by using redefined XML or JSON function format for data transfers. The architecture for the detection, tracing of the source, and mitigation of active DDoS attack described in Fig. 4.

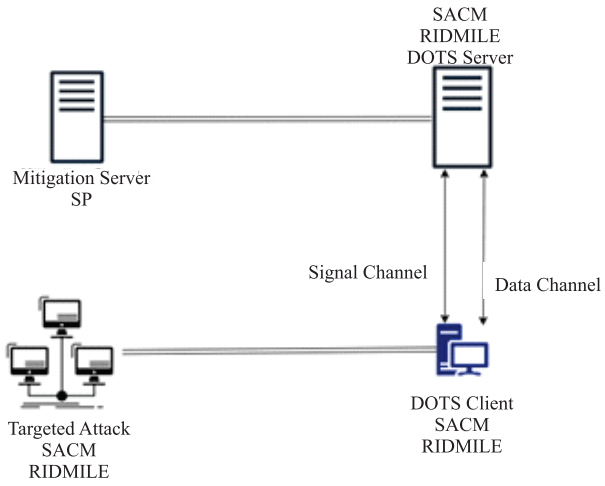

FIG. 4. PROPOSED ARCHITECTURE FOR DDOS ATTACK MITIGATION

The RID traces preemptive inter-network communication strategy to encourage sharing incident-handling information. This method will be incorporating with existing identification, tracing, source ID, and mitigation of total incident-handling solution. A secure method of incident information communication is provided by RID via enabling the interchange of IODEF (Incident Object Description and Exchange Format) [23] with XML documents. The exchange of critical information, policy, and privacy are highly considered as the security of an organization by RID.

4.1 DOTS Signaling and Data Description

For sharing incident information, the signaling has been used for defending an active DDoS attack. For this, DDoS and DOTS use the two channels for signaling and messaging. These two channels of signaling and messaging are used between DOTS clients and the DOTS server. The DOTS clients will send a signal of active DDoS attack to the DOTS servers. The DOTS server will change the destined traffic path for the attack targets; this all depends on the policy of the organization to mitigate it. Generally, the DOTS are considered more effective when there is a need for coordination regarding attack response between two or more network domains.

Table 1, the DOTS will not specify how an attack target is under DDoS attack and also does not specify how this DDoS attack will be mitigated. The request for mitigation of active DDoS attacks will be initiated by the DOTS clients. This active DDoS attack may not be mitigated at all it depends on DOTS server ability and will to mitigate it on the request of DOTS clients. But the basic function of DOTS is to share the information regarding active DDoS attacks via an alternate path on attack targets.

4.2 SACM Information Sharing and Monitoring

To mitigate or minimize the growing number of security threats there is a need for an automated process of sharing security information. And the protection of user information, the system which stores information, process, and transfers that information [24]. There are a different number of ways to detect security threats. The main objective of SACM is to collect authentic information, scalable, expression, and evaluation of that information endpoint as the main points shown in Table 2.

The SACM environment contains too many data models, protocols, and transfers that information. The SACM transfer protocol runs on the top of the TCP/IP (Transport Control Protocol/Internet Protocol). It carries different operations such as requests or responses and transfer of information. SACM is divided into a design and data concentrated off tending requirements for deciding, sharing, and utilizing stance data safely via stance data suppliers plus stance data of customers.

TABLE 1. DOTS FEATURES FOR DDOS ATTACK MITIGATION

Features	Yes	No
Message Signaling	Yes	-
Information Gathering		-
Message Security	-	No
DDoS Detection	-	
Mitigation	-	
Source Tracing	-	
Alternate Path	Yes	-

TABLE 2. SACM FEATURES

Features	Yes	No
Information Sharing	Yes	-
DDoS Detection	-	No
Information Security	Yes	-
Source Tracing	-	No
DDoS Mitigation	-	
Network Monitoring	Yes	-
Automated Processes		-

TABLE 3. MILE FEATURES

Features	Yes	No
Information Sharing	Yes	-
DDoS Detection		-
Incident Security		-
Source Tracing		-
DDoS Mitigation		-
Information Gathering		-
Network Monitoring	-	No

4.3 MILE Detection and Tracing of DDoS Attack

To facilitate communication and tracing security incident the service provider or incident response team should be prepared with tools along with processes before any attack on the attack target. For this MILE working group has given a Real-time Inter-network Defense RID framework, it will be a proactive solution used for security incidents [25]. The features of MILE are shown in Table 3.

For sharing threat intelligence, information theses should be combined with the current detection, finding, identification of the source and solution for the mitigation of DDoS attacks. This all is provided by the RID such as its nature of proactive communication within a network. The XML is used for the data in RID messages with the help of IODEF and RID documents. Security and privacy contemplations are of high worry since possibly delicate data might be gone through RID messages.

5. PROPOSED SOLUTION

The DDoS attack is a big threat to real-time service of any organization, such as Webhosting service providers, cloud computing, taxi app services, online banking, or internet service provider and so on. To avoid this, as per industry practice too many tools and techniques are used for mitigation, detection or threat information sharing. These all services of active DDoS attacks are not supported by any single tool. But they need extra tools or techniques to provide complete services, like as detection, tracing of the source, secure threat or incident information sharing, and mitigation of DDoS attack on attack targets. To get 100% results of mitigation, detection and tracing of the source as we have proposed to combine the three frameworks DDoS Open Threat Signaling DOTS, Security Automation, and Continuous Monitoring SACM, and Managed Incident Lightweight Exchange MILE of the standard body.

5.1 DDoS Mitigation and Detection Tools

To mitigate and detect active DDoS attack the SDN is used, as few of them shown in Table 4. The services provided by Cloudflare, F5 Networks, Akamai, Arbor Networks, Incapsula, Level 3, and Verisign are known as DDoSPS (Protection Service) [26]. They are providing DDoSPS for any application or for the complete network.

TABLE 4. TOOLS USED FOR DDOS DETECTION AND MITIGATION

Tools	DOTS	SACM	MLE
Cloudflare	No	No	Yes
F5 Networks			
Akamai			
Arbor Networks			
Incapsula			
Level 3			
Verisign			
Verizon			

The main functionality of DPS architecture is to divert the traffic of an application or network. This service can be enabled for always-on or on need-based.

Cloudflare provides DDoS attack mitigation as a service with a low price [27]. However, the services are provided for mitigation only and applications should be hosted at the Cloudflare platform, which is not applicable for every organization. Another tool, Verizon's, has implemented virtualized SDN-enabled architecture with the trust of the root [7]. The simulated anti-DDoS scouring programs are activated automatically close to the source of a DoS attack detected. The traffic will be routed from these functions. These functions are configured with prioritization rules to give priority to real traffic of the network dynamically and reduce the resources for the malicious traffic. Mostly these types of service for DDoS attack detection and mitigation are applied on applications with the help of router threshold.

5.2 Threat Information Sharing Tools

As the number of threats and security breach incidents are growing day by day. So that these incidents need to be detected and should be handled as soon as possible to decrease the damage of the organization. To do that there is a need for threat information sharing with a secure method. Some threat information tools are mentioned in Table 5.

The community framework known as the MISP (Malware Information Sharing Platform) is used for threat information sharing [28]. There are two main parts of the MISP data model and sharing model. In the data model, the simple and easy format has been designed. Due to the simple format, users can define which level of information will be shared with the community. The different levels of information sharing have been defined, such as organization only, the community only, connected communities, and with all as the default function of MISP communities. YARA Kim et. al. [29] is an unadulterated marker layer technology that depicts regular expression examples and conduct. YARA is an engine and language for checking documents and memory squares. At the point when a standard matches a design, YARA presumes to arrange the subject as

TABLE 5. TOOLS USED FOR THREAT INFORMATI ON SHARING AND DETECTION OF THREAT

Tools	DOTS	SACM	MLE
MISP	Yes	Yes	Yes
HELK			
SQHUNTER			
CHIRON ELK			
BANG			
YARA			
MAL TINDEX			
Onion Share			
XRay			

indicated by the standard's conduct. YARA can coordinate different string arrangements like ASCII, UTF (Unicode Transformation Format), and different encodings; YARA can likewise parse on PERL standard articulations and has Python and Ruby ties.

5.3 Prevention and Threat Information Sharing

There are a number of tools for threat information sharing and prevention, some of them are community-based and commercial. OWASP (Open Web Application Security Project) community framework to detect and prevent the websites from DoS attacks on the application layer. For a web server HTTP (Hyper-Text Transfer Protocol) headers contain noteworthy data, which is originating from the client, while the solicitations are handled, web server holds back to catch total solicitation of HTTP headers before handling for a message as an affirmation to the request sender. The HTTP slow header attack works by misusing the customer inactive break esteem on the unfortunate casualty web server [30]. This break is designed at the server side to drop a customer association if a customer was found inert during the timespan. The slow header assault finds the evaluated break worth set on the injured individual server-side and after that picks a worth which is lower than the designed worth. At that point, this assault produces HTTP demands with incomplete header or the deficient header to the injured individual web server. It keeps sending one header dependent on the chose worth with the end goal that customer inactive break won't be activated on the victim individual web server and solicitations won't be finished (Table 6).

Suricata is one of the genuine instances of open-source IDS/IPS accessible on all stages [29]. It recognizes an assault by assessing organize information against predefined standard mark rule-set accessible from developing dangers. Suricata gives name, seriousness, and kind of assault. To stay up with the latest, a logging specialist contacts the organization server to check the accessibility of new marks in the inward database. In the event that another mark is found, the logging operator naturally refreshes the Suricata ruleset.

6. CONCLUSION

To share threat information during an active DDoS attack is a big challenge for security persons. The second one is protection against the DDoS attacks on any service providers or on the network infrastructure of any organization. One existing method to detect and mitigate these types of attacks is software-defined networks SDNs. We have suggested combining three different frameworks of the standard body. By using these frameworks, the process of threat information sharing and DDoS attacks protection, and securely with the automated process. The DOTS will be used for information sharing between server and client. The security of incident messages and continuous monitoring of the attack target has been done via the SACM framework. To detect, trace the source of the attack and mitigate the active DDoS attack done with the help of MILE. The communication between two or more peers regarding incident information shared securely by RID protection techniques, such as the security and privacy policy of the organization. As we have combined all these three methods proposed solely by the standard body. The desired results can be achieved by implementing our proposed method during the active DDoS attack. The main focus was on the uptime of service provided by any organization during this attack.

TABLE 6. TOOLS USED FOR THREAT INFORMATION SHARING AND FIREWALL

Tools	DOTS	SACM	MLE
LOIC	No	No	Yes
XOIC			
HULK			
DDOSIM-Layer7			
R-U-Dead-Yet			
OWASP DOS HTTP POST			
DAVOSET			
GoldenEye HTTP Denial ofService Tool			
SURICATA	Yes	Yes	

7. FUTURE WORK

In the future we will implement it on a network to analyze it through software.

ACKNOWLEDGEMENTS

Authors are thankful to Riphah Institute of System Engineering, Islamabad, Pakistan, and Quaid-e-Awam University of Engineering, Science & Technology, Nawabshah, Pakistan, for providing facilities to conduct this research paper.

REFERENCES

[1] Mirkovic, J., and Reiher, P., "A Taxonomy of DDoS Attack and DDoS Defense Mechanisms", ACM SIGCOMM Computer Communication Review, Volume 34, No. 2, pp. 39-53, 2004.

[2] Reddy, T., Boucadair, M., Patil, P., Mortensen, A., and Teague, N., "Distributed Denial-of-Service Open Threat Signaling (DOTS) Signal Channel Specification", Internet-Draft. Reddy, 2017.

[3] Montville, A., and Munyan, B.,"Security Automation and Continuous Monitoring (SACM) Architecture", IETF Internet-Draft, 2019.

[4] Birkholz, H., Lu, J., Strassner, J., Cam-Winget, N., and Montville, A.,"Security Automation and Continuous Monitoring (SACM) Terminology", IETF Internet-Draft, 2018.

[5] Inacio, C., and Miyamoto, D., "Management Incident Lightweight Exchange (MILE) Implementation Report. Management", Internet Engineering Task Force, 2017.

[6] Steinberger, J., Kuhnert, B., Sperotto, A., Baier, H., and Pras, A., "Collaborative DDoS Defense Using Flow-Based Security Event Information". IEEE/IFIP Network Operations and Management Symposium, pp. 516-522, April, 2016.

[7] Yan, Q., Huang, W., Luo, X., Gong, Q., and Yu, F.R.,"A Multi-Level DDoS Mitigation Framework for the Industrial Internet of

Things", IEEE Communications Magazine, Volume 56, No. 2, pp. 30-36, 2018.

[8] D'Cruze, H., Wang, P., Sbeit, R.O., and Ray, A., "A Software-Defined Networking (SDN) Approach to Mitigating DDoS Attacks", Information Technology-New Generations, pp. 141-145, Springer, Cham, 2018.

[9] Aamir, M., and Zaidi, S.M.A., "DDoS Attack Detection with Feature Engineering and Machine Learning: The Framework and Performance Evaluation", International Journal of Information Security, pp. 1-25, 2019.

[10] Xia, S.M., Zhang, L., Bai, W., Zhou, X.Y., and Pan, Z.S., "DDoS Traffic Control Using Transfer Learning DQN With Structure Information", IEEE Access, Volume 7, pp. 81481-81493, 2019.

[11] Swami, R., Dave, M., and Ranga, V.,"Software-Defined Networking-Based DDoS Defense Mechanisms", ACM Computing Surveys, Volume 52, No. 2, pp. 28, 2019.

[12] Bawany, N.Z., Shamsi, J.A., and Salah, K., "DDoS Attack Detection and Mitigation Using SDN: Methods, Practices, and Solutions", Arabian Journal for Science & Engineering, Volume 42, No. 2, pp. 425-441, 2017.

[13] Hameed, S., and Khan, A.H., "SDN Based Collaborative Scheme for Mitigation of DDoS Attacks", Future Internet, Volume 10, No. 3, pp. 23, 2018.

[14] Panchen, S., Phaal, P., and McKee, N.,"InMon Corporation's sFlow: A Method for Monitoring Traffic in Switched and Routed networks", Published in RFC. 2001.

[15] Hu, D., Hong, P., and Chen, Y., "FADM: DDoS Flooding Attack Detection and Mitigation System in Software-Defined Networking", IEEE Global Communications Conference, pp. 1-7, December, 2017.

[16] Li, Y., Liu, B., Zhai, S., and Chen, M., "DDoS Attack Detection Method Based on Feature Extraction of Deep Belief Network", IOP Conference Series: Earth and Environmental Science, IOP Publishing, Volume 252, No. 3, pp. 032013, April, 2019.

[17] Kampanakis, P., "Security Automation and Threat Information-Sharing Options", IEEE Security & Privacy, Volume 12, No. 5, pp. 42-51, 2014.

[18] François, J., Aib, I., and Boutaba, R.,"FireCol: A Collaborative Protection Network for the Detection of Flooding DDoS Attacks", IEEE/ACM Transactions on Networking, Volume 20, No. 6, pp. 1828-1841, 2012.

[19] Cotton, M., "DDoS Attacks: Defending Cloud Environments", Information Technology-New Generations, pp. 907-909, Springer, Cham, 2018.

[20] Bhushan, K., and Gupta, B.B., "Distributed Denial of Service (DDoS) Attack Mitigation in a Software-Defined Network (SDN)-Based Cloud Computing Environment", Journal of Ambient Intelligence and Humanized Computing, Volume 10, No. 5, pp. 1985-1997, 2019.

[21] Tounsi, W., and Rais, H., "A Survey on Technical Threat Intelligence in the Age of Sophisticated Cyber-Attacks", Computers & Security, Volume 72, pp. 212-233, 2018.

[22] Cam-Winget, N., and Lorenzin, L., "Security Automation and Continuous Monitoring (SACM) Requirements", An IETF Working Group, 2017.

[23] Danyliw, R., Meijer, J., and Demchenko, Y., "RFC 5070: Incident Object Description Exchange Format (IODEF), Network Working Group, 2012.

[24] Cam-Winget, N., and Lorenzin, L., "RFC 8248: Security Automation and Continuous Monitoring (SACM) Requirements", Engineering, Computer Science, Published in RFC 2017.

[25] Moriarty, K., "RFC 6545: Real-Time Inter-Network Defense RID" Internet Engineering Task Force, 2012.

[26] Jonker, M., Sperotto, A., van Rijswijk-Deij, R., Sadre, R., and Pras, A.,"Measuring the Adoption of DDoS Protection Services" ACM Proceedings of Internet Measurement Conference, pp. 279-285, November, 2016.

[27] "Advanced DDoS Attack Protection", https:// www.cloudflare.com/ddos/, (Accessed on 30, July 2019).

[28] Wagner, C., Dulaunoy, A., Wagener, G., and Iklody, A., "Misp: The design and Implementation of a Collaborative Threat Intelligence Sharing Platform", ACM Proceedings of Workshop on Information Sharing and Collaborative Security, pp. 49-56, October, 2016.

[29] Kim, E., Kim, K., Shin, D., Jin, B., and Kim, H., "CyTIME: Cyber Threat Intelligence Management Framework for Automatically Generating Security Rules", ACM Proceedings of 13th International Conference on Future Internet Technologies, pp. 7, June, 2018.

[30] Behal, S., and Kumar, K.,"Characterization and Comparison of DDoS Attack Tools and Traffic Generators: A Review", International Journal of Network Security, Volume 19, No. 3, pp. 383-393, 2017.

Performance and Comparative Analysis of Speed Control of IM using Improved Hybrid Fuzzy Gain Scheduling of Proportional Integral Derivative Controller

Bilawal Nawaz Malik*, Zaira Anwar*, Aftab Ahmad*, Safee Ullah, and Inam Ul Hasan Shaikh***

* Department of Electrical Engineering, University of Engineering & Technology, Taxila, Pakistan.

** Department of Electrical Engineering, Heavy Industries Taxila Education City, Taxila, Pakistan.

bilawalnawz@gmail.com, eshmal.fatima@yahoo.com, aftab.ahmad@uettaxila.edu.pk, inam.hasan@uettaxila.edu.pk, safee10@yahoo.com

ABSTRACT

In this paper, an improved Hybrid FGS-PID (Fuzzy Gain Scheduling of Proportional Integral Derivative) controller is presented for governing the speed of IM (Induction Motor). It is compared with the existing conventional controller (PD&PID) which are extensively used in the industries, an indirect vector control technique using "Synchronously Rotating Reference" as an IM's frame model. This model has been used to governor the speed of three phase squirrel cage IM by using various controller techniques. The proposed Hybrid FGS-PID controller method has been designed, which further selects the three different gains of the PID controller by using a fuzzy inference engine while considering the inputs and outputs Fuzzy rules have been designed to calculate the optimum range of gain values. The designed controller has the flexibility of suitably fine-tuning of conventional PID controller's gains to get the desired results under various operating conditions and to fuzzify the gain parameters Gaussian membership functions were used, rules are mapped in Mamdani inference engine corresponding to their inputs and their output. The comparative results show that fresh gain parameters of designed FGS-PID controller have resolved that the limitations regarding parameters changed and load variations quite satisfactorily.

Key Words: Induction Motor, Proportional Integral Derivative, Proportional Derivative, Fuzzy Logic Controller, Proportional Integral, Indirect Field Oriented Control and Fuzzy Gain Scheduling of PID.

1. INTRODUCTION

IM are used in a wide range of industrial and domestic applications. According to the recent research, it is noted that mostly generated electrical energy is used up via electric motors in technologically advanced countries. Among all these motors, more than 90% of them are IMs [1]. The control of IM is challenging due to its intrinsic nonlinear nature and by means of study with a large number of papers and patents. A squirrel cage IMs is extensively used because of its reliability, low cost, simple maintenance and robustness, so it is important to design a controller [2]. To increase efficiency and enhancing its performance, several different techniques have been proposed. Scalar control technique is mostly used because of its easy implementation. The SC drives do not give satisfactory results for extraordinary performance applications. In this manner of control, torque and flux are decoupled and therefore the analysis of IM is greatly simplified and becomes quite similar to DC excited motor.

With the passage of time, in vector control technique, different conventional controllers have been used together for IM to improve its performance. But it is necessary to highlight that, PID controllers have a main drawback i.e. performance degradation because of the variations in its parameter. These issues rises mostly because of the fixed gains, which effect the performance. To control the speed of such motors, FLC (Fuzzy Logic Controller) delivers a positive solution [3].

FLC has the main attribute over classical PID controller is that FLC does not require any mathematical model. By using fuzzy logic, all those complex systems which are difficult to model precisely, can also be controlled effectively [4]. The IM and their robustness with respect to change in parameters can be enhanced the nonlinear techniques which fuzzy control provides [5-6]. Lately, in order to enhance the controller's performance, hybrid control techniques that consist of two or added control approaches are offered.

TS (Takagi-Sugeno) based fuzzy controller presented in [7] to achieve robust speed control of an IM. An applied conventional PI (Proportional Integral) controller as well as a Fuzzy controller has been presented in [5]. They reported that the performance of IM has been upgraded by means of starting current and rise time. The demonstrated performance of SPWM (Sinusoidal Pulse Width Modulation) presented in using different simulation technique combined with PI or FLC, the results shows a better performance of FLC. An adaptive FLC design technique using backtracking search algorithm has been presented in [8]. The results show it was better. FPI control strategy designed for IM is presented in [9] to control the speed in an improved manner. PI controller and FLC have been designed for IM drive in [7]. Fuzzy controller has been designed using TS fuzzy model. The results exposed that TSF controller showed improved performance by means of control delay to load variants. Adaptive FLC based on Levenberg–Marquardt algorithm presented in [10]. In this paper the results show that the controller is robust and is useful for load disturbance rejection. PI controller and FLC four based rules controller presented in [11] for a double star IM driven for its INFOC (Indirect Field Oriented Control). In this case, FLC shows better result than PI controller. The secondary

vector model control method for a 3-phase Induction machine using soft calculating technique. ISM (Intellectual Speed Model) is being considered with fuzzy reasoning based controllers presented in [12] and simulated experimentations were done using MATLAB or SIMULINK to attain best results.

It is definitely a challenging task to design the speed controller for induction machines [13]. Some controllers show good performance in some attributes, as from the previous study firstly scalar methods are being looked for speed regulation of the IM. Scalar control drives are easily implemented but does not provide satisfactory results for high performance applications. Vector control technique was invented by Blaschke. Vector control technique provides a decoupling mechanism for IMs such as in DC machines by controlling the torque (Γ) and flux(Θ) independently. PI regulator is most extensively adopted in engineering uses because of its modest assembly, easy structure and a very little cost. Integral control can possess the effect of least error. It has an undesirable consequence on speed of reaction as well as whole firmness of the model. PD controller has the capability to forecast the upcoming fault in system thus increasing the stability of system. PID regulator is extensively used in business and electronic systems. It mainly possesses dynamic firm responses on variation in controller parameters (D controller). FLC is the approach of "if and then" declaration for the regulator and calculated the model of network is not an obligatory in fuzzy controller therefore it can be functional on nonlinear systems. Intellectual Speed Governor is also being planned using fuzzy reasoning controllers. Diverse simulation tests were approved for achieving the finest controller. The guidelines for the mentioned controller were aimed to deal with dynamic conduct. The acts of the presented fuzzy reasoning control relying on induction machine are related with traditional machine having PI controller at various operation circumstances. Results of fuzzy control model prove the progress in stability and dynamic response.

The literature survey concludes that to improve performance parameters of an IM either fuzzy logic or neural networks have been used. By employing these techniques there has been sufficient improvement in the performance parameters but still as per today's needs and demands, the parameters further need to be improved. Therefore, this research focuses on the use of hybrid control i.e. conventional PID controller with fuzzy supervisory control.

2. MATHEMATICAL FORMULATION

2.1 Reference Model of IM

Stator Reference Model: Stator reference model presented that, the axis remains staticon d-q axis [14]. In stator reference model stator and reference frame rotate at same speed, i.e. ω_c=0.

Rotor Reference Model: Rotor reference model presented that, the d-q axes moves according to rotor's speed [15-16]. In rotor reference model stator and reference frame rotate at same speed, i.e. $\omega_c = \omega_r$ and $\theta_c = \theta_r$.

Synchronously Rotating Reference Model: Synchronously rotating reference model presented that, the d-q axes rotate with synchronous speed [15-16]. In synchronously rotating reference model stator and reference frame rotate at same speed, i.e. $\omega_c = \omega_r$ and ω_{sl}.

$$\begin{bmatrix} V_{qs}^e \\ V_{ds}^e \\ V_{qr}^e \\ V_{dr}^e \end{bmatrix} = \begin{bmatrix} R_s + L_S\frac{d}{dt} & \omega_s L_s i_{ds}^e & L_m\frac{di_{qr}^r}{dt} & \omega_s L_s i_{dr}^r \\ -\omega_s L_s & R_s + L_S\frac{d}{dt} & -\omega_s L_m & L_m\frac{d}{dt} \\ L_m\frac{d}{dt} & (\omega_s-\omega_r)L_s & R_r + L_r\frac{d}{dt} & (\omega_s-\omega_r)L_s \\ -(\omega_s-\omega_r)L_m & L_m\frac{d}{dt} & -(\omega_s-\omega_r)L_r & R_r + L_r\frac{d}{dt} \end{bmatrix} \begin{bmatrix} i_{qs}^e \\ i_{ds}^e \\ i_{qr}^e \\ i_{dr}^e \end{bmatrix}$$

In control system, because of the constant variables of the motor, synchronously rotating reference frame is used [15-16].

2.2 Derivation of Transfer Function

To design a speed controller for an IM, we assume the constant rotor flux [14-15] i.e.

λ_r = constant and

$$\frac{d\lambda_r}{dt} = 0$$

As stator voltages are given;

$$V_{qs}^e = \left(R_s + L_s\frac{d}{dt}\right)i_{qs}^e + \omega_s L_s i_{ds}^e + L_m\frac{di_{qr}^e}{dt} + \omega_s L_s i_{dr}^e \quad (2)$$

$$V_{qs}^e = -\omega_s L_s i_{qs}^e + \left(R_s + L_s\frac{d}{dt}\right)i_{ds}^e - \omega_s L_m i_{qr}^e L_m\frac{di_{dr}^e}{dt} \quad (3)$$

Where, $\omega_{sl} = \omega_s - \omega_r$

$$V_{qs}^e = \left(R_s + \sigma L_s\frac{d}{dt}\right)i_{qs}^e + \omega_s i_{ds}^e(\sigma L_s) + \omega_s L_m \quad (4)$$

Similarly,

$$V_{ds}^e = \left(R_s + \sigma L_s\frac{d}{dt}\right)i_{ds}^e - \omega_s i_{ds}^e(\sigma L_s) + \frac{L_m}{L_r}\frac{d}{dt}(\lambda_r) \quad (5)$$

As we know that i_{ds} is constant in steady state and its derivative is zero so,

$$i_{ds}^e = i_f \quad (6)$$

$$\frac{di_{ds}^e}{ss} = 0 \quad (7)$$

Hence, the torque producing component is written in Equations (8-9):

$$i_{qs}^{e} = i_T \tag{8}$$

$$V_{qs}^{e} - \omega_r\left(L_s i_f\right) = \left(R_s + \frac{R_r L_s}{L_r} + L_a \frac{d}{dt}\right) i_T \tag{9}$$

We take Laplace transform of the torque producing current component such as:

$$i_T = \frac{V_{qs}^{e} - \omega_r\left(L_a i_f\right)}{R_a\left(1 + \frac{sL_a}{R_a}\right)} \tag{10}$$

Now by substituting $K_a = \frac{1}{R_a}$ and $T_a = \frac{L_a}{R_a}$ and 1in the above expression:

$$i_T = \frac{K_a}{\left(1 + sT_a\right)} V_{qs}^{e} - \omega_r\left(L_s i_f\right) \tag{11}$$

With the help of voltage signal and speed feedback. The torque can be expressed as [15].

$$T_e = \frac{3}{2}\frac{P}{2}\frac{L_m^2}{L_r} \text{ if } i_T \tag{12}$$

$$K_t = \frac{3}{2}\frac{P}{2}\frac{L_m^2}{L_r} \text{ if } i_T \tag{13}$$

Now substitute the value of K_t in Equations (12)

$$T_e = K_t i_T \tag{14}$$

The load dynamics is represented in electromagnetic torque and load torque [17].

$$J\frac{d\omega_m}{dt} + B\omega_m = K_t i_T - B_t \omega_m \tag{15}$$

$$T_t = B_t \omega_m \tag{16}$$

Equation (15) can be shown as [12]

$$d\left(\frac{P}{2}\omega_m\right)dt + B\left(\frac{P}{2}\omega_m\right) = \frac{P}{2}K_t i_T - B_t\left(\frac{P}{2}\omega_m\right) \tag{17}$$

$$\omega_r = \frac{P}{2}\omega_m \tag{18}$$

By substituting value of ω_r

$$J\frac{d\omega_r}{dt} + B\omega_r = \frac{P}{2}K_t i_T - B_t\omega_r \tag{19}$$

By taking Laplace transform of above expression

$$Js\omega_r(s) + \left(B + B_t\right)\omega_r(s) = \frac{P}{2}K_t i_T(s) \tag{20}$$

Where, $B + B_t = B_t$

$$Js\omega_r(s) + B_t\omega_r(s) = \frac{P}{2}K_t i_T(s) \tag{21}$$

$$\omega_r(s) B_t\left(s\frac{J}{B_t} + 1\right) = \frac{P}{2}K_t i_T(s) \tag{22}$$

$$\frac{\omega_r(s)}{i_T(s)} = \frac{P}{2}\frac{K_t}{B_t}\frac{1}{\left(s\frac{J}{B_t} + 1\right)} \tag{23}$$

The above expression can be written as:

$$\frac{\omega_r(s)}{i_T(s)} = \frac{K_m}{1 + sT_m} \tag{24}$$

The Equation (24) shows the relationship between the speed and current produced by the torque in terms of transfer function. The main parameters of the IM are specified in [16] (Table 1)

Once the transfer function is computed then we have find the performance parameters of the IM in terms of settling time, rise time and overshoot.

2.3 Open Loop Response of the System

It is significant to check the open loop response of system by computing the performance of the system and the performance is measured by characteristics like settling time, rise time and overshoot. The output characteristics response of the unit step open loop system is presented below in Fig.1 and Table 2.

TABLE 1. PARAMETER OF IM [16]	
Quantity	Magnitude/Symbol
Power (P)	5 Hp
Rated voltage (V)	220 V
Poles (P)	P = 4
Stator resistance (R_s)	R_s=0.277?
Rotor resistance (R_r)	R_r=0.183?
Stator inductance (L_s)	L_s=0.0553H
Rotor inductance (L_r)	L_r=0.0583H
Frequency (f)	f=50 Hz
Mutual inductance (L_m)	L_m=0.0583H
Moment of inertia (J)	J=0.011667Kg-m
Settling time of plant (T_s)	T_S=10s
Time constant of speed filter (T_w)	T_w=0.002
Gain of current transducer (H_c)	H_C=0.333V/A
Steady state field current (i_f)	i_f=6A
Control frequency (F_c)	F_c=2000Hz

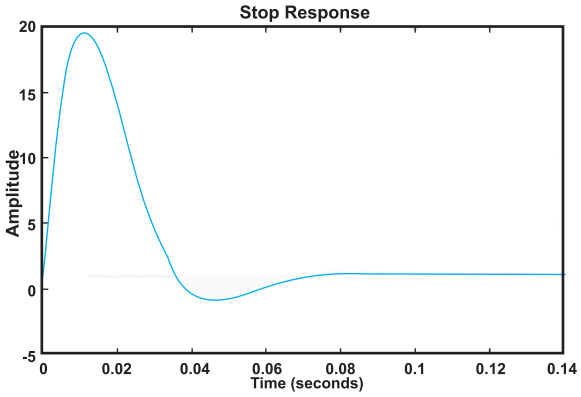

FIG. 1. OPEN LOOP RESPONSE OF THE SYSTEM

TABLE 2. PERFORMANCE PARAMETER OF THE SYSTEM	
Performance Parameters	Open Loop Response of System
Rise Time (s)	3.0799e-04
Settling Time (s)	0.0651
Overshoot	1.7896e+03

A very high overshoot has been observed in the open loop response because of the system nonlinearity and harmonics present in the system parameters. As desired performance is described in [15], so the parameters are required to be improved. For that reason, it is important to design a controller.

3. CONVENTIONAL CONTROLLER

Conventional PD along with PID controller helps in controlling of Induction motors. The conventional controller is a feedback controller. The value of error can be calculated by the difference between the measured process value and the desired set point value. It drives the controlled plant to keep the steady state error equal to zero, so here we designed the PD and PID controllers to check the performance of IM. The conventional feedback controller block diagram is shown in Fig. 2.

3.1 Proportional Derivative Controller

PD controller is also used for the speed control of IM, the pros of using this controller is to reduce the settling time, rise time and the overshoot, significantly. Therefore, it increases the bandwidth of the system. But due to the derivative operation, the noise also get amplified resulting in a system which is suspicious to noise i.e. error, which may cause a system to be unstable. Here, we have designed the PD controller for the IM and following are the gain parameters of designed PD controller; K_p = 66101 and K_d = 2.2863. The response and performance parameters are given in Fig. 3 and Table 3.

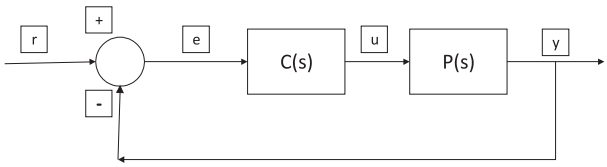

FIG. 2. FEEDBACK CONTROLLED SYSTEM BLOCK DIAGRAM [18]

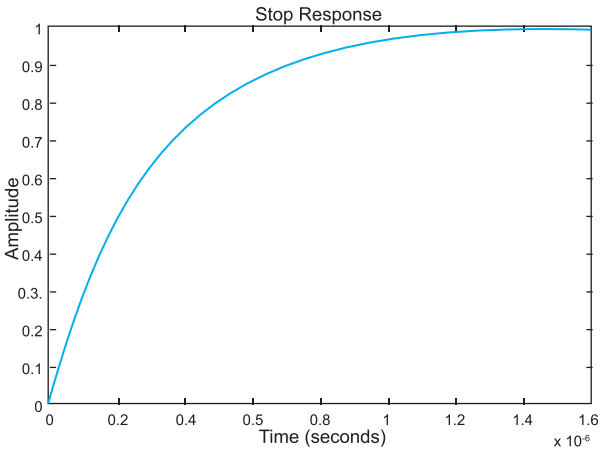

FIG. 3. STEP RESPONSE OF PD CONTROLLER

TABLE 3. PERFORMANCE PARAMETER OF THE PD CONTROLLER	
Performance Parameters	With PD Controller
Rise time (s)	6.6101e-07
Settling time (s)	1.1600e-06
Overshoot	0.0735

3.2 Proportional Integral Derivative Controller

PID controller is mostly applicable in control system of industries. PID controller has all basic features i.e. **D** controller shows fast reaction when the controller input changes. **I** controller increases the control signal which lead error towards the zero. **P** controller helps to eliminate the oscillations. Derivative mode improves the stability of system and enables increase in gain, $\mathbf{K_P}$ which increases speed of the controller response. The output of PID depends on the main three terms which are error signal, error integral and error derivative. The mathematical form is shown in Equation (25):

$$u(t) = K_P e(t) + K_I \int_0^t e(\tau)d\tau + K_D \frac{de(t)}{dt}$$

Where K_p, K_i and K_d are PI and Derivative gains respectively. It combines proportional, derivative and integral of the error signal which determine command signal 'u' for the system. In our case 'u' represents the T^*_e torque of the vector control drive for the induction motor.

The response and performance parameters of PID Controller are given below in the Fig.4 and Table 4.

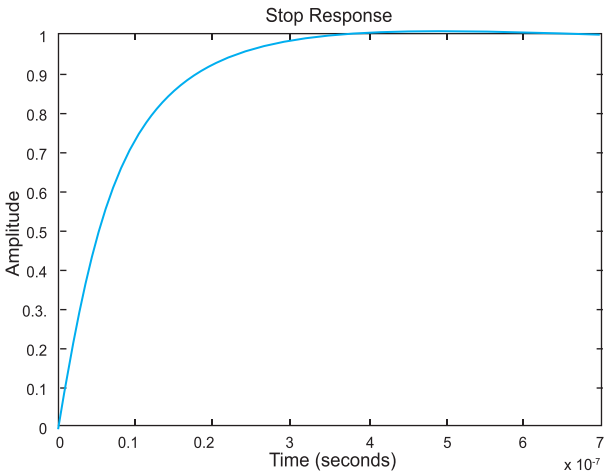

FIG. 4. STEP RESPONSE OF THE PID CONTROLLER

TABLE 4. PERFORMANCE PARAMETER OF THE PID CONTROLLER	
Performance Parameters	With PID Controller
Rise Time (s)	1.6668e-07
Settling Time (s)	2.9750e-07
Overshoot	0

It is necessary to mention that the performance degradation is the main drawback in PID controller because of parameter variations and this matter mostly arises because of fixed gain of the controller that influences on speed performance.

4. FUZZY CONTROLLER

Fuzzy control is basically applied through "if-then" statement for control process. The variables showed the antecedent (the if-part of the statement) and the consequent (the then-part of the statement). Thus, the non-linear system can be relied in this statement. Mamdani inference engine is used to map the input to their corresponding output. It is preferred over sugeno inference engine because it is more flexible and deal with the both MIMO (Multiple-Input and Multiple-Output) and MISO system Flow chart shown in Fig. 5, describes the methodology to search the solution using FLC system.

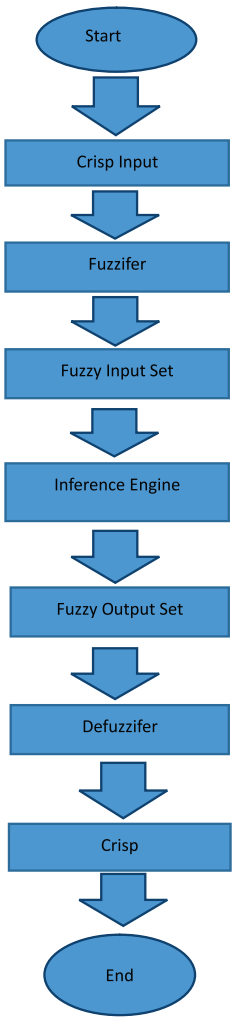

FIG. 5. FLOW CHART METHODOLOGY OF FUZZY LOGIC CONTROL

5. HYBRID FUZZY GAIN SCHEDULING OF PID CONTROLLER

Hybrid controller is designed with the incorporation of different controller. Here in our case, we have designed FGS-PID controller. In this way, we used the simple PID controller with the fuzzy controller to signify both overshoot and undershoot of the PID, which provides the optimized domino effects with the implementation of this model. Also with the help of hybrid model, it provides the increased levels of stability under different load variations.

To get the best optimized results, conventional controller is combined with the FC, hybridization of both controllers is proposed. In our proposed technique, hybrid controller works as the single controller for the speed control of the IM. In this technique, there are two input signals which are the error of the signal (E) and change in the error signal (CE) that is derivative of the error. A new error signal which is the output of the FC which is fed to the PID controller.

5.1 Inputs of Fuzzy Controller

Fuzzy controller uses "error" and "rate of change of error" as inputs. "Error" is the estimated difference between observed and true values of torque producing current

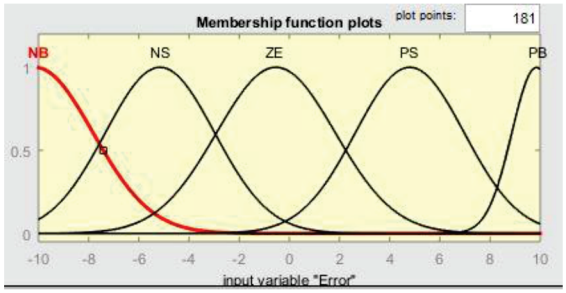

FIG. 6. MEMBERSHIP FUNCTION PLOT FOR ERROR

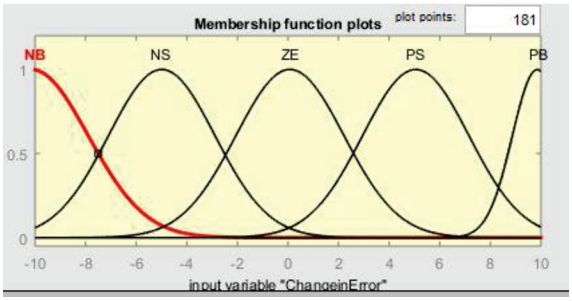

FIG. 7. MEMBERSHIP FUNCTION PLOT FOR CHANGE IN ERROR

TABLE 5.RULES BASE FOR THE FUZZY CONTROLLER

ECE	NB	NS	ZE	PS	PB
NB	NB	NB	NS	NS	ZE
NS	NB	NS	NS	ZE	PS
ZE	NS	NS	ZE	PS	PS
PS	NS	ZE	PS	PB	PB
PB	ZE	PS	PS	PB	PB

component of IM. These ranges have been partitioned as shown in Figs. 6-7. Here we use the ranges of "error" and "rate of change of error" are NL (Negative Large), NS (Negative Small), ZE (Zero), PS (Positive Small) and PL (Positive Large). There are different types of membership function i.e. triangular, Gaussian, trapezoidal. Here we use Gaussian membership function due to their smoothness and concise natures.

5.2 Rules Base for the Fuzzy Controller

The rules for the FLC is followed in this paper are given in Table 5.

5.3 Outputs of the Fuzzy Logic Controller

FLC output is the value of gain parameter for PID controller i.e. $\mathbf{K_p}$, $\mathbf{K_i}$ and $\mathbf{K_d}$. Fuzzy controller automatically adjusts the values of the gain parameters according to the load variations. The universe of discourse for these three gains have been selected after performing extensive simulations. The membership function corresponding to the controller outputs are as shown in Figs. 8-10.

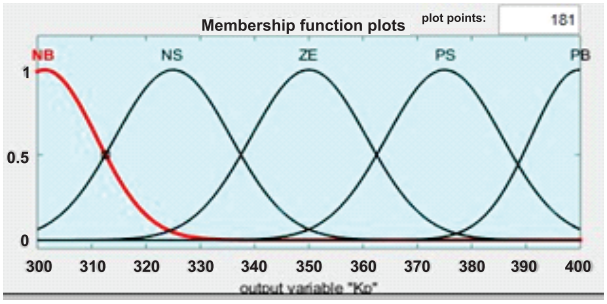

FIG. 8. MEMBERSHIP FUNCTION PLOT FOR K_p

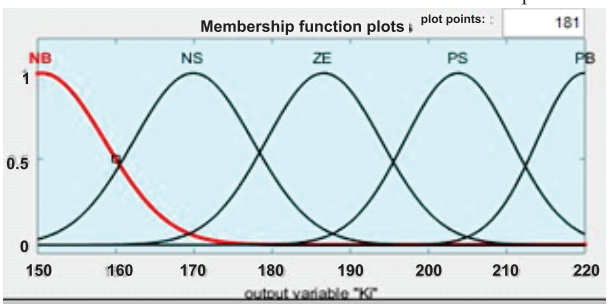

FIG. 9. MEMBERSHIP FUNCTION PLOT FOR K_i

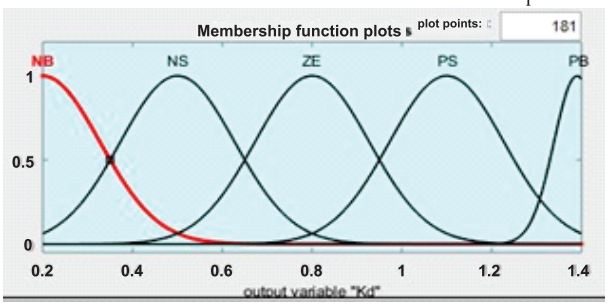

FIG. 10. MEMBERSHIP FUNCTION PLOT FOR K_d

The 3D surface view for the rules of $\mathbf{K_p}$ while considering the error and rate of change of error is shown in the Fig 11.

6. RESULTS AND DISCUSSIONS

As we have discussed earlier that our main aim is to control the speed control of IM as a purpose, we have designed the conventional controller i.e. PD and PID controller. By using these controllers, the system response become fast, as shown in Table 6. In Table 6, we do the comparison of open loop response of the system with the closed loop PD and PID control responses of the system.

The analysis indicates that overshoot value has decreased from, 1.7896×10^{3}% to 0.0735% in PD and 1.7896×10^{3}% to 0% in PID. Rise time improved from 3.0799×10^{-4}s to 6.6101×10^{-7}s in PD and 3.0799×10^{-4}s to 1.6668×10^{-7}s in PID. Settling time has improved from 0.0651s to 1.1600×10^{-6}s in PD and 0.0651s to 2.9750×10^{-7}s in PID. So the system response become fast.

Due to the limitations of the conventional controllers we designed FGS-PID controller. The results of FGS-PID controller are presented in Table 7. Considering, a case in which we change the load and according to the load variation the values of error and change in error become [-7 7] then the value of K_p, K_i and K_d are automatically updated at the values of error and change in error as shown in Fig. 12 and the step response is given in Fig. 13 respectively. At this stage, the PI and derivative gains will be 341,180 and 0.69 respectively. If we change the error values, gains will change accordingly as shown in Figs. 12-13 and Table 7.

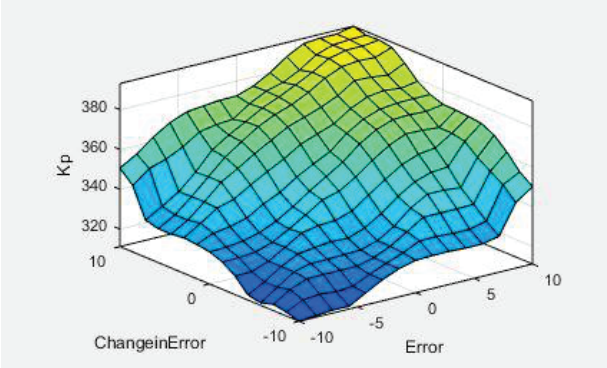

FIG. 11. 3D SURFACE VIEW

TABLE 6. COMPARISON BETWEEN ALL THE CONVENTIONAL

Performance Parameters	Step Response of System	With PD Controller	With PID Controller
Rise time (s)	3.0799e-04	6.6101e-07	1.6668e-07
Settling time (s)	0.0651	1.1600e-06	2.9750e-07
Overshoot	1.7896e+03	0.0735	0

We demonstrated from Table 7 that the FGS-PID for the IM has better performance over the conventional controller. The results in Table 7 show that if the values of "error" and "rate of change of error" is in between the designed (-10 to 10) values, the FGS set the gain values for PID controller to get the better results.

7. CONCLUSION

In this paper, our primary focus is to design a fuzzy supervisory controller to tune the classical PID controller and compare the performance of PID, PD controller and Fuzzy supervisory controller. In the first stage, we designed the PID and PD controller. The analysis indicates that the system response become fast. Conventional PID controller is extensively used but it has constant parameters, due to any change in the parameters, the controller has to re-adjust its gain values, so it is unreliable in case of noise, so to deal with this uncertainty

TABLE 7. GAIN VALUES AT RANDOM VALUES OF "ERROR" AND "CHANGE IN ERROR"

[Error, Change in Error]	K_p	K_i	K_d	Rise Time (s)	Settling Time (s)	Over Shoot
[0,0]	351	187	0.809	3.2904e-09	5.8594e-09	0
[0,0.5]	351	187	0.814	3.2740e-09	5.8300e-09	0
[0.5,0]	352	188	0.828	3.2184e-09	5.7311e-09	0
[-7,7]	341	180	0.69	3.8587e-09	6.8712e-09	0
[0,10]	373	202	1.07	2.4880e-09	4.4304e-09	0
[-10,0]	327	171	0.528	5.0451e-09	8.9842e-09	0
[-10,10]	351	187	0.808	3.2972e-09	5.8713e-09	0

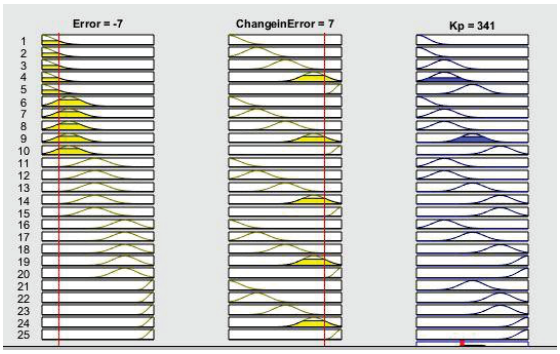

FIG. 12. VALUE OF Kp AT [-7 7]

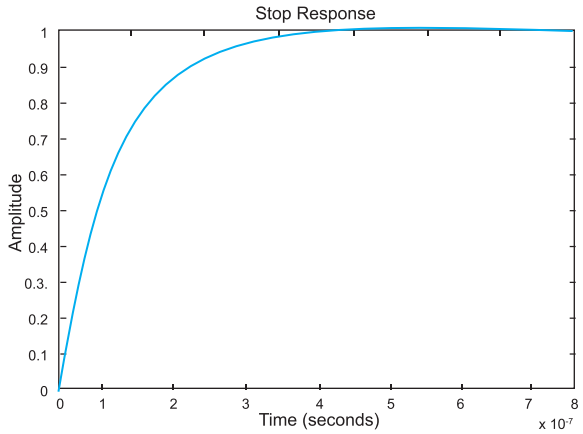

FIG. 13. FGS-PID CONTROLLER OUTPUT AT [-7 7]

FGS-PID controller is designed. In order to design a control system having fuzzy logic, various input and output ranges were assumed. Two different inputs were assumed for the controller which are "error" and "rate of change of error" for the following outputs i.e. K_p, K_i and K_d. Gaussian membership functions were used for the conversion of the crisp values into their respective fuzzy values. Rules were designed after repeated simulations and to map the input to their corresponding output Mamdani's Inference Engine is used. MATLAB plays a vital role in performing all these simulations and steps. Performance of FGS-PID controller have been assessed under different operating conditions, performance of the IM is evaluated by the control parameters i.e. peak overshoot, settling time and rise time, we demonstrated that the FGS-PID controller for the IM has improved performance above the PID controller. From the results it is cleared that if the "error" and "rate of change of error" is in between the designed (-10 to 10 unit), the FGS adjusts the gain values for PID controller to get desired performance. On the basis of the simulated results, the dynamic response takes less time to meet the steady state and controller shows better response under the quick load changes as compared with the other conventional PD and PID controller.

REFERENCES

[1] Shi, K., "Applied Intelligent Control of IM Drives", John Wiley & Sons, 2011.

[2] Kusagur, A., Kodad, S.F., and, Ram, S., "Modelling and Simulation of an ANFIS Controller for an AC Drive", World Journal of Modelling and Simulation, Volume 8, No. 1, pp. 36-49, March, 2011.

[3] Fattah, A. J., and, Qader, I.A., "Performance and Comparison Analysis of Speed Control of IMs using Improved Hybrid PID-Fuzzy Controller", IEEE International Conference on Electro/Information Technology (EIT), pp. 575-580, 2015.

[4] Kusagur, A., Kodad, S. F., and, Sankarram, B. V., "Modelling of IM& Control of Speed using Hybrid Controller Technology", Journal of Theoretical and Applied Information Technology, 2009.

[5] Patwa, S., "Control of Starting Current in Three Phase IM using Fuzzy Logic Controller", International Journal of Advanced Technology in Engineering and Science, Volume 1, No. 12, pp. 2732, December, 2013.

[6] Goel, N., Sharma, P.R., and, Bala, S., "Performance Analysis of SPWM Inverter FED 3-Phase IM Drive using MATLAB SIMULINK", International Journal of Advanced Technology in Engineering and Science, Volume 2, No. 6, pp. 183-193, June, 2014.

[7] Shaukat, N., Khan, B., Mehmood, C.A., and, Ali, S.M., "Takagi-Sugeno Fuzzy Logic Based Speed Control of IM", International Conference on Frontiers of Information Technology, pp. 280-285, December, 2016.

[8] Ali, J.A., Hannan, M.A., Mohamed, A., and, Abdolrasol, M.G.M., "Fuzzy Logic Speed Controller Optimization Approach for IM Drive using Backtracking Search Algorithm", Measurement, Volume 78, pp. 49-62, 2016.

[9] Asad, M., Arif, M., and, Khan, U., "Speed Control of IM via Fuzzy Proportional Integral (FPI) Controller", IEEE International Conference on Computing , Electronic and Electrical Engineering, April, 2016.

[10] Zeb, K., Ali, Z., Saleem, K., Uddin, W., Javed, M.A., and, Christofedes, N., "Indirect Field-Oriented Control of IM Drive Based on Adaptive Fuzzy Logic Controller", Electrical Engineering, Volume 99, No. 3, pp. 803-815, September, 2017.

[11] Tir, Z., Malik, O.P., and, Eltamaly, A.M., "Fuzzy Logic Based Speed Control of Indirect Field Oriented Controlled Double Star IMs Connected in Parallel to a Single Six-Phase Inverter Supply", Electric Power Systems Research, Volume 134,pp. 126-133, May, 2016.

[12] Shajia, P.J., and, Daniel, A.E., "An Intelligent Speed Controller Design for Indirect Vector Controlled IM Drive System", Global Colloquium in Recent Advancement and Effectual Researches in Engineering, Science and Technology, Volume 25, pp. 801-807, 2016.

[13] Behera, P.K., Behera, M.K., and Sahoo, A.K., "Comparative Analysis of Scalar & Vector Control of IM through Modeling & Simulation", International Journal of Innovative Research in Electrical, Electronics, Instrumentation and Control Engineering, Volume 2, No. 4, pp. 1340-1344, April, 2014.

[14] Wang, L. X., "A Control in Fuzzy Sytems and Control", Prentis Hall,August, 1996.

[15] Krause, P. C., and, Thomas, C.H., "Simulation of Symmetrical Induction Machinery", IEEE Transactions on Power Apparatus and Systems, Volume 84, No. 11, pp. 1038-1053, November, 1965.

[16] Krishnan, R., "Electric Motor Drives: Modeling, Analysis and Control", Pearson, February, 2001.

[17] Singh, G., and, Singh, G., "A Fuzzy Pre-Compensated-PI Controller for Indirect Field Oriented Controlled IM Drive", IEEE Innovative Applications of Computational Intelligence on Power, Energy and Controls with their Impact on Humanity, pp. 257-261, November, 2014.

[18] http://ctms.engin.umich.edu/CTMS/index.php?example=Cruise Control&section=ControlPID

Design and Development of an Omni Wheel Soccer Robot

Musharraf Ahmed Hanif*, Muhammad Sarwar Ehsan*, and Syed Atif Mehdi**
*Department of Electrical Engineering, University of Central Punjab, Lahore, Pakistan.
**Department of Computer Science, University of Central Punjab, Lahore, Pakistan.
musharraf.hanif@ucp.edu.pk, sarwar.ehsan@ucp.edu.pk, syed.atif@ucp.edu.pk

ABSTRACT

This paper presents the design of soccer playing robots developed for the RoboSprint 2015 national competition by the team from University of Central Punjab, Lahore, Pakistan. This competition was envisioned to be a stepping stone to encourage locally developed robots to take part in the international RoboCup matches. Some of the biggest challenges for competing in the international RoboCup was the necessary leap in design capability that was missing in most national competitions. Our main design criteria was to develop robots with good performance without the usual high costs associated with such designs. In this regard, we were able to design and build two robots that had about half the speed and acceleration for less than a quarter of the total cost of the typical designs employed by the leading teams in the RoboCup SSL (Small Size League). Another design choice normally not found in such robots is the implementation of an internal closed loop feedback control in addition to the external closed loop control incorporating the shared vision server and the team server. This internal feedback loop architecture was developed to reduce the responsibility on the team server, leaving it free to form strategy without having to be concerned with the micro-management of the two robots. Test measurements show that these performance goals are achieved with a low-costrobot.

Key Words: Omni Wheel Robot, Soccer Robot, RoboSprint.

1. INTRODUCTION

Robotics is gaining popularity among younger generation, which is quite evident by the tremendous increase in robotic competitions all over the world. Most of these challenges require indigenously developed robots that can perform a particular task in a very controlled environment [1]. Among these, one popular competition is where robots play in a field with a ball and score goals. There are different variants of this Robot Football. In some versions, humanoid robots are used to play against each other [2-3]. In other versions, groups are encouraged to develop their own wheeled robots and these robots play the game [4-5].

The RoboSprint was the most popular robot football competition in Pakistan. It was aimed to promote research in the field of autonomous robotics in Pakistan [6]. Therefore, the competition required teams to have their own indigenous robots to play the game. Its eventual aim was to evolve as a local version of the international SSL of the RoboCup competition. The main goal of the RoboCup is "By the middle of the 21st century, a team of fully autonomous humanoid robot soccer players shall win a soccer game, complying with the official rules of FIFA, against the winner of the most recent World Cup" [7]. The last RoboSprint was organized in 2015. The design presented in this paper participated in the 2015 competition and was later updated in anticipation of future events.

A high degree of mobility and controllability is required for wheeled robots to play a soccer game. In many cases it is not feasible that a wheeled robot may take full turn like a car when it is trying to fetch the ball. This will not only increase the turning radius but also cause un-necessary delay in picking the ball. Similarly, the design of the robot should be such that it may hold the ball when it is moving towards the goal. Eventually, when the robot reaches its target location, it may able to shoot the ball with some force so that it may go for a goal. These design, budget and performance constraints led to U-bot – an indigenous soccer robot. U-bot, Fig. 1, is a unique robot in its performance and design. Details of the robot and its capabilities are discussed in detail.

In this paper, we were able to design and build two robots that had about half the speed and acceleration for less than a quarter of the total cost of the typical designs employed by the leading teams in the RoboCup SSL. We also employed an internal closed loop feedback control in addition to the external closed loop control incorporating the shared vision server and the team server. This internal

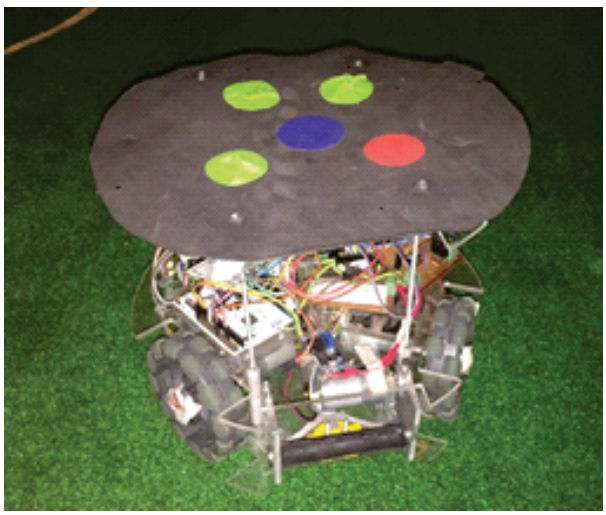

FIG. 1. ONE OF THE ASSEMBLED U-BOT ROBOTS WITHOUT ITS PROTECTIVE SIDEWALL

feedback loop architecture was developed to reduce the responsibility on the team server, leaving it free to form strategy without having to be concerned with the micro-management of the two robots.

The rest of the paper is organized as follows: Section-II, describes an overview of already existing robotic systems that play soccer. Section-III, focuses on design on U-bot. Section-IV describes and discusses performance of U-bot in actual testing. Section-V, concludes the paper and gives an outlook to the future work.

2. LITERATURE REVIEW

RoboCup soccer started in 1997 to foster research in robotics, AI (Artificial Intelligence), Computer Science and Engineering [8].

A very comprehensive view about RoboCup has been [9]. The authors described rules for SSL and team formation. It also described the playing area that is monitored by a roof mounted camera providing whole view of the field to the server. This information is communicated to the robots playing the game and can be used for developing strategies or to intercept the ball in the field.

A unique mechanism for dribbling the soccer ball for small size robot was developed by Ruizand Weitzenfeld [10]. Their catch and dribble strategy provided more control on the ball during movement of the robot. There is still room for improvement and further experiments to make the mechanism more effective.

A mechatronic design for small sized soccer robot has been presented in [11]. They have used omni-directional wheels to move the robot in the environment. These wheels gave advantage to move the robot in any direction without rotation of the robot itself. They have also developed a kicking mechanism alongside dribbling to pass ball or shoot it towards the goal.

The robot developed in [12], focuses on distributed control architecture and a mechanism for communication between robots in the team was developed. It also includes PI (Proportional Integral) controller to control speed of the robot when it is approaching the ball or another robot.

Recognizing team player in the field of SSL is a challenging task. Bruce and Veloso [13], a fast and accurate method based on vision has been described to detect pattern. This pattern can be placed on top of the robots and top mounted camera in SSL field will transmit the images to the server. From the images, the image processing algorithm can be used to identify exact location and orientation of the robot in the field.

A unique omni-directional navigation system, omni-vision system and omni-kick mechanism has been described in [14]. The robots developed in their paper are based on no-head direction (i.e. their direction of movement and the orientation on the field are independent of each other) and respond more quickly in the MSL (Medium Size League) arena. Their robots are capable of more sophisticated behaviors like ball passing or goal keeping.

The RoboSprint 2015 rules were published to enable potential participants to build their system according to common specifications. These rules dictated that each team have two robots in the field. Fig. 2 shows both teams would get access to the locations of the robots and the ball on the field from RoboCup SSLs shared vision system. The rules also specified the dimensions and weights of the robot [15].

Four team description papers [16-19], provide a basis of components and techniques used by some of the leading teams in the SSL competition.

3. ROBOT DESIGN

System Overview: Fig. 3 shows the block diagram of the developed robots. Each robot has three brushed DC motors with gear boxes driving omni wheels. The motors also have integrated quadrature encoders that allow direct measurement of wheel velocities and displacements.

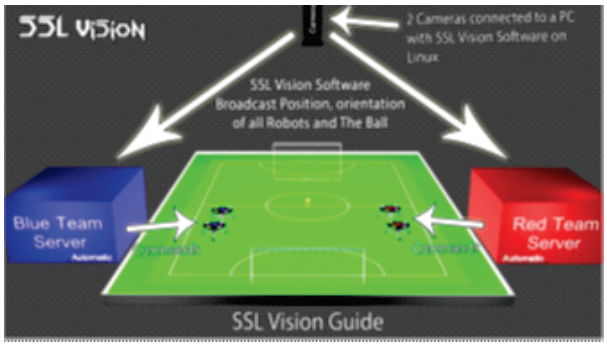

FIG. 2. OVERVIEW OF THE SHARED VISION SYSTEM USED BY THE ROBOCUP SMALL SIZE LEAGUE [15]

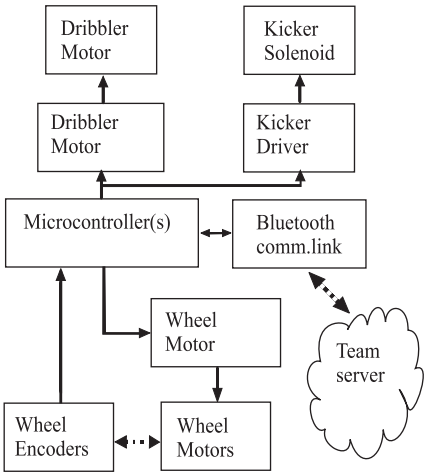

FIG. 3. ROBOT BLOCK DIAGRAM

The kicking mechanism uses a solenoid with a 25 mm travel pusher. The kicker driver allows control of the actuation power applied to the solenoid, which in turn controls the amount of force exerted on the ball.

A Bluetooth transceiver is used to provide a bidirectional link to the team server. This link is used to both receive commands as well as to send the robot's telemetry and status report back to the team server. The link can also be used to tune the gains of the PID (Proportional Integral Derivate) controllers using serial commands and getting the results of the step commands to the system.

Mechanical Layout and Corresponding Orientation Transforms: The developed robot uses three omni wheels arranged 120° apart in a circular pattern as shown in Fig. 4. The front of the robot also houses the ball handling mechanism which comprises of a dribbler and a flat kicker (indicated in Fig. 4 with a hashed rectangle).

With the used omni wheel arrangement, the transform matrices for converting between the robot frame velocities (v_f, v_n and ω_r) and the wheel velocities (v_1, v_2 and v_3) are given by Equations (1-2). These Equations (1-2) allow us to compute the lateral velocities from the measured wheel velocities as well as to compute desired wheel velocities for a known set of translational velocities.

$$\begin{bmatrix} v_f \\ v_n \\ \omega_r \end{bmatrix} = \begin{bmatrix} \sqrt{\frac{3}{3}} & -\sqrt{\frac{3}{3}} & 0 \\ \frac{1}{3} & \frac{1}{3} & -\frac{2}{3} \\ \frac{1}{3R} & \frac{1}{3R} & \frac{1}{3R} \end{bmatrix} \begin{bmatrix} v_1 \\ v_2 \\ v_3 \end{bmatrix} \quad (1)$$

$$\begin{bmatrix} v_1 \\ v_2 \\ v_3 \end{bmatrix} = \begin{bmatrix} \sqrt{\frac{3}{2}} & \frac{1}{2} & R \\ -\sqrt{\frac{3}{2}} & \frac{1}{2} & R \\ 0 & -1 & R \end{bmatrix} \begin{bmatrix} v_f \\ v_n \\ \omega_r \end{bmatrix} \quad (2)$$

where v_1, v_2 and v_3 correspond to the velocities of the three wheels, v_f is the forward velocity of the robot, v_n is the lateral velocity of the robot and ω_r is the rotational velocity of the robot frame and R is the distance from the centre of the robot to the wheels.

Similarly, transform matrices are required for converting between the absolute frame of reference (i.e. the match area) and robot frame of reference (i.e. robot chassis). Fig. 5 shows a robot at an angle θ_r to the x axis and with its center at coordinates x_r and y_r. Equations (3-4) provide the relationship for converting between the world frame coordinates and velocities and the robot frame velocities.

$$\begin{bmatrix} v_x \\ v_y \\ \omega_w \end{bmatrix} = \begin{bmatrix} \cos\theta_r & -\sin\theta_r & 0 \\ \sin\theta_r & \cos\theta_r & 0 \\ 0 & 0 & 1 \end{bmatrix} \begin{bmatrix} v_f \\ v_n \\ \omega_r \end{bmatrix} \quad (3)$$

$$\begin{bmatrix} v_f \\ v_n \\ \omega_r \end{bmatrix} = \begin{bmatrix} \cos\theta_r & \sin\theta_r & 0 \\ -\sin\theta_r & \cos\theta_r & 0 \\ 0 & 0 & 1 \end{bmatrix} \begin{bmatrix} v_x \\ v_y \\ \omega_w \end{bmatrix} \quad (4)$$

where v_x and v_y are the components of the robot velocity along the x and y axis of the absolute frame, ω_w correspond to the rotational velocity of the robot in the context of the world frame, x_r and y_r are the coordinates of the location of the robot on the absolute frame and θ_r is angle of the robot chases to the absolute frame.

Position Determination: SSL Vision and Deadreckoning: The SSL vision system calculates the position of all the robots and the ball on the field with an error of less than 5mm. Special markers placed on top the robots allows the system to identify the different robots on the field and their orientations. These are then passed to both the team servers using UDP (User Datagram Protocol) multicast packets. In our testing in the lab, it is

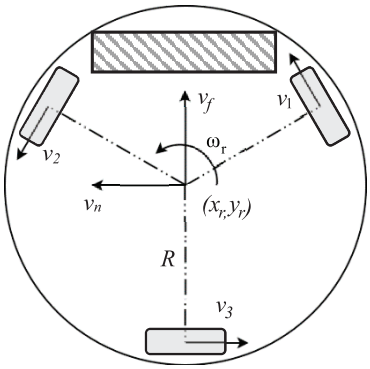

FIG. 4. LAYOUT OF THE ROBOT PLATFORM, THE VELOCITY VECTORS FOR THE THREE WHEELS AND THE ROBOT FRAME VELOCITIES

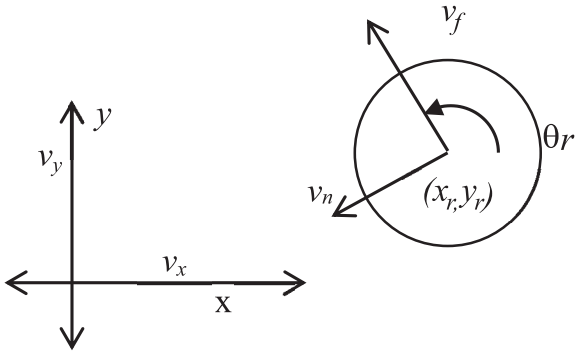

FIG. 5. ABSOLUTEFRAME AND ROBOT FRAME VELOCITIES

observed that due to some combination of the specified low-cost cameras and various other factors that we were unable to determine conclusively, there is a delay of up to 1s in positions received from the server and the actual positions on the field.

The world frame velocities can also be calculated from measured wheel velocities using Equations (1-2). These world frame velocities can then be used to calculate the change in the position and orientation of the robot on the playing field independently of the shared vision system. This approach provides a rapidly updated output. However, due to limitations of the sensors, gearbox backlash and slight wheel slip during hard accelerations, the error in the calculated position tends to compound quickly (an error of up to 100 mm can be reached within 10 seconds if aggressive maneuvering is being performed).

In order to fuse the position data from the two sources, a new algorithm has been devised and implemented. It overcomes the latency of the precise location and the poor accuracy of the responsive mechanism by maintaining a log of all the computed positions for the last 1 second. When an updated precise position is received, it calculates the correction factor for that moment in time (using past values) and applies it to all reading from that time forward. This technique offers much better performance than what is possible by either of the techniques acting alone.

Control Hierarchy: The overall control system comprises of a total of six PID controllers shown in Fig. 6. The velocity of each wheel is controlled with a PID controller. The output of the controller is used to control the direction and speed of each wheel. For the feedback of wheel speed, the angular displacement and speed of each wheel is calculated from the input of the corresponding wheel encoder. The gains of these controllers are set using online tuning through the use of Bluetooth telemetry. This online tuning mode makes it possible to change controller gains and then command step responses without having to recompile and reprogram the controller.

The reference inputs for the lower level wheel speed controllers are obtained from three higher level controllers, each of which is responsible for one of the three parameters (i.e. the position in x and y coordinates and the orientation angle). The outputs of these position controllers are then transformed to desired robot wheel velocities. The feedback for the position controller is taken from the position fusion algorithm described above.

Telemetry: Command and Status Packets: The robot expects a fixed length command packet from the team server. The minimum time between two commands is limited by only the transmission limit of the Bluetooth communication channel. In practice, team server could send as many as 60 commands per second. In the absence of a new command, the robot completes the execution of the last command and then holds the last commanded position. Any new command received before the completion of the previous command result in the command being performed being overwritten. This is intentional as the situation can be rapidly evolving during a match and might require a change in the game plan where completing the previous commands might no longer be beneficial.

Table 1 show the format of the command packets. There were three major parts of the packet. The first part is reserved for the commanded position and orientation. The second part is reserved for actual position and

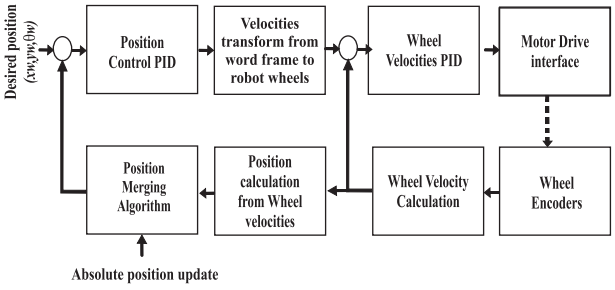

FIG. 6. COMPLETE CONTROL LOOP

TABLE 1. FORMAT OF THE COMMAND PACKETS RECEIVED FROM TEAM SERVER

Bytes	Contents	Description of Contents
1	'$'	Header
5	x	Commanded position and orientation in mm and degrees (with sign)
5	y	
4	θ	
5	x	Observed position and orientation from the vision system in mm and degrees. *t* is the age of position in this segment represented in ms.
5	y	
4	θ	
3	t	
3	Commands, force and speed	Kicker force, kicker commands and dribbler speed command
1	Status	Packet status (indicates which fields are valid)
1	';'	Terminator

orientation received from the shared vision system and also includes an age of the information based on the timestamps on the UDP packets. The third part is reserved for the ball handling commands and covers the kick strategy, kick force as well as the speed for the ball dribbler. Finally, the status indicates which of these three fields contain valid data. It is possible to send out commands where only one, two or all three fields contain valid data.

Table 2 shows the format of the status packets sent to the team server. Like the command packets above, these also had three fields. These are used to report back the last valid command received, the internally calculated position and to acknowledge the commands to the ball included consisted of the feedback from the ball detection sensor. There is no packet status as all fields always contained valid information regardless of the configuration of the last received command. The robot sends status packets every 20 milliseconds.

Overall System Integration: The overall system integration is achieved by implementing cooperative tasks and by using a cooperative time triggered task scheduler. Fig. 7 shows the complete data flow diagram of the robot. Following is a brief description of the various processes or tasks.

The Wheel Speed Measurement task periodically calculates the individual wheel speeds from the wheel encoders. These wheel speeds are then used by the Position Dead reckoning task to get the responsive but error prone position and orientation of the robot. This data along with the desired wheel speed data is also used by the

TABLE 2. FORMAT OF THE STATUS PACKETS SENT TO TEAM SERVER

Bytes	Contents	Description of Contents
1	'#'	Header
5	x	Last commanded position and orientation in mm and degrees (with sign)
5	y	
4	θ	
5	x	Current internally calculated position and orientation from the vision system in mm and degrees.
5	y	
4	θ	
3	Commands, force, speed and possession	Last commanded kicker force, kicker commands and dribbler speed command
1	';'	Terminator

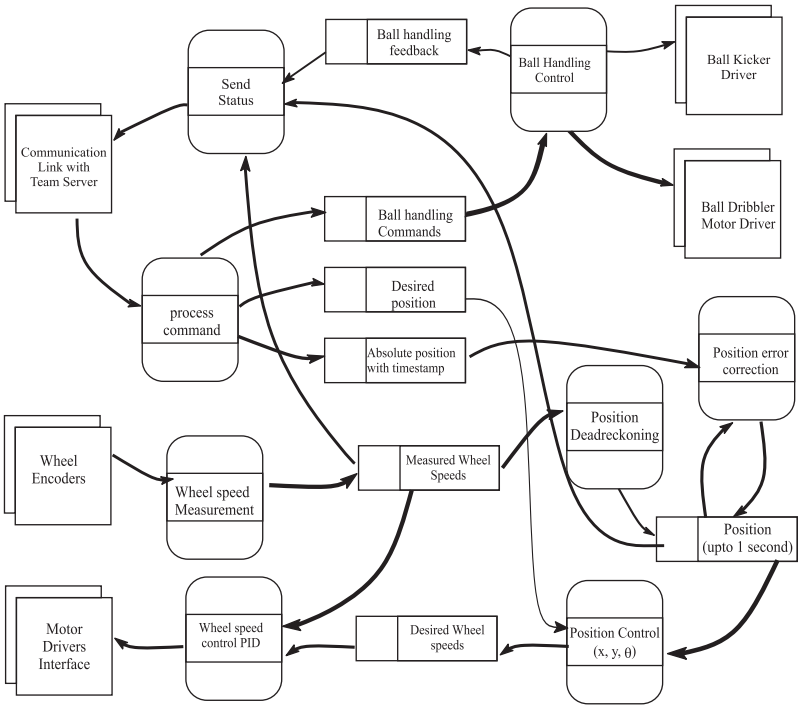

FIG 7 . DATA FLOW DIAGRAM FOR THE ROBOT

Wheel Speed Control PID task to control the power to the wheel motors.

The Process Command task gets data received from the team server and stores it into variables used by the ball handling control task, position error correction task and the position control task. The Send Status task sends the feedback from the ball handling control, as well as the internally measured wheel speeds and calculated position of the robot back to the team server.

The Position Error Correction task uses implements the position fusion algorithm described in the Position Determination subsection. The fused position information is used by the Position Control task to figure out the desired wheel speeds to bring the robot into the desired position and orientation received from the team server.

The Ball Handling Control task is responsible for executing the relevant commands received from the team server. This could be to capture the ball by inducing a backspin using the dribbler. The amount of backspin is controlled via commands. Similarly, the force with which to kick the ball as well as the moment to kick is also controlled via commands.

The main control loop repeats every 20 milliseconds. This time period was selected based on the responsiveness of the open loop system. The total CPU utilization when running at 72MHz is under 20%. The tasks are staggered so as not to overload any time tick of the cooperative scheduler. An added benefit of the staggering is that the task launch jitter in all the tasks used for sampling data and for updating the outputs is minimized. The sequence of tasks in the control loop is as follows:

(1) Wheel Speed Measurement

(2) Position Deadreckoning

(3) Process Command

(4) Position Error Correction

(5) Position Control

(6) Wheel Speed Control

(7) Ball Handling Control

(8) Send Status

Robot Hardware Cost Comparison: One of the stated goals of the project was to develop the robots at a significantly lower cost than those used by the major teams in RoboCup. The design utilized by a lot of the teams (e.g. SKUBA, CMDragons, etc.)used either four 30 Watt Maxon flat brushless DC motors to drive the four wheels through custom built gear boxes or larger 50 Watt motors in a direct drive configuration [16-19]. These translate to around US$150for the motor, gear box and encoder per wheel, thus, a total of US$600 for only drive mechanism of a single robot. By contrast, our design uses a total of three geared permanent magnet brushed DC motors with built in encoders costing US$40 or US$120 in total for one robot. Similarly, the elimination of chip kicker from the usual designs also helped to reduce the cost of the ball handling mechanism. The downside is that our design is too big to enter RoboCup SSL matches but is sufficient for the requirements for the RoboSprint competition. The other tradeoff is the performance, where our robot has about two thirds of the top speed and half of the acceleration in some of the top teams of the time [16-18].The developed robots can be seen in action during a tournament match in Fig. 8.

4. PERFORMANCE

The dynamic performance of the robots on the field was measured by using the SSL vision system. The lag of the vision system was then compensated for during the processing of test data. To access the performance of the developed robots, short and long displacement move commands were given to the robot. For each type of command, the robot was put in at starting point and was ordered to move a predetermined distance at orientation angles of 0, 45, 90 and 180^{o} for the robot with regards to the direction of commanded motion. The time taken by the robot to move to withing 50mm of the destination was measured. The maximum time taken to reach the destination over twenty tries was noted.

For multiple small move commands of 0.5m displacement in any direction while keeping the orientation (i.e. θ_r) constant, the robot reached 50mm of the destination within 1.7s, with error in the angle under $\pm 3^{o}$.

For multiple larger move commands specifying a destination with a displacement of 4m from the starting point in any direction while keeping the orientation constant, the robot reached 50mm of the destination within 4.2s, with error in the angle under $\pm 5^{o}$.

It should be noted that a wait of an additional 1s allowed the robot to reorient and reposition more correctly by utilizing the accurate position information from the SSL vision system. This reorientation was not dependent on any additional commands from the team server but relied on continuous position updates from the vision system.

The enhanced electronic drive for flat kicker was able to kick the ball with a speed of 2.8m/s. This was a significant improvement over the initial system that was employed in RoboSprint 2015 as it was only able to manage 1.4 m/s.

FIG. 8. YELLOW TEAM COMPOSED OF TWO U-BOTS (LEFT HALF OF THE PICTURE) DURING A MATCH IN ROBOSPRINT 2015

5. CONCLUSION

This paper presents a detailed design of a small size robot used in a RoboCup style competition in Pakistan called RoboSprint. The design philosophy as well as the "Design and Development of an Omni Wheel Soccer Robot"robots developed due to it are presented along the real-time measurements in the playing field. These measurements show the successful working of the developed design. The total cost for each of the developed robot is less than the quarter of the cost of drive mechanism in some of the leading team robots in the RoboCup SSL.

6. FUTURE WORK

For future work, the ball handling mechanism will be enhanced by developing a chip kicker in addition to the existing flat kicker. Moreover, an onboard computer vision system will be added to enhance and extend the systems capability in close quarters situations during a match. Finally, torque control instead of speed control for the wheel motors should be implemented.

ACKNOWLEDGEMENT

Authors would like to thank the Faculty of Engineering, and Faculty of Information Technology, University of Central Punjab, Lahore, Pakistan, for their support, feedback and suggestions.

REFERENCES

[1] Mitchell, O., "What Has Twenty Years Of RoboCup Taught Us?," Robot Rabbi, 21 May 2017. [Online]. Available: https://robotrabbi.com/2017/05/21/robocup/. [Accessed 23 October 2018].

[2] RoboCup.org, "RoboCupSoccer - Humanoid," [Online]. Available: https://www.robocup.org/leagues/3. [Accessed 25November 2019].

[3] RoboCup.org, "RoboCupSoccer - Standard Platform," [Online]. Available: https://www.robocup.org/leagues/5. [Accessed 25 November 2019].

[4] RoboCup.org, "RoboCupSoccer - Small Size," [Online]. Available: https://www.robocup.org/leagues/7. [Accessed 25 November 2019].

[5] RoboCup.org, "RoboCupSoccer - Middle Size," [Online]. Available: https://www.robocup.org/leagues/6. [Accessed 25 November 2019].

[6] Aftab, H., "CASE Robosprint: Fostering Love for Robotics and Technology," Pro Pakistani, 26 March 2015. [Online]. Available: https://propakistani.pk/2015/03/26/case-robosprint-fostering-love-for-robotics-and-technology/. [Accessed 23 October 2018].

[7] RoboCup.org, "Objective - RoboCup.org," [Online]. Available: https://www.robocup.org/objective. [Accessed 23 October 2018].

[8] Veloso, M., and Stone, P., "Video: RoboCup Robot Soccer History 1997 – 2011",IEEE/RSJ International Conference on Intelligent Robots and Systems, Vilamoura, Portugal, 2012.

[9] Weitzenfeld, A., Biswas, J.,Akar, M., and Sukvichai, K., "RoboCup Small-Size League: Past, Present and Future",RoboCup 2014: Robot World Cup XVIII, Springer, 2015.

[10] Ruiz, M.S., and Weitzenfeld, A., "Soccer Dribbler Design for the Eagle Knights RoboCup Small Size Robot",IEEE 3rd Latin American Robotics Symposium, Santiago, Chile, 2006.

[11] Witte, J.D., "Mechatronic Design of a Soccer Robot for the Small-Size League of RoboCup", Vrije Universiteit Brussel, Brussel, 2010.

[12] Smit,A., "Development of a Robot for RoboCup Small Size League, Utilizing a Distributed Control Architecture for a Multi-Robot System Development Platform", Stellenbosch University, Stellenbosch, South Africa, 2011.

[13] Bruce, J., and Veloso, M., "Fast and Accurate Vision-Based Pattern Detection and Identification", IEEE International Conference on Robotics and Automation, Taipei, Taiwan, 2003.

[14] Samani, H.A., Abdollahi, A., Ostadi, H., and Rad, S.Z., "Design and Development of a Comprehensive Omni directional Soccer Player Robot",International Journal of Advanced Robotic Systems, Volume 1, No. 3, pp. 191-200, 2004.

[15] CASE and PAF-KIET, "Robo Sprint 2015 Rulebook," CASE and PAF-KIET, 2015. [Online]. Available: https://www.scribd.com/document/346184177/Robo-Sprint-2015-Rulebook. [Accessed 23 October 2018].

[16] Panyapiang, T., Chaiso, K., Sukvichai, K., and Lertariyasakchai, P., "Skuba 2013 Team Description", RoboCup SSL Team Description 2013, Available: https://ssl.robocup.org/wp-content/uploads/2019/01 /2013_TDP_Skuba.pdf [Accessed 25 November 2019]

[17] Biswas, J., Mendoza, J.P., Zhu, D., Etling, P.A., Klee, S., Choi, B., Licitra, M., and Veloso, M., "CMDragons 2013 Team Description", RoboCup SSL Team Description 2013, Available: https://ssl.robocup.org/wp-content/uploads/2019/01/2013_TDP_CMDragons.pdf [Accessed 25 November 2019]

[18] Almagro, J., Avidano, C., Lindbeck, C., Neiger, J., Olkin, Z., Peterson, E., Stachowicz, K., Stuckey, W., White, M., Woodward, M., and Burdel, G.P., "RoboJackets 2019 Team Description Paper", RoboCup SSL Team Description, Available: https://ssl.robocup.org/ wp-content/uploads/2019/03/2019_ TDP_RoboJackets.pdf [Accessed 5 February 2020]

[19] Ito, M., Suzuki, R., Isokawa, S., Du, J., Suzuki, R., Nakayama, M., Ando, Y., Umeda, Y., Ono, Y., Kashiwamori, F., Kishi, F., Ban, K., Yamada, T., Adachi, Y., and Naruse. T., "RoboDragons 2019 Extended Team Description", RoboCup SSL Team Description", 2019, Available: https://ssl.robocup.org/wp-content/uploads/ 2019/03/2019_ETDP_RoboDragons.pdf [Accessed 5 February 2020]

Designing and Analyzing a Planer Butler Matrix for Phased Array Antenna for Future 5G Applications

Irshad Ullah*, Muhammad Irfan Khattak*, and Muhammad Farooq**

*Department of Electrical Engineering, University of Engineering & Technology, Peshawar, Kohat Campus, Pakistan.

**Department of Electrical Engineering, University of Engineering & Technology, Peshawar, Pakistan.
irshadullah@uetpeshawar.edu.pk, M.I.Khattak@uetpeshawar.edu.pk, farooq3956@gmail.com

ABSTRACT

Future 5G (Fifth Generation) wireless communication claims for many fold increase in data rates, quality of service and connectivity. This gaga bits per second data rate is made possible by steerable antennas and mm-wave spectrum. This paper presents a design consists of 4-elements linear phased array feed by 4x4 Butler matrix for future 5G wireless communication networks. However, the Building block of Butler matrix are hybrid couple, crossover, and phase shifter. Both the Butler matrix and micro strip antenna array are designed on a single layer Roger RT5880 substrate having dielectric constant is 2.2 (r=2.2) and thickness 0.254mm. The dimensions of Butler matrix, its components and micro strip antenna are designed and optimized in CST (Computer Simulated Technology) microwave studio. The area of Butler matrix is 30x17mm^2 and the overall area is. The reflection from each input port and its coupling with other input ports are investigated and they are below -10dB in the whole band. The S_{11} parameters of array shows a wide BW (Band Width) having frequency band from 26.3-29.55GHz. The insertion loss on average equal to 6.9dB. The radiation pattern for different input port excitation shows that beams are pointing at +10, -38, +38 and -10^o, from broad-side and their corresponding gains are 12, 10.4, 10.4 and 12dB respectively. The side lobe level are -11.5, -6.2, -6.3 and -11.6 while half power beam width are 29.2^o, 30.4^o, 30.2^o and 29.3^o respectively. Apart from this array pattern synthesis and analysis are discussed which conform simulated results.

Key Words: Fifth Generation, Hybrid Coupler, Crossover, Phase Shifter, Butler Matrix, Microstrip Antenna, Array Factor.

1. INTRODUCTION

Future 5G wireless communication will enhance data rates, QoS (Quality of Service) and connectivity. This amazing technology will support IoT (Internet of Things), IoV (Internet of Vehicle) and smart grid [1]. This gaga bits per second data rate is made possible by steerable antennas and mm-wave spectrum [2]. Apart from this, as the number of users increase, co-channel interference increases and hence degrade the QoS; which is also controlled by beam steerable antennas [3]. Beam steerable antenna is an antenna which transmit signal in desired direction and stop transmitting in undesired direction. Thus, a beam steerable antenna provide a significant improvement in system performance and system capacity [4-5]. This new technology will use the unused BW ranging from 3-300GHz [1]. There are different mm-wave bands proposed for 5G wireless network. The 28 and 38 GHz bands are completely discussed in [2]. In this paper building penetration, reflection, propagation, path loss, angle of arrival, angle of departure and RMS (Root Mean Square) delay spread both for rural and urban environment are analyzed and discussed. Furthermore a statistical model for urban environment is also developed.

There are different techniques used for beam steering like mechanical steering, integrated lens antennas, switched beam antennas, traveling wave antennas, reflect-array antennas, retro-directive antennas, beam-forming antennas and meta-material antennas [6]. But here in this work, analog multi-beam antenna which is a type of beam-forming antenna is used. The multi-beam antenna have many applications: in satellite communication, electronic counter measure, radar and cellular networks, for instance. The feed to multi-beam antenna comes from beam-former which is either network or lens. The lens may be Rotman Lens, Dome Lenses, Bootlace Lenses or some other lenses. While network may be Power Divider BFN, Blass and Nolen Matrices, Butler Matrix, the 2D (Two-Dimensional) BFN, or McFarland 2D Matrix [7]. In this work the Butler matrix was proposed because of its simple structure, low insertion loss, wider BW, orthogonal beam generation and easy realization [3,8].

Butler matrix is passive NxN beam forming network for uniform array, having N input ports and N output ports [9-10]. These N output ports have excitation signals that have same amplitude and progressive phase shift for each input port excitation [10-12]. These N output ports are connected with1xN linear array, which results in N orthogonal beams formation [12]. The Butler matrix along with array act as a reciprocal network that can be use either in a transmitter or in a receiver [12-13].

The Butler matrix for beam steering applications was investigated in literature [3-4,8,12,14-26]. In these designs the Butler matrix was designed for lower frequencies, mostly 2.4GHz, while [27-34] for higher frequencies. Apart from this, the technologies used for higher frequency bands are either SIW (Substrate Integrated Waveguide), multi-layer or semiconductors. Several research articles target 5G application [8,31-36]. But they are either on SIW technology or multi-layer technology. The author in [32] has used single layer micro-strip technology but has not discussed all the individual components and integration of Butler matrix

with antenna. In general, the microstrip planer single layer structure has is very attractive due to its numerous advantages like compact size, simple structure, low cost and easy fabrication.

In this work, the Butler matrix was designed on a single layer microstrip technology as shown in the Fig. 1, which consists of four Hybrid couplers, two crossovers and two 45 degree phase shifters [27]. The design uses 50Ω line width, which is too wide at the designed frequency, and will overlap [14,27]. Thus, a low dielectric constant thin material is used. Therefore, Rogers RT5880 has dielectric constant 2.2 and thickness 0.254mm is used for effective designing. The performance of the BM is totally dependent upon these components and any error occurred in one of these components will be repeated as many times as the component is repeated and hence, the final output will degrade seriously [25]. Thus, good performance components should be designed and optimized in CST before the actual designing of the butler matrix [14]. Finally, Butler matrix is designed by combining these components. This optimized Butler matrix has net- area equal to 30x17mm^2. A micro-strip inset feed antenna is developed and integrated with the Butler matrix. This will result in 30x25mm^2 overall area. All the results of the simulation show good agreement with theory.

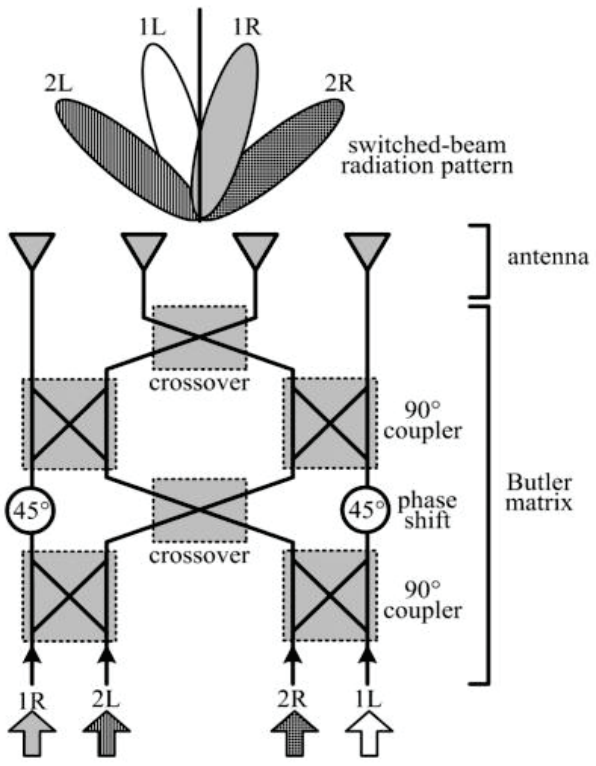

FIG. 1. BLOCK DIAGRAM OF BUTLER MATRIX

The work is organized as follows. In section-1 introduction is given. In section-2 the detail design of Butler matrix and its individual components are presented. In sections 3-5 the design of micro-strip antenna, array and array factor synthesis and analysis, designing and simulation results are discussed respectively. Finally, in section-6 concluded remarks are given.

2. DESIGNING OF BUTLER MATRIX AND ITS INDIVIDUAL COMPONENTS

In this section Butler matrix and its individual components designing is presented. For optimal Butler matrix the individual components are designed and optimized first. These components are then combined to make optimal Butler matrix. The individual components designing is discussed below.

2.1 Hybrid Coupler Designing

Hybrid coupler is a symmetric four port network. Any port can be taken as input port whose adjacent port will be isolated and it is opposite two ports will be consider as output ports. This can also be evident from the scattering matrix [37].

$$[s] = \frac{-1}{\sqrt{2}} \begin{bmatrix} 0 & j & 1 & 0 \\ j & 0 & 0 & 0 \\ 1 & 0 & 0 & j \\ 0 & 1 & j & 0 \end{bmatrix}$$

The Hybrid coupler is composed of two primary and two secondary transmission line, the secondary transmission line are connected in shunt and are quarter wavelength apart [23,28]. The impedance between two shunt lines is $Z_o/2$; where Z_o is the impedance of primary and secondary transmission lines [37].

This circuit was designed and optimized using CST microwave studio as shown in Fig. 2. The detail dimensions are given in Table 1.The magnitude and phases are plotted in Fig. 3(a-b) respectively. Reflection coefficient (S_{11}) and isolation level (S_{41}) both are below -20dB. The power is equally divide between port-2 and port-3 i.e. $S_{21}$is nearly equal toS_{31}. The insertion loss on average is 3.35dB. The phase difference between port-2 and port-3 is 89°.

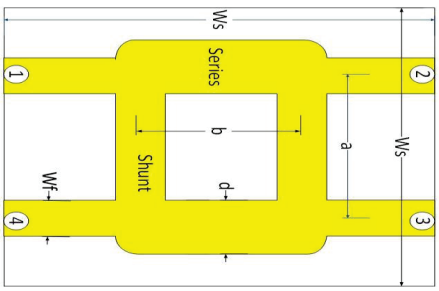

FIG. 2. HYBRID COUPLER FOR 5G APPLICATIONS

2.2 Crossover

Crossover is used for crossing two transmission lines and prevent coupling between them [15]. The optimal crossover designing is very challenging task in the designing of butler matrix [14]. It is a symmetrical network having two ports on either side [14]. Itis designed to pass the power to the port diagonally opposite to the input port [25]. Crossover is designed on micro-strip [38-41] and is used in many microwave circuits like butler matrix etc. In this paper a two section crossover is used as shown in Fig. 4(a). The ideal crossover is designed using Equations (1-2) [41].

$$Z_3 = \frac{50 \times Z_2}{Z_C^2} \quad (1)$$

$$Z_1 = \frac{Z_C^2}{50} \quad (2)$$

This crossover was designed in CST as shown in Fig. 4(b) and its dimensions are given in Table 2. The scattering parameters are shown in Fig. 5. Its isolation loss is below -25 dB while its insertion loss, return loss and S_{41} is 0.52, 26 and -17.8dB respectively.

TABLE 1. DESIGN DIMENSION OF HYBRID COUPLER

W_s	L_s	h_s	W_f	a	b	d
6	4	0.254	0.8	3	1.7	1.216

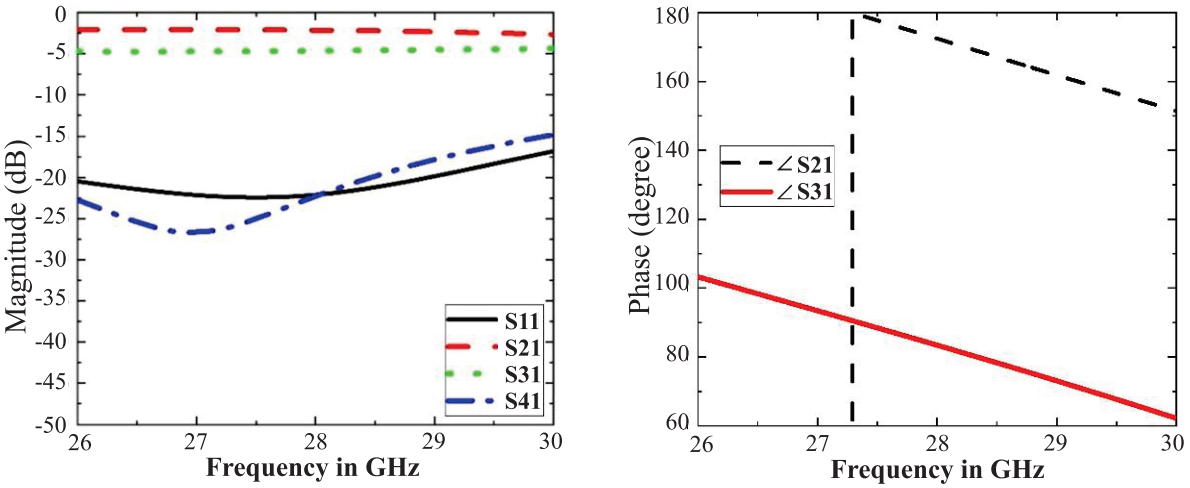

(a) MAGNITUDE PLOT (b) PHASE PLOT

FIG. 3. SIMULATED S-PARAMETERS OF HYBRIDCOUPLER FOR 5G APPLICATIONS

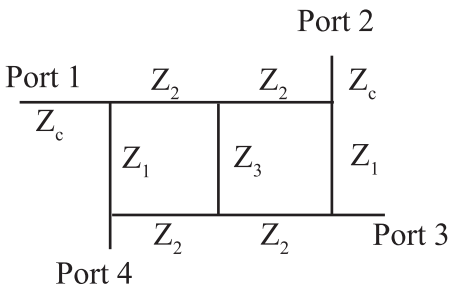

FIG. 4 (a). BLOCK DIAGRAM OF CROSSOVER

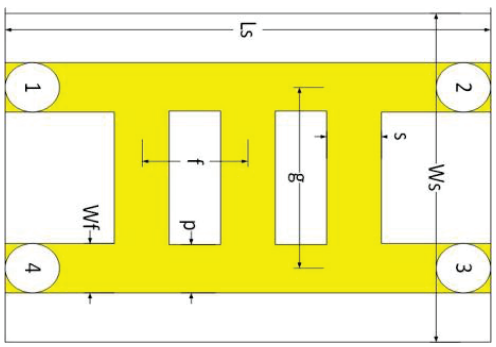

FIG. 4 (b). CROSSOVER FOR 5G APPLICATIONS

TABLE 2. DESIGN DIMENSION OF CROSSOVER FOR 5G PPLICATIONS

W_s	L_s	h_s	W_f	f	g	p	s
6.85	8	0.254	0.8	2	2.75	0.769	0.8

2.3 Phase Shifter

A transmission line delays signal and acts as a phase shifting network and the phase shift relation with length is given by Equation (3)

$$\varphi = \left(\frac{2\pi}{\lambda_g}\right)\Delta \qquad (3)$$

Where

$$\lambda_g = \frac{\lambda_o}{\sqrt{\epsilon_e}}$$

Where $_e$is effective dielectric constant.

The phase shifter is designed as shown in Fig. 6. The Δ_l between straight and u shaped part is equal to 45°.

2.4 Final Design

All the individual components that were designed and optimized are combined on a single layer Rogers RT5880 substrate to make Butler matrix. The final Butler matrix is shown in Fig. 7. The total area of the Butler matrix is 30x17mm^2. The simulated magnitude are shown in Fig. 8(a-d) for all input port excitation. The magnitude plot shows that the return losses i.e. S_{11}, S_{22}, S_{33}, and S_{44} are below -10dB in an entire bandwidth. The transmission coefficient on average is equal to 6.89 dB for port-1 and port-4 and 6.98 dB for port-2 and port-3, as shown in Table 3. The coupling with other input ports are below -10 dB in the whole range.

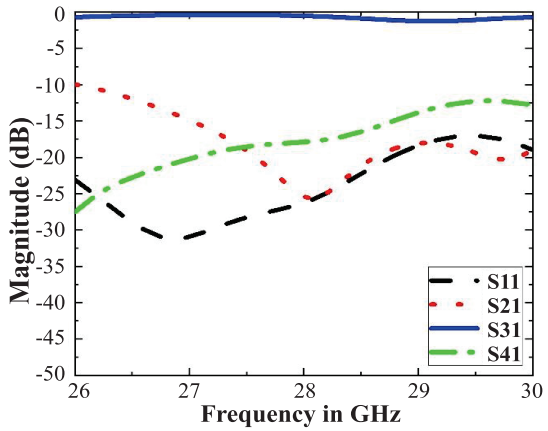

FIG. 5. SIMULATED S-PARAMETERS OF CROSSOVER FOR 5G APPLICATIONS

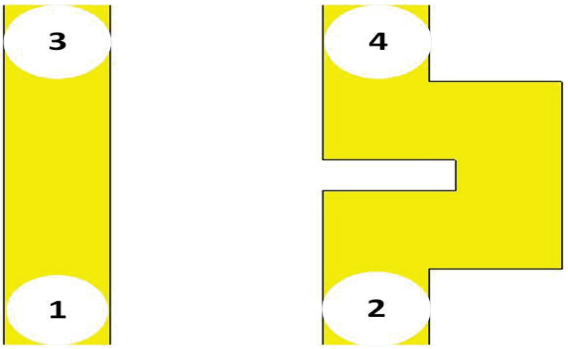

FIG. 6. PHASE SHIFTER FOR 5G APPLICATIONS

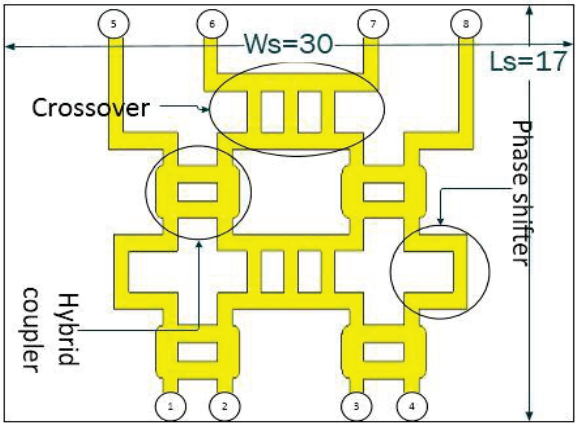

FIG. 7. BUTLER MATRIX FOR 5G APPLICATION

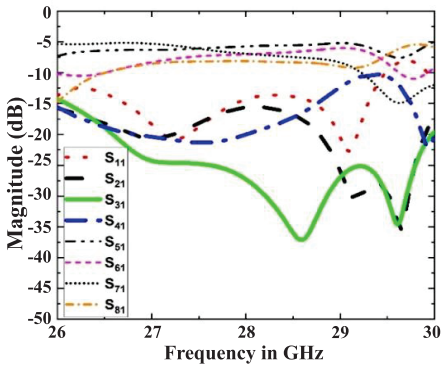

(a) MAGNITUDE PLOT WHEN PORT 1 IS EXITED

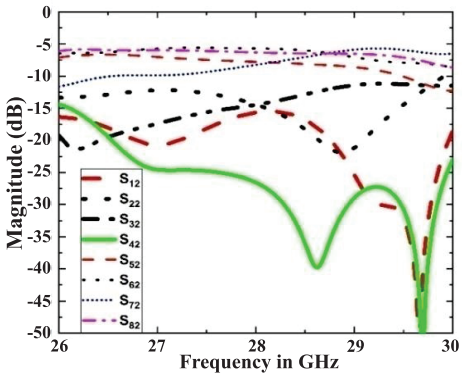

(b) MAGNITUDE PLOT WHEN PORT 2 IS EXITED

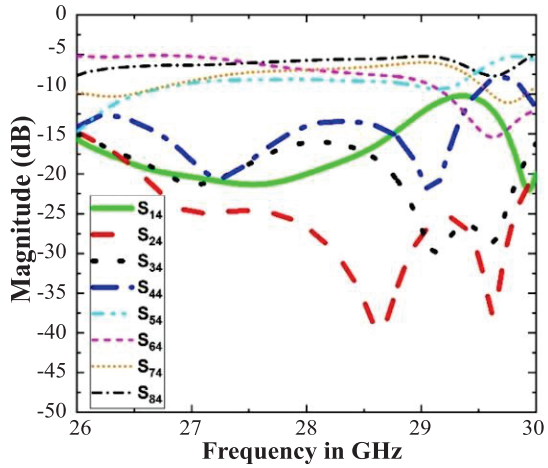

(c) MAGNITUDE PLOT WHEN PORT 3 IS EXITED

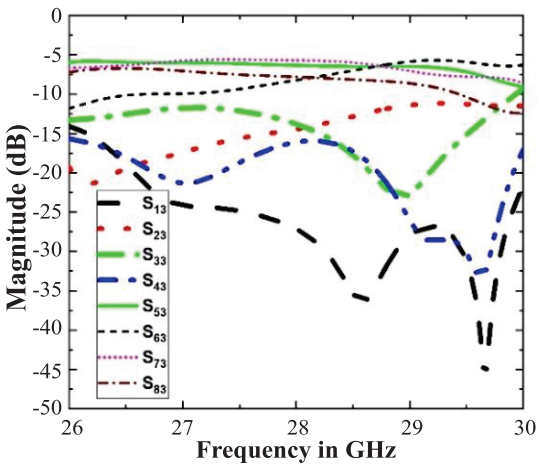

(d) MAGNITUDE PLOT WHEN PORT 4 IS EXITED

FIG. 8. SIMULATED S-PARAMETERS OF BUTLER MATRIX FOR 5G APPLICATIONS

TABLE 3. TRANSMISSION COEFFICIENT OF BUTLER MATRIX

Ports	Port-5	Port-6	Port-7	Port-8
Port-1	-5.54	-6.65	-7.44	-8.03
Port-2	-7.78	-6.89	-6.9	-5.70
Port-3	-6.32	-8.18	-5.69	-7.81
Port-4	-6.32	-8.18	-5.69	-7.81

The phase response is plotted in Fig. 9(a-d). The average progressive phase shift between output ports, i.e. S_{6i}, S_{5i} = - S_{6i} = S_{8i} - S_{7i}, for each input port i are 46.75, -134.3, 134.8 and 46.24 respectively. These phase differences are plotted in Fig. 10(a-d). The respective phases are shown in Table 4. A minute phase difference occur due to coupling with isolated ports and among different sections of butler matrix. The reflection from other ports, bends and junctions also degrade the performance. Furthermore, at higher frequencies there ismutual coupling between different sections of Butler matrix.

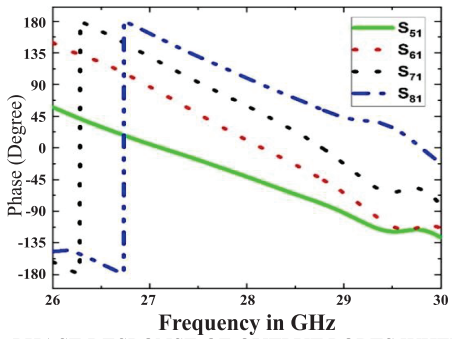

(a) PHASE RESPONSE OF OUTPUT PORTS WHEN PORT-1 IS EXCITED

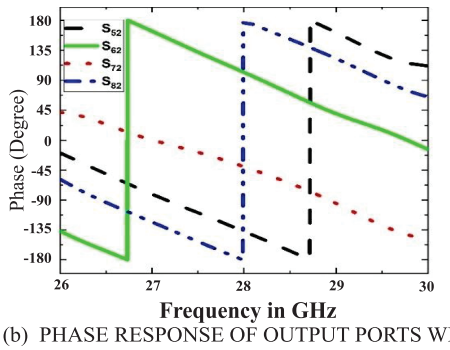

(b) PHASE RESPONSE OF OUTPUT PORTS WHEN PORT-2 IS EXCITED

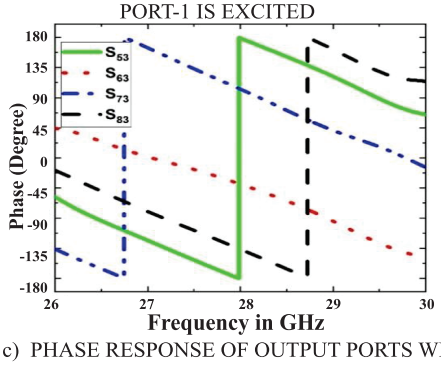

(c) PHASE RESPONSE OF OUTPUT PORTS WHEN PORT-3 IS EXCITED

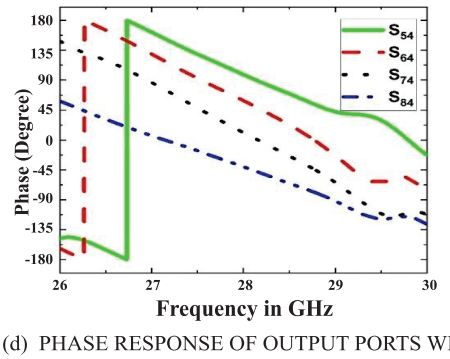

(d) PHASE RESPONSE OF OUTPUT PORTS WHEN PORT-4 IS EXCITED

FIG. 9. SIMULATED PHASE RESPONSE OF THE OUTPUT PORTS OF BUTLER MATRIX FOR 5G APPLICATION

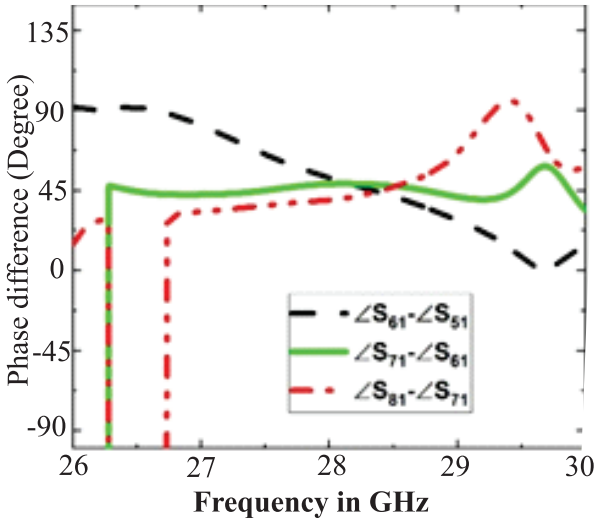

(a) PHASE DIFFERENCE BETWEEN OUTPUT PORTS WHEN PORT-1 IS EXCITED

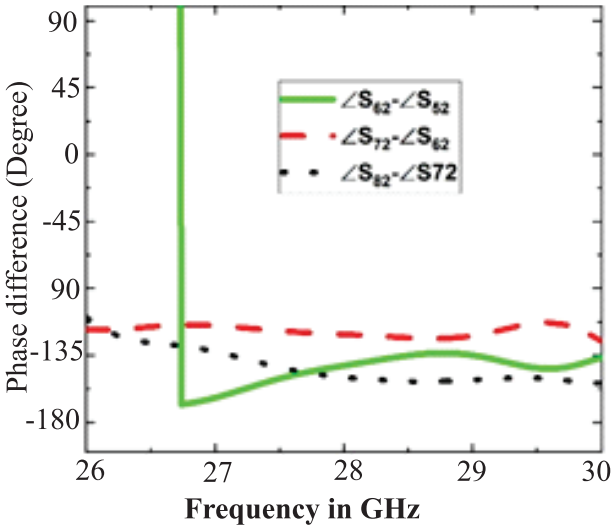

(b) PHASE DIFFERENCE BETWEEN OUTPUT PORTS WHEN PORT-2 IS EXCITED

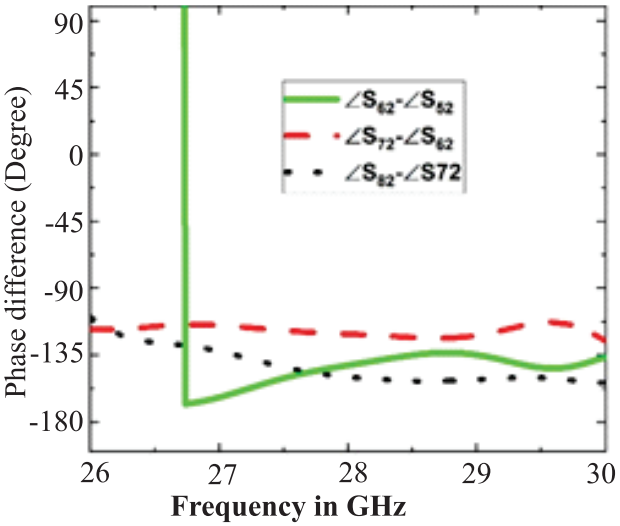

(c) PHASE DIFFERENCE BETWEEN OUTPUT PORTS WHEN PORT-3 IS EXCITED

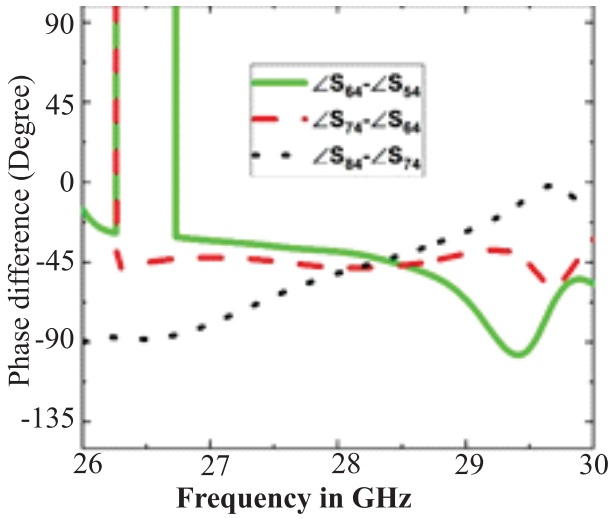

(d) PHASE DIFFERENCE BETWEEN OUTPUT PORTS WHEN PORT-4 IS EXCITED

FIG. 10. SIMULATED PHASE DIFFERENCE BETWEEN THE OUTPUT PORTS OF BUTLER MATRIX FOR 5G APPLICATIONS

TABLE 4. PHASE SHIFT BETWEEN ADJACENT PORTS FOR EACH INPUT PORT EXCITATION

Ports	Port-5	Port-6	Port-7	Port-8
Port-1	-64.95	-22.92	24.67	71.25
Port-2	-137.3	101.83	-40.04	179.25
Port-3	178.33	-39.97	101.88	-137.3
Port-4	98.31	59.05	10.89	-40.46

3. MICROSTRIP ANTENNA DESIGNING

The unit cell (microstrip patch antenna) of 1x4 phased array is shown in Fig. 11and its dimensions are shown in Table 5.Its return loss at 28GHz is -31dB and has a bandwidth of 833 MHz as shown in Fig. 12. The 3D radiation pattern is shown in Fig. 13. The peak gain at operating frequency is 7.47 dB, the HPBW is 79.3° and side lobe level is -17dB.

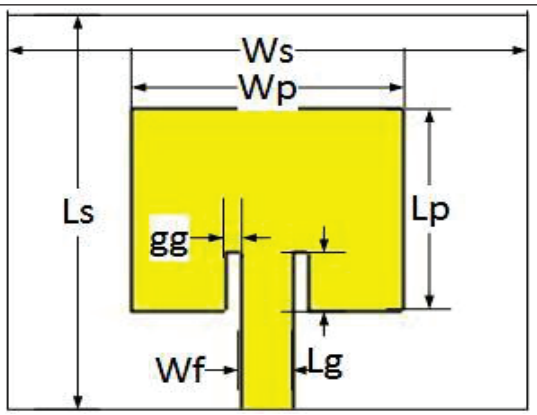

FIG. 11. DESIGN MICRO-STRIP ANTENNA

TABLE 5. DESIGN DIMENSION OF MICROSTRIP ANTENNA							
W_s	L_s	h_s	W_p	L_p	W_f	L_g	g_g
6.485	6.88786	0.254	4.2425	3.44393	0.8	1	0.25

4. ARRAY AND ARRAY FACTOR SYNTHESIS AND ANALYSIS

Let us consider four microstrip antennas placed along z-axis to make a linear array of four elements. The distance between two adjacent elements is d and p(x,y,z) is the point of observation of fields at distance r from the origin as shown in the Fig. 14. In order to avoid grating lobe in scanning array, the distance between antenna elements is taken $0.5\lambda_o$ [10,24].

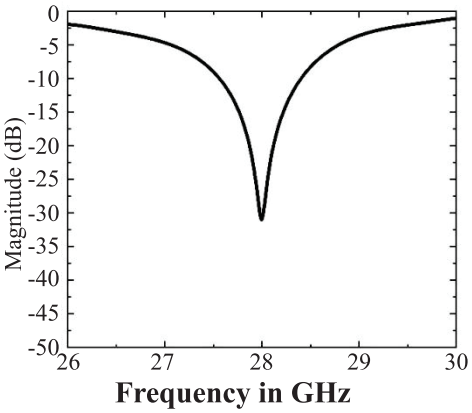

FIG. 12. S-PARAMETERS OF MICRO-STRIP ANTENNA

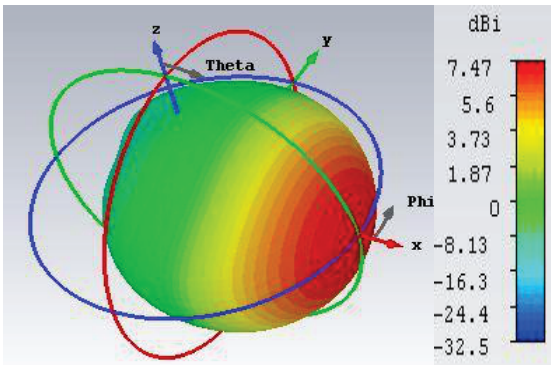

FIG. 13. 3D RADIATION PATTERN OF PATCH ANTENNA

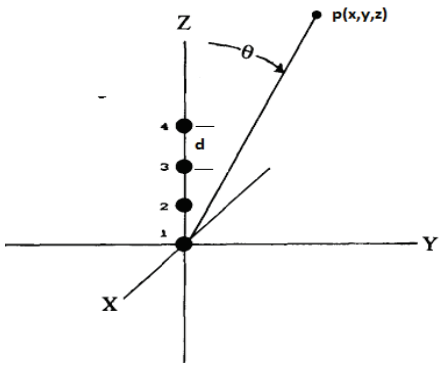

FIG. 14. GEOMETRY OF 4 ELEMENT LINEAR ARRAY PLACE ALONG Z-AXIS

4.1 Array Factor Synthesis and Analysis

The electric field for n^{th} element is given by Equation (4).

$$E_n(x,y,z) = \frac{e^{-jkr}}{r} A_{mn} I_{en} e^{j(n-1)[kd\cos\theta+\beta]} \quad (4)$$

Where k is wave number, d is the distance between adjacent element, (n-1)d is the distance of n^{th}element from the origin, A_{mn} is the behavior of individual microstrip antenna in term of orientation and polarization of electric fields, θ is the angle from source axes to field point position vector (as in spherical coordinate system), I_{en} is the excitation current amplitude of n^{th} element, (n-1) kd cosθ is the spatial phase shift and (n-1)β is the electrical phase shift to n^{th} element. Also note that β is the electrical phase shift between two adjacent elements and (n-1)[kd cos θ + β] is the total phase shift.

The field at point p is the superposition of all the fields radiated by all antenna elements is given by Equation (5).

$$E_n(x,y,z) = \sum_{n=1}^{4} E_n(x,y,z) \quad (5)$$

$$E_n(x,y,z) = \frac{e^{-jkr}}{r} A_m \sum_{n=1}^{4} I_{en} e^{j(n-1)[kd\cos\theta+\beta]}$$

$$E_n(x,y,z) = \frac{e^{-jkr}}{r} A_m \times AF$$

Where AF is called array factor which is given by Equation (6).

$$AF = \sum_{n=1}^{4} I_{en} e^{j(n-1)[kd\cos\theta+\beta]} \quad (6)$$

Let us consider all the elementshave excitation amplitude equal to 1 for the sake of easy visualization of the array pattern. The simplified array factor is given by Equation (7).

$$AF = \sum_{n=1}^{4} e^{j(n-1)[kd\cos\theta+\beta]} \quad (7)$$

To simplify the analysis of pattern, put Ψ=kd cos θ + β. Now the array factor will look like

$$AF = \sum_{n=1}^{4} e^{j(n-1)\psi}$$

Here inside the summation is complex exponential which will be maximum at ψ = 0. Let θ corresponding to maximum amplitude is θ_o which is calculated as follow:

$$kd\cos\theta_o + \beta = 0$$

$$\cos\theta_o = \frac{-\beta}{kd}$$

$$\theta_o = \cos^{-1}\left(\frac{-\beta}{kd}\right) \quad (8)$$

After simplification

$$\theta_o = \cos^{-1}\left(\frac{-\beta}{\pi}\right) \quad (9)$$

The Equation(8-9) gives the beam direction from z-axis. The beam direction is usually measured from broadside or from xy-plane which is given Equation (10).

$$\theta_o = \cos^{-1}\left(\frac{-\beta}{\pi}\right) - 90^o \quad (10)$$

The beam direction corresponding to Butler matrix progressive phase shift are calculated and given in Table 6

4.2 Half Power Beam Width

The half power beam width for scanning array is given by Equation (11) [42].

$$HPBW = \cos^{-1}\left(\cos\theta_o - \frac{2.782}{N\pi}\right) - \cos^{-1}\left(\cos\theta_o + \frac{2.782}{N\pi}\right) \quad (11)$$

The calculated beam width is given in Table 7. The error occurs because the Butler matrix does not provide uniform phase shift and the calculation involves approximation.

5. ARRAY DESIGNING AND SIMULATION RESULTS

The direction of main beam from z-axis for port-1 to port-4 excitation are 100, 52, 128 and 80° respectively as shown in Fig. 15(a), while the direction of main beam from broadside were 10, -38, 38 and -10° respectively as shown in Fig. 15(b), which are summarized and compared with calculation in Table 6. Half power beam width are 29.2, 30.4, 30.2 and 29.3° respectively, they are also summarized and compared with calculation in Table 7. The side lobe level were -11.5, -6.2, -6.3 and -11.6dB. The gains of this array are 12, 10.4, 10.4 and 12dBi respectively.

TABLE 6. COMPARISON BETWEEN SIMULATED AND CALCULATED BEAM STEERING ANGLE. C1: PORT NUMBER; C2: PROGRESSIVE PHASE SHIFT CORRESPONDING TO BM; C3: CALCULATED PHASE SCAN ANGLE FROM Z-AXIS; C3: CALCULATED PHASE SCAN ANGLE FROM BROADSIDE; C4: SIMULATED PHASE SCAN ANGLE FROM Z-AXIS C5: SIMULATED PHASE SCAN ANGLE FROM BROAD-SIDE

C1	C2	C3	C4	C5	C6
1	45.35	104	14	100	10
2	-134.5	41.63	-48.3	52	-38
3	134.77	138.48	48.48	128	38
4	-46.25	75	-15	80	-10

TABLE 1. COMPARISON BETWEEN SIMULATED AND CALCULATED HPBW. C1: PORT NUMBER; C2: PROGRESSIVE PHASE SHIFT CORRESPONDING TO BM; C3: CALCULATED PHASE SCAN ANGLE FROM Z-AXIS; C4: CALCULATED HPBW; C5: SIMULATED HPBW

C1	C2	C3	C4	C5
1	45.35	104	26.4	29
2	-134.53	41.63	43	30.4
3	134.77	138.48	44	30.5
4	-46.25	75	27	29.3

The antenna system has a wide bandwidth from 26.3-29.55GHz as shown in Fig. 16.

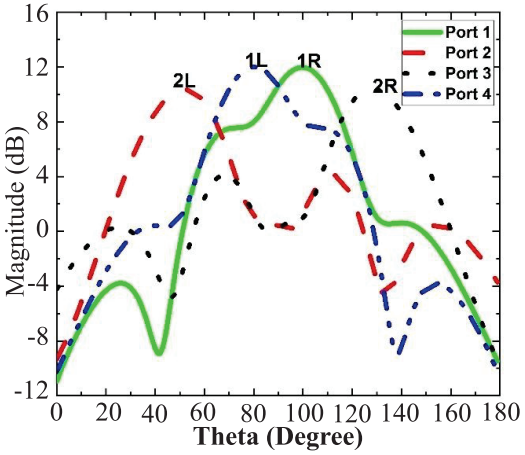

(a) THETA FROM Z-AXIS

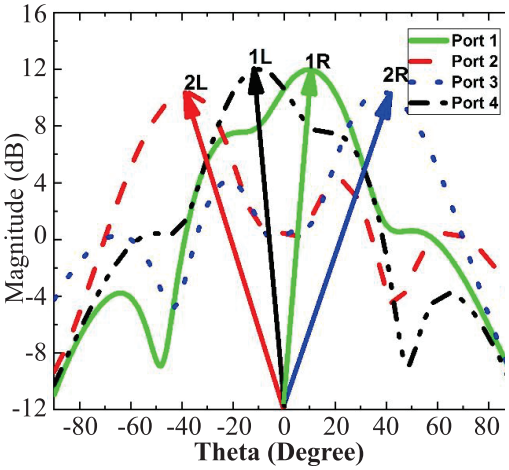

(b) THETA FROM BROADSIDE

FIG. 15. SIMULATED RADIATION PATTERN AT FOR DIFFERENT INPUT PORT EXCITATION

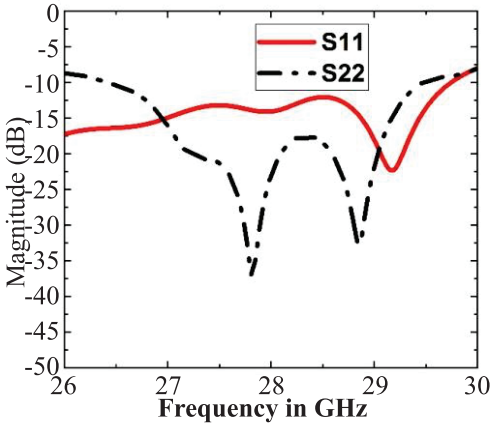

FIG. 16. S-PARAMETERS OF THE BEAM STEERING ANTENNA SYSTEM FOR 5

The 4 element linear array fed by 4x4 Butler matrix was designed in CST and all input ports were excited one by one as shown in Fig. 17. Here, in this designed both the array and Butler matrix are designed on the same substrate. The array elements are placed along z-axis above origin and keep the inter element spacing $0.5\lambda_o$. The total area of the Butler matrix is $30x25mm^2$. The detail parameters are given in Table 8.

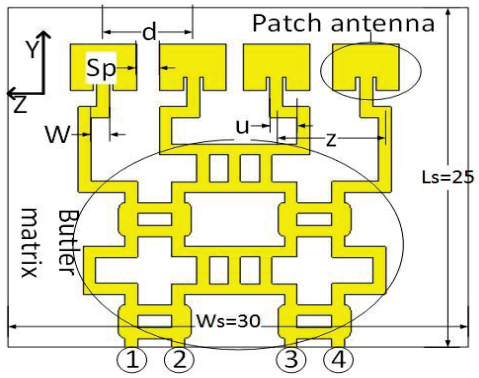

FIG. 17. 1X4 BEAM STEERING ARRAY SYSTEM FOR 5G APPLICATIONS

TABLE 8. PARAMETERS OF BEAM STEERABLE ANTENNA SYSTEM FOR 5G APPLICATIONS

u	d	z	w	Sp
1.32	5.357	5.75	0.39	1.1

6. CONCLUSION

In this paper, a 1x4 linear array of micro-strip antenna integrated with 4x4 Butler matrix is presented. Both the Butler matrix and micro-strip antenna are designed on a single layer Roger RT5880 substrate having $_r$ = 2.2 and thickness 0.254mm. This antenna cover 28GHz band for future 5G wireless communication networks. The beam is steered from broadside to +10 and +38 degrees. The gain for single element is 7.47dB while, for array the gain is 12, 10.4, 10.4 and 12dB for the respective input port. The half power beam width are 29.2°, 30.4°, 30.2° and 29.3° respectively. The side lobe level were -11.5, -6.2, -6.3 and -11.6 respectively.

ACKNOWLEDGEMENT

The authors are grateful to all the teachers, students, colleagues, and classmates for their help and encouragement. The authors also want to acknowledge the support of University Engineering &Technology, Peshawar, Pakistan, in higher study.

REFERENCES

[1] Agiwal, M., Roy, A., and Saxena, N., "Next Generation 5G Wireless Networks: A Comprehensive Survey", IEEE Communications Surveys & Tutorials, Volume 18, pp. 1617-1655, 2016.

[2] Rappaport, T.S., Sun, S., Mayzus, R., Zhao, H., Azar, Y., Wang, K., Wong, G.N., Schulz, J.K., Samimi, M., and Gutierrez, F., "Millimeter Wave Mobile Communications for 5G Cellular: It Will Work!", IEEE Access, Volume 1, pp. 335-349, 2013.

[3] Barro, O.A., and Himdi, M., "Single Layered 4x4 Butler Matrix Without Phase-Shifters and Crossovers", IEEE Accesss, Volume XX, Volume 6, pp77289-77298, 2018.

[4] Chen, Q., Lai, S., and Zheng, S., "Compact Butler Matrix Based on Patch Element for X-Band Applications", Asia-Pacific Microwave Conference, pp. 1-3, 2015.

[5] Wincza, K., Gruszczynski, S., and Sachse, K., "Reduced Sidelobe Four-Beam Antenna Array Fed by Modified Butler Matrix", Electronics Letters, Volume 42, pp. 508-509, 2006.

[6] Uchendu, I., and Kelly, J.R.,"Survey of Beam Steering Techniques Available for Millimeter Wave Applications", Progress in Electromagnetics Research, Volume 68, pp. 35-54, 2016.

[7] Hansen, R.C., "Phased Array Antennas", Volume 213, John Wiley & Sons, 2009.

[8] Chu, H.N., and Ma, T.-G., "An Extended $4\Times 4$ Butler Matrix with Enhanced Beam Controllability and Widened Spatial Coverage", IEEE Transactions on Microwave Theory and Techniques, Volume 66, pp. 1301-1311, 2017.

[9] Moody, H., "The Systematic Design of the Butler Matrix", IEEE Transactions on Antennas and Propagation, Volume 12, pp. 786-788, 1964.

[10] Ibrahim, S., Rahim, M., Masri, T., Karim, M., and Aziz, M.A., "Multibeam Antenna Array with Butler Matrix for WLAN Applications", 2nd European Conference on Antennas and Propagation, 2007.

[11] Dall'Omo, C., Monediere, T., Jecko, B., Lamour, F., Wolk, I., and Elkael, M., "Design and Realization of a 4x4 Microstrip Butler Matrix Without any Crossing in Millimeter Waves", Microwave and Optical Technology Letters, Volume 38, pp. 462-465, 2003.

[12] Traii, M., Nedil, M., Gharsallah, A., and Denidni, T.A., "A New Design of Compact: A New Design of Compact", International Journal of Microwave Science and Technology, 2008.

[13] Patterson, C.E., Khan, W.T., Ponchak, G.E., May, G.S., and Papapolymerou, J., "A 60-GHz Active Receiving Switched-Beam Antenna Array with Integrated Butler Matrix and GaAs Amplifiers", IEEE Transactions on Microwave Theory and Techniques, Volume 60, pp. 3599-3607, 2012.

[14] Errifi, H., Baghdad, A., Badri, A., and Sahel, A.,"Design and Simulation of a Plannar 4x4 Butler Matrix in Microstrip Technology for X-Band Application", Mediterranean Telecommunications Journal, Volume 7, No. 1, January, 2017.

[15] Madany, Y.M., Elkamchouchi, H.M., and Salama, A.A., "Design and Analysis of Miniaturized Smart Antenna System Using 1x8 Switched Butler Matrix", IFLA Newspaper Conference, April, 2012.

[16] Angelucci, A., Audagnotto, P., Corda, P., Obino, P., Piarulli, F., and Piovano, B., "High Performance Microstrip Networks for Multibeam and Reconfigurable Operation in Mobile-Radio Systems", IEEE GLOBECOM. Communications: The Global Bridge, pp. 1717-1721, 1994.

[17] Bona, M., Manholm, L., Starski, J., and Svensson, B., "Low-Loss Compact Butler Matrix for a Microstrip Antenna", IEEE Transactions on Microwave Theory and Techniques, Volume 50, pp. 2069-2075, 2002.

[18] Ahmad, S.R., and Seman, F.C.,"4-Port Butler Matrix for Switched Multibeam Antenna Array", Asia-Pacific Conference

on Applied Electromagnetics, pp. 5, 2005.

[19] El-Tager, A.,"Design and Implementation of a Smart Antenna Using Butler Matrix for ISM-Band", Progress in Electromagnetics Research Symposium, Beijing, China, March, 2009.

[20] Bhowmik, W., and Srivastava, S.,"Optimum Design of a 4x4 Planar Butler Matrix Array for WLAN Application", arXiv Preprint arXiv:1004.4821, 2010.

[21] Djerafi, T., Fonseca, N.J., and Wu, K.,"Design and Implementation of a Planar 4x4 Butler Matrix in SIW Technology for Wide Band High Power Applications", Progress in Electromagnetics Research, Volume 35, pp. 29-51, 2011.

[22] Gundpujari, S., and Annadate, S., "A Switched Multibeam Antenna Array using Butler Matrix Feed Network", International Journal of Application or Innovation in Engineering Management, 2013.

[23] Debbarma, K., Moyra, T., and Yadav, D., "Size Reduction of 4x4 Butler Matrix Using Defected Microstrip Structure", Emerging Trends in Computing and Communication, pp. 33-41, Springer, 2014.

[24] Bhowmik, P., and Moyra, T.,"Modelling and Validation of a Compact Planar Butler Matrix by Removing Crossover", Wireless Personal Communications, Volume 95, pp. 5121-5132, 2017.

[25] Rao, P.H., Sajin, J.S., and Kudesia, K., "Miniaturisation of Switched Beam Array Antenna Using Phase Delay Properties of CSRR-Loaded Transmission Line", IET Microwaves, Antennas & Propagation, Volume 12, pp. 1960-1966, 2018.

[26] Adamidis, G.A., Vardiambasis, I.O., Ioannidou, M.P., and Kapetanakis, T.N.,"Design and Implementation of Single-Layer 4x4 and 8x8 Butler Matrices for Multibeam Antenna Arrays", International Journal of Antennas and Propagation, 2019.

[27] Tseng, C.-H., Chen, C.-J., and Chu, T.-H., "A Low-Cost 60-GHz Switched-Beam Patch Antenna Array with Butler Matrix Network", IEEE Antennas and Wireless Propagation Letters, Volume 7, pp. 432-435, 2008.

[28] Murad, N., Lancaster, M., Wang, Y., and Ke, M., "Micromachined Millimeter-Wave Butler Matrix with a Patch Antenna Array", Mediterrannean Microwave Symposium, pp. 1-4, 2009.

[29] Chen, C.-J., and Chu, T.-H.,"Design of a 60-GHz Substrate Integrated Waveguide Butler Matrix - A Systematic approach", IEEE Transactions on Microwave Theory and Techniques, Volume 58, pp. 1724-1733, 2010.

[30] Zhang, J., and Vincent, F., "Design a V-Band 4x4 Butler Matrix for Switched Beam-Forming Operation", IET Seminar Active RF Devices, Belfast, UK, September, 2011.

[31] Djerafi, T. and Wu, K.,"A Low-Cost Wideband 77-GHz Planar Butler Matrix in SIW Technology", IEEE Transactions on Antennas and Propagation, Volume 60, pp. 4949-4954, 2012.

[32] Orakwue, S.I., Ngah, R., Rahman, T., and Al-Khafaji, H.M., "A 4x4 Butler Matrix for 28 GHz Switched Multi-Beam Antenna", International Journal of Engineering and Technology, Volume 7, 2015.

[33] Klionovski, K., Shamim, A., and Sharawi, M.S.,"5G Antenna Array with Wide-Angle Beam Steering and Dual Linear Polarizations", IEEE International Symposium on Antennas and Propagation & USNC/URSI National Radio Science Meeting, pp. 1469-1470, 2017.

[34] Klionovski, K., Sharawi, M.S., and Shamim, A., "A Dual-Polarization-Switched Beam Patch Antenna Array for Millimeter-Wave Applications", IEEE Transactions on Antennas and Propagation, Volume 67, pp. 3510-3515, 2019.

[35] Yang, Q.-L., Ban, Y.-L., Kang, K., and Wu, G.,"SIW Multibeam Array for 5G Mobile Devices", IEEE Access, Volume 4, pp. 2788-2796, 2016.

[36] Zhong, L.-H., Ban, Y.-L., Lian, J.-W., Yang, Q.-L., Guo, J., and Yu, Z.-F., "Miniaturized SIW Multibeam Antenna Array Fed by Dual-Layer 8x8 Butler Matrix", IEEE Antennas and Wireless Propagation Letters, Volume 16, pp. 3018-3021, 2017.

[37] Pozar, D.M., "Microwave Engineering", 3rd Edition, John Wiley&Sons, Inc, 2005.

[38] Abbasi, M.A.B., Antoniades, M.A., and Nikolaou, S., "A Compact Microstrip Crossover Using NRI□TL Metamaterial Lines", Microwave and Optical Technology Letters, Volume 60, pp. 2839-2843, 2018.

[39] Henin, B., and Abbosh, A., "Wideband Planar Microstrip Crossover with High Power Handling Capability and Low Distortion", Microwave and Optical Technology Letters, Volume 55, pp. 439-443, 2013.

[40] Lee, Z.-W., and Pang, Y.-H., "Compact Planar Dual-Band Crossover Using Two-Section Branch-Line Coupler", Electronics Letters, Volume 48, pp. 1348-1349, 2012.

[41] Yao, J., Lee, C., and Yeo, S.P.,"Microstrip Branch-Line Couplers for Crossover Applications", IEEE Transactions on Microwave Theory and Techniques", Volume 59, pp. 87-92, 2010.

42] Balanis, C.A., "Antenna Theory: Analysis and Design", John Wiley & Sons, 2016

Comparison of Least Mean Square Based Techniques for Spur Cancellation in Fractional N-Frequency Synthesizer

Muhammad Sarwar Ehsan*, Musharraf Ahmad Hanif*, and Maryam Javed*
* Department of Electrical Engineering, University of Central Punjab, Lahore, Pakistan.
sarwar.ehsan@ucp.edu.pk, musharraf.hanif@ucp.edu.pk, maryam.javed@ucp.edu.pk

ABSTRACT

Owing to scarcity of frequency spectrum, the frequency allocation must be provided more precisely. This can be achieved by use of the systems that can maintain precise frequency control. Fractional N-frequency synthesizer is a controllable system to generate the accurately defined signals at different frequencies. In this paper, we present the LMS (Least Mean Square) based adaptive filtering methodology for spur noise reduction in digital fractional N-frequency synthesizer and investigates the noise performance response of the system against different variants of LMS algorithm. In literature only LMS was implemented, we have not only implemented different variants of LMS but also compare their performance. A digital fractional N-frequency system have been implemented in MATLAB using SIMULINK tools and noise performance of system have been analyzed in terms of SNR (Signal to Noise Ratio), spur noise and jitter by applying basic LMS, normalized LMS algorithms in adaptive filter. On comparing the performance results, normalized LMS is found to be better and efficient algorithm as it improved the system SNR by 28.09 dBc and reduces the spur noise by 9.56 dBc along with 2.9 ps improvement in jitter.

Key Words: Least Mean Square, Frequency Synthesizer, Fractional N.

1. INTRODUCTION

As frequency spectrum is limited and the allocation must be provided more precisely which can be achieved by use of the systems that can maintain precise frequency control. Frequency synthesizer is a controllable system to generate the accurately defined signals at different frequencies. A module of delta sigma modulator is used in fractional N synthesizer to generate fractional frequencies, however, it also degrades the performance of synthesizer. In the past many techniques have been proposed to achieve better performance of analogue synthesizer.

Zhang et. al. [1] presented the design of wideband fractional N-frequency synthesizer. Their proposed model uses least mean square algorithm with DAC (Digital to Analog Converter) gain calibration technique for cancellation of quantization noise and reduction of spurs by delta sigma modulator. Spur limits the performance of phase noise in wide band PLL (Phase Locked Loop) and these induced spurs cannot be reduced through loop filter. This technique requires a very precise gain mismatching of the cancellation path. Mismatching error is detected at the output of loop filter and correlated with the accumulated quantization error. Least mean square algorithm can adaptively minimize the mismatches by adjusting DAC gain according to the output errors of loop filter. Effect of DC offset at the output of loop filter can be eliminated by using differential loop filter and integrator topologies. Gain mismatch path is calibrated outside the PLL loop to avoid the non-linearity being introduced in the system [2]. When the desired reference current is achieved the gain calibrated circuit is disabled.

Analog loop filter occupies large area and its reconfiguring is difficult. To overcome these drawbacks, Elkholy et. al. [3], proposed model of digital fractional N-frequency synthesizer based on time to digital converter, digital loop filter and digital voltage control oscillator. Due to digital nature of building blocks of digital fractional N-frequency synthesizer, loop dynamics are easier to reconfigure and they are also easier to port from one process generation to other. Impact of delta sigma modulator quantization noise or error is same on digital and analogue PLL.

Simulating results of proposed work in [3] shows that at 50 MHz reference frequency PLL with bandwidth of 3 MHz generates 4.5 GHz output frequency with in band phase noise of -106 dBc/Hz and consuming 3.7 mW power. Gupta Song [4], presented the model of wideband fractional N-frequency synthesizer to achieve low phase noise by using least mean square based DAC gain calibration technique for spur cancellation. Initially DAC based spur cancellation technique is applied on first order fractional N PLLs but later on it is generalized for higher order fractional N PLLs. Spurs are generated due to non-linearity of phase frequency detector, leakage current in charge pump and harmonics generates at output of voltage control oscillator. Spur cancellation block is used to reduce the delta sigma divider ratio noise and spur correlation block is used to detect the DAC and charge pump current gain mismatching.

Digital synthesizer has all these advantages over analog synthesizer as it offers less circuitry, flexible design, low cost, and easy verification of test results. However the digital building components induces harmonics and disturbances at their respective outputs, resultantly we always get noise, spurs and jitter at the output signals of digital fractional N-frequency synthesizers [5-7]. To the best of our knowledge, no implementation of variants of LMS exists for fractional-N-frequency synthesizers. This implementation in MATLAB/SIMULINK and their comparison is our contribution.

In this paper, we implement a model of digital fractional N-frequency synthesizer in MATLAB and SIMULINK. Delta sigma modulator is the fundamental source of generating spurs in output frequency along with other blocks. As spurs usually have much higher signal powers so simple filters cannot whip it out, therefore an approach of adaptive filtering is proposed in this work where LMS [8] gain calibration technique is used to reduce the spurs.

The rest of the paper is organized as follows: Section-II will illustrate the fundamentals of analog and digital fractional N-frequency synthesizer. Section-III is based on the variants of least mean square algorithms used in adaptive filter for noise cancellation. Section-IV is composed of working, specification used in proposed model and results of model. Section-V is based on future work and conclusion drawn from simulated results.

2. NOISE CANCELLATION IN FRACTIONAL N-FREQUENCY SYNTHESIZER

Fractional N-frequency synthesizer is the most advanced form of frequency synthesizer. The function of fractional N-frequency synthesizer is to produce a periodic output signals with a frequency that is fractional ratio of the reference frequency [4].

$$F_{out} = (N + \alpha)F_{ref} \quad (1)$$

where, N is an integer. α is a fractional value between 0 and 1. F_{out} is output frequency of synthesizer. F_{ref} is input frequency.

Analogue Fractional N-frequency Synthesizer: Analog fractional N-frequency synthesizer is generally consists of PFD (Phase Frequency Detector), CP (Charge Pump), LF (Loop Filter), VCO (Voltage Controlled Oscillator), frequency divider, and $\Delta\sum$ modulator. General block diagram of fractional N-frequency synthesizer is given in Fig. 1.

Digital Fractional N-Frequency Synthesizer: Digital fractional N-frequency synthesizer is gaining more popularity due to better performance, low cost, smart in size and consuming less power as compared to the analogue fractional N-frequency synthesizer. Digital fractional N-frequency synthesizer has the same principal as of the analogue synthesizer. In digital fractional N synthesizer, time to digital converter, digital loop filter and DCO are used in place of PFD and CP, loop filter and VCO respectively.

Design of analogue fractional N-frequency synthesizer is more complex because large capacitance is required in design of analogue filter for reducing ripples in V_{ctrl}, which occupies more space. Though digital fractional N-frequency synthesizer has many advantages as compared to digital N synthesizer, but analogue synthesizer has better jitter performance. However, circuit design of digital fractional N is more flexible in terms of better test ability, programmability, and the components of digital synthesizer operate at low voltages and low in cost as well.

Adaptive Noise Cancellation Scheme: Each component of PLL introduces noise due to disturbance occurred at their outputs. Sources of noise in synthesizer are PFD, VCO, active/passive devices of DLF and quantization noise of delta sigma modulator. These noise sources affects the performance of frequency spectrum of synthesizer. For eliminating noise added by different blocks of synthesizer, adaptive filter uses the appropriate weights to estimate and remove the estimated noise signal from available information signal. Adaptive filters are widely used in applications of signal processing. These filters are usually made of FIR (Finite Impulse Response) filters for which coefficients are updated using minimization criterion. The output of adaptive filter is weighted sum of current and previous input samples. Adaptive noise cancellation scheme structure is shown in Fig. 2. The main objective of a noise cancellation system is to generate an output that is a best fit in the least square sense to the signal which can be done by applying feedback to adaptive filter then filter coefficients are adjusted using the LMS based adaptive algorithm [8].

Least Mean Square Algorithm: LMS technique was first proposed Widrow and Stearn [9]. It is the most used adaptive filter algorithm. In this algorithm, weight coefficients are adjusted from sample to sample in such a way to minimize the MSE (Mean Square Error). This algorithm is considered very reliable for noise cancellation in various communication system

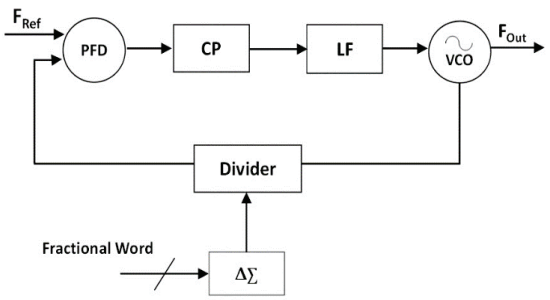

FIG. 1. FRACTIONAL N-FREQUENCY SYNTHESIZER [3]

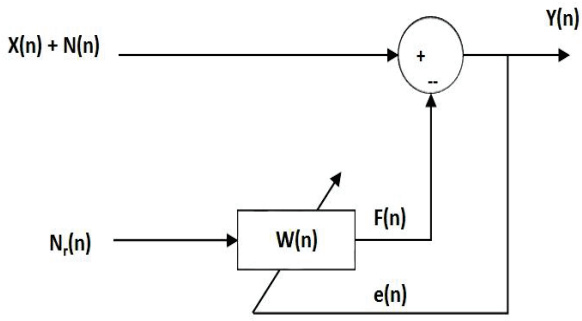

FIG. 2. ADAPTIVE NOISE CANCELLATION SCHEME [4]

applications. Aim of the algorithm is reduction of the error signal which is calculated in between output of filter and the desired signal by estimation process. The complete process is done through filtration and adaptation. In filtration, the output signal is corrupted for the adaptive filter, pertaining to the applied input signal to the filter and thus error signal is computed by taking the difference between actual output signal and desired output signal. Whereas in adaptation part, the adjustment of the filter weights is done with the help of estimated error signal [10]. The updating equation for the LMS algorithm is:

$$\mathbf{w}(n+1) = \mathbf{w}(n) + \mu_e(n)\mathbf{u}(n) \quad (2)$$
$$e(n) = s(n) - y(n) \quad (3)$$

where μ is the step size of the adaptive filter, **w**(n) is the filter coefficients vector, **u**(n) is the filter input vector, d(n) is desired scalar signal and y(n) is additive noise.

Normalized Least Mean Square Algorithm: Normalized LMS is the modified form of the LMS algorithm which removes the instability problem of LMS by applying normalization to the input power. NLMS updating the coefficients of adaptive filter by using the equation mentioned in [4].

$$w(n+1) = w(n) + \mu e(n)\frac{u(n)}{\|u(n)\|^2} \quad (4)$$

Where $\mu(n) = \frac{u}{\|u(n)\|^2}$ putting this expression in Equation (4) to get the new Equation (5).

$$\mathbf{w}(n+1) = \mathbf{w}(n) + \mu(n)e(n)\mathbf{u}(n) \quad (5)$$

3. SIMULATION RESULTS

To verify the impact of LMS based filtering scheme on noise performance we have implemented the model of digital fractional N-frequency synthesizer for spur reduction which deals with digital signals and uses both analogue and digital function parameters of SIMULINK/MATLAB. We have analyzed the simulation results for SNR, spur noise and jitter to assess the noise performance of our system.

Proposed Model: Digital fractional N-frequency synthesizer is a closed loop feedback system [11] that comprises of phase frequency detector subsystem, digital loop filter subsystem, voltage control oscillator, frequency divider subsystem, delta sigma modulator subsystem, LMS filter, single tone frequency estimator subsystem and jitter measurement subsystem. The working of digital fractional N-frequency synthesizer is to compare the phase of reference signal with the feedback signal i.e. divided synthesized signal through phase frequency detector and generates the phase error signal. Output of the phase frequency detector becomes the input of the digital loop filter which removes the high frequency components and allows to pass low frequency signals. The output of digital loop filter is feed to the VCO to control the oscillating frequency and phase depend upon the input signal. The output signal frequency is viewed through single tone frequency estimator subsystem and jitter is analyzed through jitter measurement subsystem. Digital output of VCO is given to frequency divider which divides down the frequency of output signal by N or N+1, this divided value is decided by delta sigma modulator. For spur noise reduction we use LMS filter. SIMULINK diagram of our proposed model is shown in Fig. 3.

Reference Signal: Reference signal of 50 MHz is generated through sine wave source block parameter in SIMULINK by using frequency in rad/sec i.e. $2\pi\times50\times10^6$ with the phase of π and sampled at $2x10^{-10}$. Sine wave block parameter generates discrete waveform which is passed through square wave subsystem to convert it in to a square wave signal.

Phase Frequency Detector Subsystem: PFD subsystem has two input ports and one output port. Reference signal and divided synthesized signal (feedback signal) are the inputs of PFD. SIMULINK diagram of PFD in time domain is shown in Fig. 4.

PFD will compare the phases of two input signals and generate the phase error. Resultantly, UP and DOWN signals are obtained at the Q output port of 1st and 2nd D flip flop respectively. Function of D flip flops is to detect the rising edge of both input signals. If the reference frequency signal is leading the synthesized signal, UP

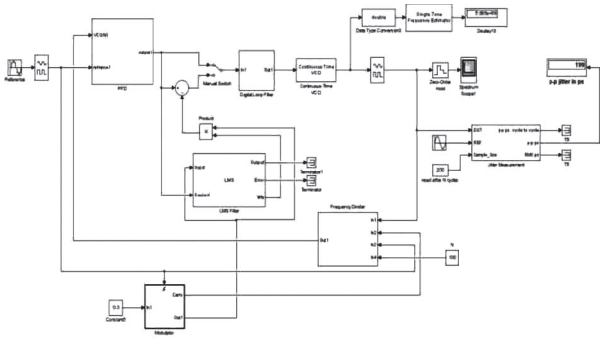

FIG. 3. SIMULINK MODEL OF DIGITAL FRACTIONAL N-FREQUENCY SYNTHESIZER

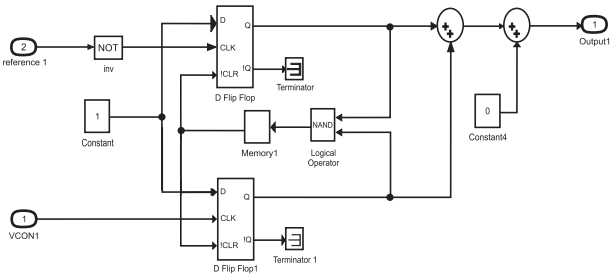

FIG. 4. SIMULINK MODEL OF PFD

signal is high and phase difference is proportional to the pulse width of Q2 therefore Q1 represents the short pulses. NAND gate is used to reset D flip flops when both Q1 and Q2 are high after a specified delay.

Digital Loop Filter Subsystem: Digital loop filter subsystem [12-13] consists of one input and one output port. Phase error generated by PFD becomes the input of digital loop filter. Digital loop filter subsystem consists of IIR low pass digital filter cascaded with proportional and integrated gains. Diagram of SIMULINK model of digital loop filter is shown in Fig. 5.

We have tweaked the parameters to allow low frequency signals to pass. We set the parameters of IIR digital filter so that it allows to pass 50-100kHz signal and set the values of proportional and integral gains i.e. 0.21 and 0.04. These gain values are used to obtain the loop bandwidth, stability and damping coefficient by using the following formulae of

Damping frequency:

$$F_n = \frac{\omega_n}{2\pi} \quad (6)$$

$$\omega_n = F_{rwf}\sqrt{K_I} \quad (7)$$

where, ω_n is natural frequency, F_{ref} is input frequency and K_I is integral gain of digital filter.

Damping coefficient:

$$\zeta = \frac{K_P}{2\sqrt{K_I}} \quad (8)$$

Where ζ is damping coefficient. K_P and K_I is proportional and integral gain of digital loop filter.

Transfer function of PI filter is:

$$H(z) = K_P + K_I \frac{z^{-1}}{1 - z^{-1}} \quad (9)$$

where K_p is proportional gain of digital loop filter and K_I is integral gain of digital loop filter.

Voltage Control Oscillator: We have used VCO function block in SIMULINK and set the parameters so that it will generate the output synthesized signal with frequency which is equal to $(N+\alpha)F_{ref}$. The output of digital loop filter becomes the input of VCO which will generate output signal of frequency range 4.797-5.163 GHz. Output frequency changes w.r.t. to the amplitude variation of the input signal. Set the parameters in VCO block parameters like quiescent frequency is 5.1 GHz and input sensitivity is 1 GHz. Spectrum of output waveform is analyzed through spectrum analyzer. Output spectrum waveform of synthesized signal frequency is shown in Fig. 6.

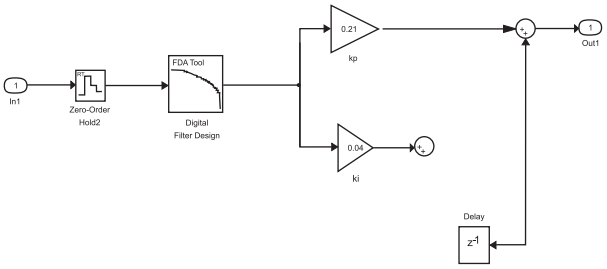

FIG. 5. SIMULINK MODEL OF DIGITAL LOOP FILTER.

Without applying LMS filter in proposed digital model, the output on spectrum analyzer in Fig. 6 clearly shows the non-uniform spread of the signal and its embedded noise which consequently results in relatively low performance in terms of SNR and jitter.

Frequency Divider: Frequency divider subsystem having four input ports and one output port. The function of frequency divider is to divided down the output synthesized frequency by the average value between N or N+1. SIMULINK model of frequency divider is shown in the Fig. 7. The output digital signal of VCO becomes the 1st input of frequency divider subsystem. 2nd input comes from carry output port of delta sigma modulator.

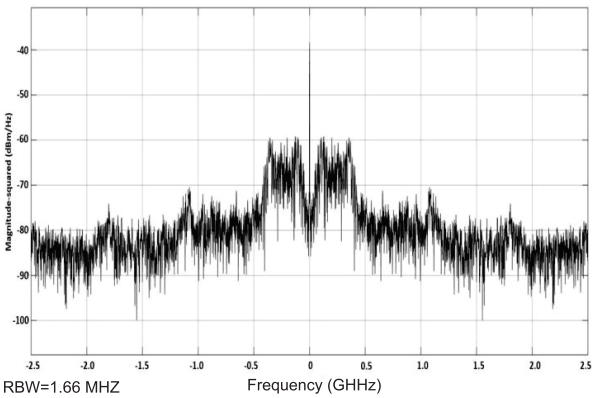

FIG. 6. OUTPUT SPECTRUM OF VCO

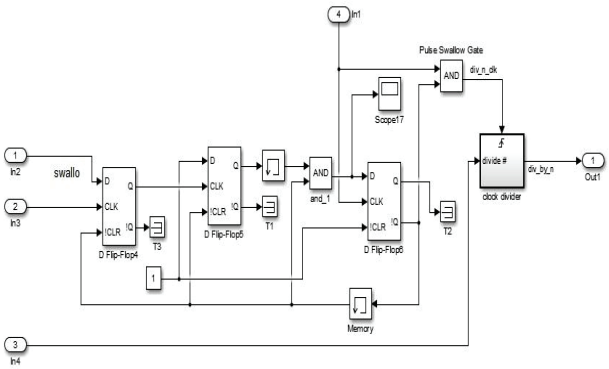

FIG. 7. SIMULINK MODEL OF FREQUENCY DIVIDER SUBSYSTEM

3rd input is the digital reference signal while 4th input is the N integer value which is used as 100 here to divide the synthesized signal frequency. The frequency divider subsystem divides the output signal frequency by N when the carry out port of delta sigma modulator is zero and divides output signal frequency by N + 1 when the carry output of delta sigma modulator subsystem is 1. α is the fractional value which is 0.3.

Delta Sigma Modulator: Delta sigma modulator subsystem having one input port and two output ports i.e. carry output port and state output port. Subsystem consists of an adder, modulator function and delay parameters. We have arranged these parameters so that carry out put port is 0 or 1 and quantization error signal is generated at the state output port. SIMULINK model of delta sigma modulator subsystem is shown in Fig. 8.

The function of this subsystem to repeatedly add the fractional value α which is 0.3 in the sum operator. When the sum is less than 1 the carry output port show 0 result. When the sum is greater than or equal to 1, carry output port shows 1 in the result. Sum operator is reset to its fractional part.

Single Tone Frequency Estimator Subsystem: Single tone frequency estimator is not the building block of digital fractional N-frequency synthesizer its function is to display the output synthesized signal frequency on display scope. We will get the different values of synthesized signal frequency with or without using LMS filter. Without using LMS filter the value of output synthesized signal frequency is 5.109GHz. The remaining values will be presented in LMS filter section.

Jitter Measurement Subsystem: Jitter measurement subsystem is also not the building block of digital fractional N-frequency synthesizer and this subsystem will help to display the jitter value on display scope. We will get different values of jitter in pico seconds with or without using LMS filter. The jitter value is 199 ps without using LMS filter.

Least Mean Square Filter: LMS Algorithm is extensively used in many application of communication due to its simplicity and robustness. The LMS algorithm can be used to minimize the mismatches between the input signals by adjusting the coefficients (gains) according to the errors at the loop filter output. We will use LMS algorithm for reduction of spur noise in proposed architecture. In SIMULINK library there is built in feature of LMS filter available. Set the parameters in LMS filter block accordingly like

Filter Length=1, Step Size (μ)=0.03 and Leakage Factor=1.

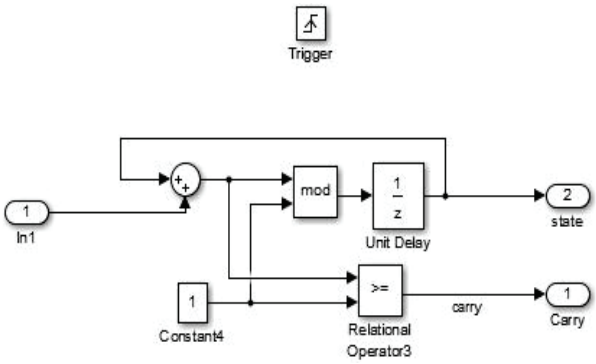

FIG. 8. SIMULINK MODEL OF DELTA SIGMA MODULATOR SUBSYSTEM

TABLE 1. RESULTS OBTAINED WITHOUT USING LMS FILTER.	
Output Frequency	5.109 GHz
Jitter	199 ps
SNR	-17.66 dBc
Spur Noise	-6.404 dBc

TABLE 2. RESULTS OBTAINED BY USING LMS FILTER.	
Output Frequency	5.138 GHz
Jitter	196.6 ps
SNR	-9.51 dBc
Spur Noise	-8.041 dBc

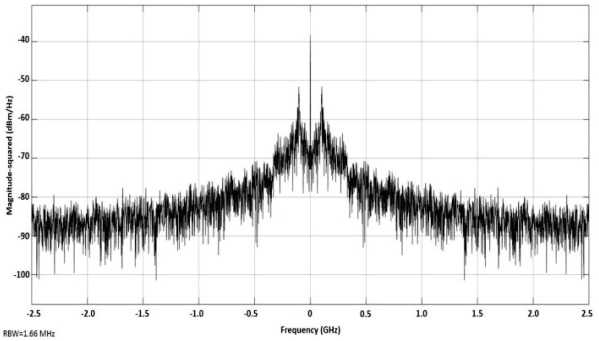

FIG. 9. OUTPUT SIGNAL SPECTRUM BY USING SIMPLE LMS FILTER

TABLE 3. RESULTS OBTAINED BY USING NORMALIZED LMS ALGORITHM IN LMS FILTER	
Output Frequency	4.797 GHz
Jitter	197.8 ps
SNR	-1.17 dBc
Spur Noise	-13.418 dBc

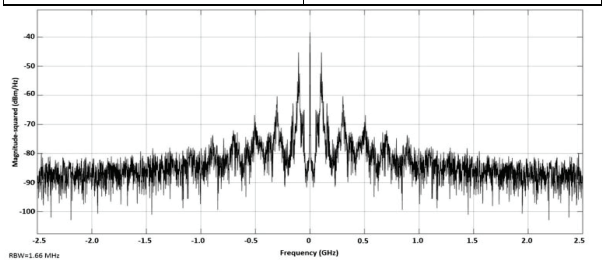

FIG. 10. OUTPUT SIGNAL SPECTRUM WITH NORMALIZED LMS FILTRE

The LMS filter offer different variants of LMS algorithm. Following are different form of LMS algorithm: simple LMS algorithm, normalized LMS algorithm, sign- error LMS algorithm, sign-data LMS algorithm, and sign-sign LMS algorithm. All the mentioned algorithms differ in the ways they adapt coefficients, regardless of how they execute convolution operations. Setting the parameters in LMS filter block and the model will shows a result in Table 2.

Fig. 9 shows the noise performance by using basic LMS algorithm based adaptive filter in our proposed digital frequency N synthesizer model, SNR is improved up to 8.15 dBc, obtain better jitter and spur noise is reduced up to 1.637 dBc.

Normalized LMS: When select the normalized LMS in LMS filter and get results mentioned in Table 3.

In Fig. 10 with the use of normalized LMS algorithm in adaptive noise filter of our model, the spectrum analyzer output is achieved with highly improved performance in terms of SNR, spur noise and jitter. Spur noise reduced up to 7.014 dBc and SNR improved upto 16.49 dBc.

Impact of Different Values of Step Size 'μ' in Noise Performance of Digital Fractional N-Frequency Synthesizer: The value of step size of LMS filter directly impacts the convergence speed, stability and steady state error of the adaptive filter. Smaller step size is used to ensure small steady state error but it also reduces the convergence speed of the filter. On the other hand, step size can be increased to speed up the convergence though it might incur instability to the filter as well. In digital fractional N-frequency synthesizer, we changed the value of step size and observed its impact on noise performance in terms of SNR, spur noise and jitter. Output values with μ=0.5, μ=1 and μ=1.2 have been summarized in Table 4 by applying simple LMS, normalized LMS, sign-error, sign-data and sign-sign LMS algorithms in filter.

It can be seen that every LMS algorithm shows different values of performance parameters on varying the value of step size (μ). However it is quite evident that normalized LMS algorithm displays the best performance as compared to any other LMS variant for each and every value of μ. It is also proven that the most optimal value of for normalized LMS is 1 where all performance parameters of digital fractional frequency synthesizer shows the best values with the improvement of SNR by 28.09 dBc, reduction of spur noise by 9.56 dBc and jitter reduction of 2.9 ps as compared to the results if no LMS filter is used.

TABLE 4. EFFECT OF STEP SIZE ON SNR AND SPUR NOISE

Output	μ = 0.03	μ = 0.5	μ = 1	μ= 1.2
Output freq	4.797 GHz	5.1 GHz	5.1 GHz	5.1 GHz
Jitter	197.8 ps	196.1 ps	196.1 ps	196.1 ps
SNR	-1.17 dBc	7.69 dBc	10.43 dBc	10.30 dBc
Spur noise	-13.418 dBc	-18.17 dBc	-15.971 dBc	-15.819 dBc

4. CONCLUSION

Though spur noise cannot be completely cancelled out however significant improvement in noise performance can be achieved by applying adaptive filters with LMS algorithm and its different versions. In our work, we have observed impact of LMS variants on noise performance of propose digital fractional N-frequency synthesizer model in terms of SNR, jitter and spur noise. Some LMS version improves one variable to some extent while the other degrades the same to different extent so there can be a tradeoff among these indicators with the use of LMS variants. If we compare the results, normalized LMS has been found to be the most efficient one to improve the system noise performance as it improves the SNR by 28.09 dBc and reduces the spurious noise by 9.56 dBc along with 2.9 ps improvement in jitter as well. We have implemented the proposed model for testing and verification MATLAB/SIMULINK as high frequency radio communication hardware chips are not readily available in Pakistan. The designing of circuit level implantation is next area of focus to evaluate the real time performance results which involves CMOS chip fabrication process as well. Apart from this, proper schematic of TDC (Time to Digital Converter) is not available in SIMULINK, so we had to use PFD in place of TDC to generate the result. Further we will try to design the TDC to simulate and study its impact on the overall noise performance of our model. Implementation of this work in hardware to validate the results is one area for future work. Another area for future research is to reduce the intrinsic noise.

5. FUTURE WORK

In future, same comparative analysis can be extended for other Adaptive algorithms like RLS (Restless legs syndrome), RMS (Root Mean Square) and APA (Affine Projection Algorithm).Analysis may be extended for comparison of more advanced performance parameters like speed, complexity and stability. Designing circuit level implantation to evaluate real time performance results. Another area for future research is to reduce the intrinsic noise.

ACKNOWLEDGEMENT

Authors would like to thank faculty members at Faculty Engineering, University of Central Punjab, Lahore, Pakistan, for their feedback and suggestions.

REFERENCES

[1] Zhang, Y., Mueller, J.H., Mohr, B., Liao, L., Atac, A., Wunderlich, R., and Heinen, S., "A Multi-Frequency Multi- Standard Wideband Fractional-PLL with Adaptive Phase-Noise Cancellation for Low-Power Short-Range Standards", IEEE Transactions on Microwave Theory and Techniques, Volume 64, No. 4, 2016.

[2] Kozak, M., and Friedman, E., "Design and Simulation of Fractional N PLL Frequency Synthesizers", IEEE International Symposium on Circuits and Systems, 2004.

[3] Elkholy, A., Anand, T., Choi, W., Elshazly, A., and Hanumolu, P.K., "A 3.7 mW Low-Noise Wide-Bandwidth 4.5 GHz Digital Fractional N PLL Using Time Amplifier-Based TDC", IEEE Journal of Solid-State Circuits, Volume 50, No. 4, pp. 1-15, April, 2015.

[4] Gupta, M., and Song, B., "A 1.8-GHz Spur-Cancelled Fractional N-frequency Synthesizer with LMS Based DAC Gain Calibration", IEEE Journal of Solid-State Circuits, Volume 41, No. 12, pp 2842-2851, December, 2006.

[5] Hung, S., and Pamarti, S., "6.4 A 0.5-to-2.5GHz Multi-Output Fractional Frequency Synthesizer with 90 fs Jitter and -106dBc Spurious Tones Based on Digital Spur Cancellation", IEEE International Solid-State Circuits Conference, 2019.

[6] Vo, T.M., and Samori, C., "Salvatore Levantino A Novel LMS-Based Calibration Scheme for Fractional-N Digital PLLs", IEEE International Solid- State Circuits Conference, 2018.

[7] Elkholy, A., Saxena, S., Shu, G., Elshazly, A., and Hanumolu, P.K., "Low-Jitter Multi-Output All-Digital Clock Generator Using DTC-Based Open Loop Fractional Dividers", IEEE Journal of Solid-State Circuits, Volume 53, No. 6, 2018.

[8] Sayed, A.H., "Adaptive Filters", John Wiley and Sons, Inc., Hoboken, New Jersey, University of California, Los Angeles, 2008.

[9] Widrow, B., and Stearns, S.D., "Adaptive Signal Processing", Prentice Hall, 1985.

[10] Poularikas, A.D., and Ramadan, Z.M., "Filtering Primer with MATLAB", Taylor and Francis Group, Boca Raton, London, New York, 2006.

[11] Liu, Y., "Design of All Digital Phase Locked Loop in Serial Link Communication", Master's Thesis, Graduate College, University of Illinois, Urbana, Illinois, 2015.

[12] Bilhan, E., Ying, F., Meiners, J.M., and Xiu, L., "Spur Free Fractional N PLL Utilizing PrecisioN-frequency and Phase Selection", IEEE Dallas/CAS Workshop on Design Applications Integration and Software, 2006.

[13] Hui, B., and Nang, N., "FPGA Implementation of DSSS RF Front-End Based on Software Radio", International Symposium on Antennas Propagation and EM Theory, 2008.

Short Circuit Analysis of EHT Network and Solutions for De−Rated Equipment

Muhammad Ibrar-ul-Haque*, Usama Ahmed*, Sana Anwar*, Umm-e-Laila, and Shakeel Ahmed Khan***

* Department of Electrical Engineering, Sir Syed University of Engineering & Technology, Karachi, Pakistan.

**Department of Computer Engineering, Sir Syed University of Engineering & Technology, Karachi, Pakistan.

mihaque@ssuet.edu.pk, usamaehmed@gmail.com, sanaanwar077@gmail.com, ulaila@ssuet.edu.pk, shakilak@ssuet.edu.pk

ABSTRACT

In any power system, load growth occurs due to increase in various activities including industrial expansion, infrastructure development, population growth etc. To meet power demand, the electrical network of utility company required addition in transmission lines, grid stations and power generation. The heavy current that flows due to short circuits causes different types of internal and external faults on the power system which may damage the equipment in the grid station if the fault is not cleared in time. The equipment in the grid station must have the capability to withstand the heavy short circuit level. If unusually high currents exceed the capability of protective devices in the power system, a short-circuit can cause the devices to explode like a bomb, which may ultimately result in collapse of entire system leading to brown out or black out. All these expansion leads to increase in short circuit levels. The short circuit current passes the high voltage, network equipment including circuit breakers, disconnectors, current transformers, potential transformers, surge arresters etc. The high voltage equipment's need to be check due to increase in short circuit current due to addition in power plants, auto transformers, power transformers and transmission lines. The equipment's that are already installed are required to withstand short circuit at all time. In the presented work, short circuit levels are calculated by using a software ETAP (Electrical Transient Analysis Program), followed with the analysis of existing equipment's as whether it can withstand the short circuit level. The proposed period of study is set to be 5 years (till year 2023). Furthermore, three different types of solutions are provided for the derating equipment in the K- electric 220V and 132KV transmission lines

Key Words: Short Circuit Level, Faults in Power System, rotective Devices, Load Growth, Power Demand, Electrical Transient Analysis Program, System Analysis, Black Out.

1. INTRODUCTION

The proposed research work which is implemented under the name of "Short-circuit analysis of EHT (Extra High Tension) network of K-Electric for five years (2018-2023) and solutions for de-rated equipment" is a simulation-based research work in which EHT Network of Karachi City is considered. The term EHT in our research work is used for 220 and 132KV.

K-Electric is the main vertically integrated power utility in Pakistan, managing all three categories generation, transmission and distribution [1]. Various researchers have performed their studies in this domain [2-4]. All the related data is taken from K-Electric. This research work is carried out through a prominent software ETAP and is based on the load flow analysis which is implemented for whole K-Electric network including 220, 132 and 66KV circuits so as to match the results of simulation. Further short circuit analysis is done on the network on different levels. The basic purpose is to find the de-rated equipment in K-Electric EHT Network. The de-rated equipment means the protective equipment which are present in the system has reduces its capacity since many years despite that system has expanded and may expand further. Equipment are usually chosen according to the system short circuit level at the time of installation which after sometime may have increased [5-9]. The equipment must therefore be changed for the effective working of the system. The research work has a provision for this, in which short circuit level of K-Electric existing EHT Network will be observed and solutions of de- rated equipment will be given as per the conditions.

2. POWER FLOW STUDIES

ETAP software has been used for the load flow study with the consideration of removing issues related to under voltage scenarios. The load flow study is used for calculating required size and location of capacitors for removing the issue of under voltage. What-if scenarios can be investigated by these studies specially related to sudden addition and removal of loads to the system. These studies also indicate the fluctuations in system voltages and capacity utilization of system equipment, under various contingencies.

Studies related to load flow are frequently used to pinpoint the necessity for the:

(a) Added generation.

(b) Inductive or Capacitive VAR (Volt-Ampere Reactive) support.

(c) The employment of capacitors and/or the reactors for maintaining the voltages of system within designated margins.

Power flow studies of the K-Electric system has done through these steps which are mentioned below.

- The analysis of technical aspects.
- Load Flow Study for the steady state stability.
- Stability analysis results are to be matched with the

K-Electric network data.

- Short circuit analysis to determine the magnitude of short circuit current.
- Short circuit levels that the system can produce under faulty condition.
- Comparing magnitudes with the ratings of interrupting, over current protective components.
- Sequence of events consisting of the initial loss of a single generator or transmission component.

3. LOAD FLOW AND ETAP SIMULATION

In this work, load flow study using ETAP software is carried out with an approach to overcome the problem of an under and over voltage at buses. Load flow studies using ETAP software is an excellent tool for system planning. A number of operating procedures can be analyzed such as the loss of generator, a transmission line, a transformer or a load. Load flow studies can be used to determine the optimum size and location of capacitors to surmount the problem of an under voltage. Also, they are useful in determining the system voltage sunder conditions of suddenly applied or disconnected loads.

Load flow studies determine if system voltages remain within specified limits under various contingency conditions, and whether equipment such as transformers and conductors are over loaded. Load flow studies are often used to identify the need for additional generation, capacitive, or inductive VAR support, or the placemen to capacitors and/or reactors to maintain system voltages within specified limits.

Some of the screenshots of simulation work is shown in Fig 1. The Fig. 1 is the whole semantic of utility company network created using ETAP software. It Contains 66, 132 and 220 kV buses layout with generators feeding the system.

Fig. 2 shows the load flow data on CCP (Competition Commission of Pakistan) bus which consists of six generators four of which are rated at 40MW and are operating at a reactive power of 29.8 MVAR with current outflows of 2404 Amperes and after the stepping up of the voltage levels the reactive power drops down to 27.8MVAR and current out flows to 125.7 Amperes. The remaining two generators are operating at 15 MW with reactive power equal to 15.3 MVAR which drops down to 14.1 MVAR and the current outflows from 1064 Amperes drops down to 53.2 Amperes. The CCP is operating at 222.5 kV.

Fig. 3 shows the load flow data on Dhabajee bus with connected loads.

There are a total of two power transformers connected as loads on the Dhabeji grid rated at 16 and 27 MVA. The active power being drawn out 14.4 and 24.3 MW respectively. The reactive power being 6.97 11.8 MVAR respectively. The currents being 64.4 115.8 Amperes respectively. The bus operating voltage is found to be 129.1 kV.

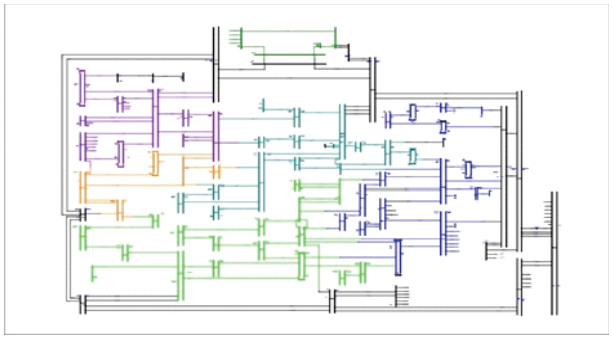

FIG. 1. NETWORK DIAGRAM ON ETAP SOFTWARE

4. SHORT CIRCUIT ANALYSIS

4.1 Short Circuit Faults

When the insulation of the system fails at one or more points or a conducting object comes into contact with alive point, a short circuit or a fault occurs.

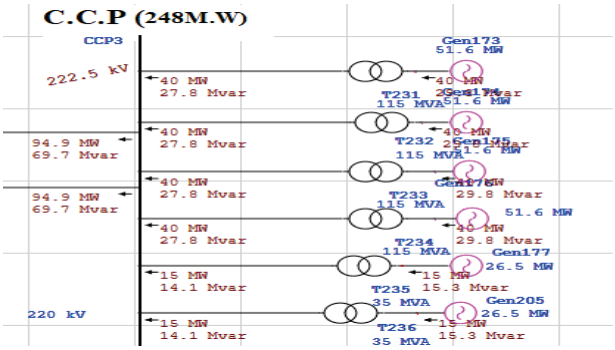

FIG. 2. LOAD FLOW CCP BUS USING ETAP SOFTWARE

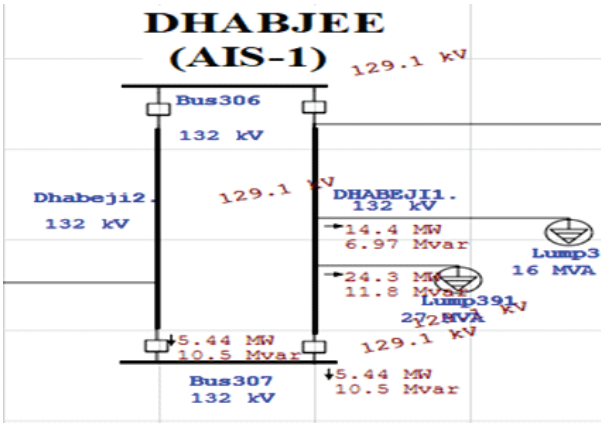

FIG. 3. LOAD FLOW ON DHABAJEE BUS USING ETAP SOFTWARE

There are mainly two character of faulting in the electrical power system. Those are:

- Symmetrical faults or balanced three phase faults
- Unsymmetrical faults or unbalanced faults.

4.2 Effect of Short Circuit Faults

The Over Current: After the occurrence of fault, a very low impedance path is created for the current flow. Due to this, very high current s being drawn from the supply, which causes the tripping of relay, also damage components and insulation of equipment.

Risk to the Operating Workers: Fault existence can also bring shocks to the persons. The Severity of shocks be governed by the voltage and current at the location of fault and may also lead to the death.

5. DAMAGE OF EQUIPMENT

The heavy currents due to the short circuit fault result in the damage of components, can burn completely and this leads to inappropriate working of the equipment or device. At times substantial fire can cause complete equipment burnout.

Study on K-Electric Network: Electrical fault is an abnormal status, caused by equipment failures such as transformer and rotating machine, human errors and environmental conditions. Theses faults cause interruption to electric flows, equipment amends and even cause death of humans, birds and animals.

The existing condition of grid stations at 220 KV of K-Electric is not much satisfactory with regards to the increased short circuit current levels. The protection scheme of K-Electric was designed years ago primarily in regards to the short circuit level of that time. However, the system has expanded in terms of generators and loads, which contributes towards increased short circuit level of each grid. The existing protection scheme may not be able to operate correctly for some grid stations, as there is an increase in the short circuit current level. This happens due to the gap between designed protection scheme current carrying capacity and the short circuit current level of grid stations. As the main concern of this research work is to provide solution for 220 KV grid stations of K-Electric , therefore the concentration of the research work revolves mainly around the 220 KV network. There are ten grid stations of 220 KV in K-Electric limited.

Respective Results: The results of our studies for different 220 KV grid stations are depicted in Table 1 showing all the grids that needs immediate replacement.

The following results are obtained using ETAP, by inserting the generator and transformer ratings/ parameters.

As observed from Table 1, at BQPS-1 (Bin Qasim Power Station), BQPS-II, ICI (Imperial Chemical Industries), KDA (Karachi Development Authority) and Pipri West, the protective equipment rating is shown to be 40 KA but the existing short circuit level at the grid is exceeding the rated capacity of the breaker, thus, the protective device needs immediate replacement.

TABLE 1. RESULTS OF SHORT CIR CUIT LEVELS AT 220KV GRIDS

Grid Stations	Existing Short Circuit Current Level (KV)	Protective Equipment Rating (KV)	Identification of Protective Equipment/Scheme
BQPS-I	43.29	43.29	De-Rated
BQPS-II	43.29	40.00	De-Rated
Baldia	40.5 0	40.00	Not De-Rated
CCP, KPC (Knowledge, Practices and Coverage)	19.08	40.00	Not De-Rated
ICI	42.24	42.24	De-Rated
KCR (Karachi Circular Railway)	23.90	23.90	Not De-Rated
KDA	42.90	42.93	De-Rated
Lakazar	23.00	40.00	Not De-Rated
Maripur	24.40	40.00	Not De-Rated
Pipri West	43.39	40.00	De-Rated

6. SOLUTION TO REDUCE SHORT CIRCUIT LEVELS

General Solution: The topography of the power system networks continues to change as country's economy grows and consumption increases. The major impact is the increase in short circuit currents in the power system due to the growth of the power system and the expansion of the complex transmission network. The increased short circuit current affects every protective power system equipment that causes heat loss and mechanical stress. This is because the protection system was designed many years ago according to the expected short circuit current, but the current short circuit is due to the expansion of the power system network and the load growth. To address this problem, we must reduce the power system network's short circuit current. Some techniques are used to reduce the short circuit currents. They are as listed below:

(i) Technique-1: Split bus bars
(ii) Technique-2: Split network
(iii) Technique-3: Use of current limiter
(iv) Technique-4: Change the neutral earth policy
(v) Technique-5: Changing some lines from AC-DC
(vi) Technique-6: New transmission network
(vii) New protection scheme

Types of Solutions: They can be classified into three main categories as following:

Interim/Immediate Solution: An interim solution is a problem-solving technique that uses the fastest solution available to the given problem. This solution is not permanent and can ever betray.

Solution for Short Period: A short-term solution is a problem-solving technique that uses sustainable

solutions rather than interim solutions. This solution could be permanent, but it can only survive until the near future.

Solution for Long Period: Along-term solution is a problem-solving technique that uses the most significant and durable solution of the given problem. The methods used in this solution are permanent and could solve the problem forever. It is one of the most sustainable solutions. This solution could be expensive.

Typical and Quantitative Analysis for Solution: The techniques involved in reducing short circuit current are categorized as solutions reliability and network reliability, as shown in Table 2.

TABLE 2. TYPICAL ANALYSIS FOR SOLUTIONS

Techniques	Solutions Reliability	Network Reliability
Splitting of Bus bar	Solution for short term	Maximum
Splitting of Network		Medium
Use of Current Limiter		Maximum
Change of Neutral Earth Policy	Interim solution	Minimum
Changing some lines from AC-DC		
New transmission network	Solution for long term	Maximum

Implementation on K-Electric Network: The existing K-Electric condition does not coincide with the above-mentioned solutions. Since the technology of changing neutral earth policy cannot work for this case, this technique usually works close to the distribution side and for asymmetrical faults that are not the scope of this research work. Other new transmission network techniques and the new protection scheme would impose an unfeasible high cost on K-Electric. Therefore, the remaining techniques that include changing certain lines from AC-DC, splitting bus bars and using the current limiter are considered much more practical for the K-Electric network.

Identification of Derated Equipment in 220KV Network: Each 220 KV grid stations have been analyzed in detail. On the basis of our study, the identification of the de-rated equipment at each grid station of 220 KV network of K-Electric is carried out, which is described above in respective results.

Apparent Replacement Plan: The replace-ment plan for some grid station at 220KV, which can be shown in Tables 3.

TABLE 3. APPARENT REPLACEMENT PLAN

No.	Grid Station	Required Immediate Action	Suggested Future Action
1.	BQPS-I	Interim Solution	Long Term Solution
2.	BQPS-II		
3.	Baldia		Short Term/Long Term
4.	ICI		Long Term Solution
5.	CCP	Nil	No Action until the system is expands
6.	KCR		
7.	KDA	Interim Solution	Long Term Solution

On the basis of above analysis, implementation of following techniques has been suggested to reduce or cater the problem of increased level of short circuit current at each grid station of 220 kV network of K-Electric shown in Table 4.

TABLE 4. APPARENT REPLACEMENT PLAN USING TECHNIQUE

Grid Station	Interim Solution	Short Term Solution	Long Term Solution
BQPS-I	Split Bus bar	Current Limiter	Current Limiter/New Protection Scheme
BQPS-II			
Baldia	No Immediate Action Required	Split Bus bar/Current Limiter	
ICI	Split Bus bar	Use of Current Limiter	
CCP	No Immediate Action Required	No action required in future until the system has not expanded	No action required in future until the system has not expanded
KCR		Split Bus bar/Current Limiter	Current Limiter/New Protection Scheme
KDA		Current Limiter	
Lalazar		Split Bus bar/Current Limiter	
Maripur		Split Bus bar/Current Limiter	
NKI		Current Limiter	
Pipre West	Split Bus bar		

7. CONCLUSION

It has been concluded from the studies that the short circuit levels of Karachi are increasing with time and hence there is a need for are placement plan. The need of replacing the breakers to a larger capacity is very necessary as many of the breakers on the 220 KV transmission side are near to saturation. They must be replaced so that the breakers may operate properly for more 8-10 years. The current rating of the circuit breakers are 40 KA.

The main reason of system equipment failure is usually the implementation of low design margins. Power electrical equipment is subjected to two types of stresses.

(i) Electrical Stress: The equipment may go out of service due to excessive voltage, current or power.
(ii) Thermal Stress: Due to equipment's own and nearby equipment's energy dissipation.

A reduction in electrical stress results in a corresponding reduction in thermal stresses. The system's reliability consequently increases. In this research work, the reliability of system is increased by introducing comparatively high design margins, i.e. design capacity over anticipated stress. The reliability of the system can be improved by implementation of a comprehensive derating policy. Neglecting this may result in degraded performance and accelerated failure.

ACKNOWLEDGEMENT

First and foremost, we would like to thank Almighty Allah for His countless Blessings on us that leads us towards the completion of this research work in the best regards. Our profound gratitude and deep regards towards the university management for encouragement, counselling along with constant monitoring throughout the research work. Authors would also like to take this opportunity to extend our regards to the Deputy General Manager Transmission, K-Electric, for providing us assistance that was needed to complete this work.

REFERENCES

[1] "Who We Are", 2019. website: https://www.ke.com.pk/ourcompany/who-we _(Retrieved June 24, 2019).

[2] Gilany, M., and Al-Hasawi, W.," Reducing the Short Circuit Levels in Kuwait Transmission Network: A Case Study", International Journal of Electrical and Computer Engineering, Volume 3, No. 5, pp. 592-596, 2009.

[3] Oswald, M., and Trench, A., "Short-Circuit Current Limitation by Series Reactors", Energize, Volume 4, pp. 45-49, October, 2009.

[4] Mehta, V.K., "Principles of Power System", Chand & Company, [ISBN 10: 8121924960, [ISBN 13: 9788121924962], New Delhi, India, 2006.

[5] Davis, W.P., "Analysis of Faults in Overhead Transmission Lines", Thesis, California State University, Sacramento, 2012.

[6] Maisuriya, R.H., and Patel, D.K., "Simulation of Short Circuit Condition and Fault Analysis in Power System", International Journal for Technological Research in Engineering [ISSN (Online): 2347-4718], February, 2018.

[7] What is Short Circuit Analysis, and Why is it Done? | Carelabz.com., from Carelabs.website:https://carelabz.com/what-short-circuit-analysis-done-shy/. (Assessed November 21, 2019).

[8] Kubis, A., Rüberg, S., and Rehtanz, C., "Development of Available Short-Circuit Power in Germany from 2011 up to 2033", CIRED Workshop - Rome, 11-12 June, 2014.

[9] Ali, S.A., Larik, A.S., and Irshad, A., "Short Circuit Analysis of 500 KV Hubco Power Transmission Network and Improvement of Voltage Stability", Mehran University Research Journal of Engineering & Technology, [ISSN: 0254-7821], Volume 30, No. 4, pp. 707–714, Jamshoro, Pakistan, 2011.

[10] Ayokunle A., Mbamaluikem, P., and Samuel, I.A., "Artificial Neural Networks for Intelligent Fault Location on the 33-Kv Nigeria Transmission Line", International Journal of Engineering Trends and Technology, Volume 54, No. 3, pp. 147-155 December, 2017.

[11] Mbamaluikem, P., Aderemi, O., Oluwaseum, S., and Ayokunle, A., "Fault Identification System Using Artificial Neural Networks for Nigeria Electric Power Line", International Journal of Scientific and Engineering Research, [ISSN 2229-5518], Volume 9, No. 2, February, 2018

[12] Elnozahy, A., and Sayed, K., "Artificial Neural Network Based Fault Classification and Location for Transmission Lines", IEEE Conference on Power Electronics and Renewable Energy, pp. 140-144, Egypt, October 23-25, 2019.

Investigation of Dynamical Systems with XPPAUT

Bilal Ahmad*, Sajid Iqbal*, Ayesha Safdar*, Kashif Ali Khan, and Shah Muhammad*****

*Department of Mechatronics & Control Engineering, University of Engineering & Technology, Lahore, Pakistan.

**Department of Mathematics, University of Engineering & Technology, Lahore, Pakistan,

***Department of Mathematics, King Saud University, Saudi Arabia.

bilalahmadadil@gmail.com,sajid.iqbal@uet.edu.pk, ayeshasafdar1993@gmail.com, kashifali@uet.edu.pk, skabeer@ksu.edu.sa

ABSTRACT

The mathematical modeling and computer simulations are extensively used in engineering problems and scientific research. The analysis of the system model gives us idea of understanding of the system whereas the simulation explains the feasibility whether system is implementable or not. Simulation also gives insight of the system realization. This paper focuses on interactive computational and simulation software XPPAUT (X-Windows Phase Plane Auto). Many Softwares i.e. MATLAB, MATHEMATICA, MAPLE are currently used for modeling and simulations of dynamical systems, but numerically integrating the differential equations is slower than that can be achieved with XPPAUT. Some problems incorporating the well-known linear and non-linear differential equations i-e radioactive decay, simple pendulum, Lorenz system, initial value problems and direction fields along-with null-clines has been coded, simulated and the results are presented to substantiate the claim.

Key Words: AUTO, Direction Field, Ordinary Differential Equations, Lorenz System, Simulation, XPPAUT.

1. INTRODUCTION

XPPAUT is freeware and it was developed by Ermentrout [1]. XPPAUT is an interactive package for differential equations, difference equations, delayed functions and boundary value problems. This computationally efficient analyzing tool can handle 590 differential equations at a time. The XPPAUT has two interactive and switchable parts XPP (X-Windows Phase Plane) and AUTO. It is an efficient and dedicated tool that is used for differential equations, difference equations, delayed function, initial value problems, stochastic problems and boundary value problems. XPP has 12 in-built ODEs (Ordinary Differential Equations) solvers that can integrate systems up to 590 differential equations [2]. It can pop-up 10 graphics windows in response to invoked inputs. It has user-friendly way of setting up the differential equations. It also supports equations with dirac-delta functions [1-3]. Nullclines, directions fields and phase planes can be plotted in much easier way as compared to any other numerical analysis tool. Just by clicking on nullclines, direction field options readily available in menu bar can plot nullclines and direction fields respectively.

The system requirements for installation are comparatively much lesser than any other technical and computational environments. The ODEs written is XPPAUT require less coding skills for the computing the response of the system under consideration. Many options are readily available as menu items of XPP main windows [2].

A prototype or model is an essential component for computer simulation. Fairly well representations of models are algebraic equations or differential equations [4-5]. Differential equation is a great tool for system modeling and simulation. The intrinsic behavior of the physical system can be predicted from the model and verified through the simulations. Differential equations are basically used to relate functions with their derivatives [5]. Thus differential equations help us understanding physical phenomena, laws of nature and system behaviors.

Dynamical systems are time dependent systems whose parameters or conditions may change with time [6]. These time-variant systems are modeled either as set of differential equations or difference equations. When systems are described by differential equations they are known as continuous dynamical systems and when these are modeled in terms of difference equations they are referred to as discrete dynamical systems. Both categories are analyzed and simulated for understanding and response of system through interactive simulating softwares. Analytical studies remains incomplete unless system is simulated and analyzed through any simulating tool so that system response and claim about system behavior can be justified [7].

2. COMPARISON WITH MATLAB, MAPLE AND MATHEMATICA

Scientists and researchers use MATLAB, MATHEMATICA, MAPLE to study and analyze the dynamical system [8-11]. These simulating packages are available for integration or simulation. MATLAB has flexibility regarding symbolic analysis and numerical simulations. It is decked with powerful parsing tool. In addition to this it has many built-in functions and libraries that enable it to solve problems related to dynamical systems. It comes with many example ODEs that are sufficient to explore, learn and familiarize one with the syntax, commands and functions. Its interface for writing up equations is very easy. Researchers with less programming knowledge can program or code equations very easily than that of any other simulating software. Likewise, in engineering education, circuit simulators are used to reinforce the student understanding of theoretical concepts using graphical aids [12-13].

XPP, which stands for X-windows phase space, is a graphical interface to AUTO. Qualitative analysis and numerical integration of dynamical systems is slower and effort requiring than that in XPPAUT.A big reason to use XPPAUT is that none of the other packages provide interface to AUTO facility [1]. AUTO is a package that allows you to see the response of dynamical systems as their initial conditions and parameters are varied [14-15]. AUTO is capable of finding the fixed points of the system as the parameter varies as well as tracking solutions to the differential equations.

3. SIMULATION RESULTS

Example-1: In this section, we will explore the radioactive decay model from the xppall/ode file that was downloaded with XPPAUT [2]. A simple program that is described by linear differential equations is discussed here. It has one parameter k. Then we set the initial conditions to execute the simulation. The linear ODE is a radioactive decay function that describes the decay of a radioactive element. The relation depicts that decay is independent of the initial amount of the substance. Decay just depends upon the half-life of the element.

The system is modeled as Equation (1).

$$\frac{dx}{dx} = -kx \qquad (1)$$

Where x is the amount of substance available at any time t. The simulation code for linear ODE is as under:

```
(1) init x = 100
(2) par k = 0.054
(3) dx/dt = - kx
(4) @ dt= 0.025, total = 30, xplot = x, yplot = y, axes = 2d
(5) @ xmin = -30, x_max = 30, y_min = - 40, y_max = 40
(6) @ xlo = - 1.5, ylo = - 2, xhi = 1.5, yhi = 2
(7) done
```

The plot of radioactive decay of a certain substance is shown in Fig. 1. The curve is a decreasing function which shows decay of radioactive substance no matter with what initial condition we proceed. The negative sign in the ODE is an indication of decay of substance.

Example-2: In this section, we will now explore the Lorenz model from the xppall/ode file that was downloaded with XPPAUT [2]. Lorenz system is a non-linear, non-periodic three dimensional deterministic model for atmospheric convection. It consists of ODEs which are famous for their chaotic behavior due to change of parameters and initial conditions. Lorenz system is set of chaotic solution curves which upon plotting resembles a buttery or eight-curve.

The Lorenz system is described by following set of differential Equations (2-4).

$$\frac{dx}{dx} = s(-x + y) \qquad (2)$$

$$\frac{dy}{dx} = rx - y - xz \qquad (3)$$

$$\frac{dz}{dt} = -bz + xy \qquad (4)$$

Where x, y and z describes the system state and b, r and s are system parameters.

The code is as follows:

```
(1)      x = - 7.5 y = - 3.6 z = 30
(2) par  r = 27 s = 10  b = 2.6
(3) dx/dt = s*(-x+y)
(4) dy/dt = r*x-y-x*z)
(5) dz/dt = - b*z + x *y
(6) @ dt = 0.025, total = 50, xplot =  x, yplot = y, zplot =
    z, axes = 3d
(7) @ xmin = -30, xmax = 30, ymin = - 30, ymax = 30,
    zmin = 0, zmax = 40
(8) @ xlo = - 2.5, ylo = - 3, xhi = 2.5, yhi = 3
(9) @ maxstor = 25000
(10) @ phi = 60
(11) @ runnow = 1
(12) done
```

The plot is obtained for parameters as r =27,s=10=2.67.

We can see that two wings of the butterfly correspond to two different sets of physical behavior of the system as illustrated in Fig. 2. Any point on the plot represents a particular physical state, and curve shows the path followed by such a point during a finite period of time. Notice how the curve spirals around one wing a few moments before switching to the other wing.

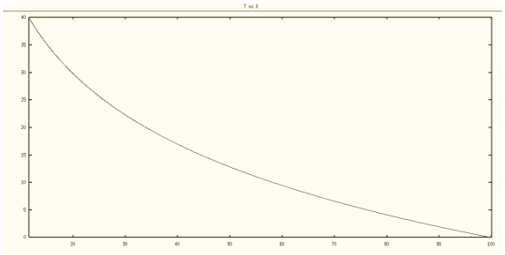

FIG. 1. RADIOACTIVE DECAY DESCRIBED BY LINEAR ODE

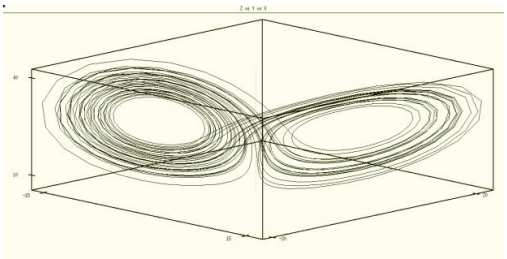

FIG. 2. 3D PLOT OF LORENZ SYSTEM

Example-3: In this section, we are going to explore simple pendulum model from the xppall/ode file that was downloaded with XPPAUT [2]. A simple pendulum consists of a bob of mass m suspended by light string of length l that is pivoted at some point P. When displaced to an initial angle and released, the pendulum will execute to and fro motion with some definite period. This system comprises of non-linear differential equations which are simulated with small angle approximations for understanding of physics of the system.

The system model is described by differential Equation (5).

$$\frac{d^2\theta}{dt^2} + \frac{g}{1}\sin\theta = 0 \qquad (5)$$

The simulation code is as follows.

```
(1)  dx/dt = xp
(2)  dxp/dt = (- mu*xp- m*g*sin(x)/ (m*l))
(3)  PE = m*g*(1- cos(x))
(4)  KE = 0.5*m*l*xpaux^2
(5)  PE = PEaux
(6)  KE = KEaux
(7)  TE = PE + KE
(8)  param m = 15, mu = 2, g = 9.81, l = 1
(9)  param scale = 0.0083
(10) @ xp = x,yp = xp, xlo= - 5, xhi = 5, ylo = -10, yhi = 10
(11) @ bounds = 1000
(12) x(0) = 2
(13) done
```

The simulation is carried out and results are plotted with simulation tool. Plot describes that system response is periodic for given set of initial conditions. The simple pendulum while swinging has two forms of mechanical energies namely kinetic and potential. At extreme positions on either side it has max PE and at mean positions it has max KE. The system keeps on oscillating unless it loses all of its mechanical energy. The plot in the simulation consist of orbits that shows periodicity and oscillator orbit termination is an indication of the fact the system ultimately loses all of its energy. The plot is phase portrait which comprises of angle at which bob is displaced from mean position and angular velocity.

The system is periodic with period T as Equation (6).

$$T = 2\pi\sqrt{\frac{1}{g}} \qquad (6)$$

Example-4: Now we will analyze and simulate a boundary value problem from the xppall/ode file that was downloaded with XPPAUT [2]. In the domain of ODEs, a BVP (Boundary Value Problem) is a pair of differential equations with some constraints. A solution of any BVP is solution to the differential equation which satisfies the given ODE and boundary conditions as well. We here discuss a non-linear BVP which consist of a differential equation and a set of boundary values. In XPPAUT we have "bdry" as keyword to specify boundary conditions [2].

We can simulate the problem with the following code.

```
(1) du/dt = v
(2) dv/dt = sin(t*u)
(3) bdry u- 1
(4) bdry du/dt
(5) init u = 10,v = - 10
(6) @ total = 20, bell = 0, xhi = 15
(7) done
```

The BVP has been analyzed and simulated. Some initial and boundary constraints have been provided by using XPPAUT commands "init" and "bdry" [2]. The results are simulated for total time of 10 seconds as shown in Fig 3. The highest value of x is taken as 10, specified by "xhi" whereas "xlo" is by-default 0.

Example-5: Finally, we will analyze and simulate an exact ODE for direction field and null clines. In XPPAUT there are commands "Direction Field" and "Null Clines". Just by clicking on this button we can obtain direction fields and null clines [2]. To analyze the direction field and null clines following code is compiled and executed.

The general form of an exact ODE is as Equation (7).

$$M(x, y) + N(x, y)\frac{dy}{dx} = 0 \qquad (7)$$

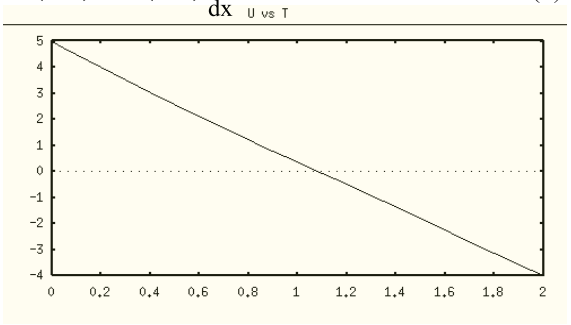

FIG. 3. A NON-LINEAR BOUNDARY VALUE PROBLEM

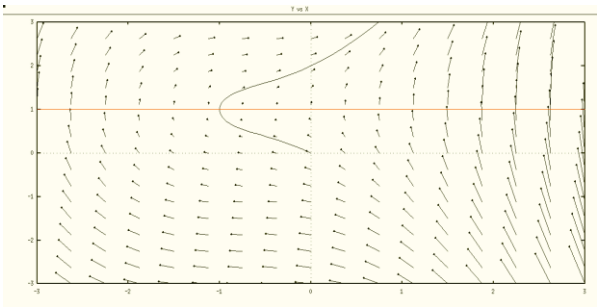

FIG. 4. DIRECTION FIELDS AND NULL CLINE

The equation selected for direction field is as Equation (8):

$$-(3x^2 + 4x + 2)\,dx + 2(y-1)dy = 0 \qquad (8)$$

(1) M(x,y) = - (3*x*x+4*x+2)
(2) N(x,y) = 2*(y- 1)
(3) dx/dt = N(x,y)
(4) dy/dt = - M(x,y)
(5) @ xp = x, yp = y, xlo = -5, xhi = 5, ylo = -5, yhi = 5
(6) done

In this section, qualitative attributes like direction fields and null clines are shown in Fig. 4. Null-cline is shown with red colored horizontal line while small lines with arrows indicate the direction field. Null cline is the curve where rate of change is zero. A solution curve is also plotted along with the said features.

4. DISCUSSION

The linear, non-linear differential equations and BVP were explored using XPPAUT. XPPAUT is a combination of XPP and AUTO [1-3]. It has been found great simulating software. It can interactively solve the given system of differential equations that means solution can be seen before the process termination, while MAPLE and MATHEMATICA are unable to do so [16-17]. AUTO is used for continuation and bifurcation of dynamical systems. In future its AUTO version will be explored.

AUTO option is available in XPP menu window that enable and prepare it for continuation and bifurcation analysis of the currently loaded problem. Continuation analysis describes the gradual development of solutions to differential equations over parameters, while bifurcation shows how solution curve appear and disappear as any of the system parameter is varied [1].

The qualitative methods i.e. phase portrait and directions fields give the general insight and interpretations of fluctuating dynamics of the system with perturbations in initial conditions and parametric variations [18-21]. The phase portrait in Fig. 5 describes the existence of any attractor, repeller and limit cycle with change of initial conditions and variations in parameters. In Fig. 5, we see limit cycle for different set of initial conditions.

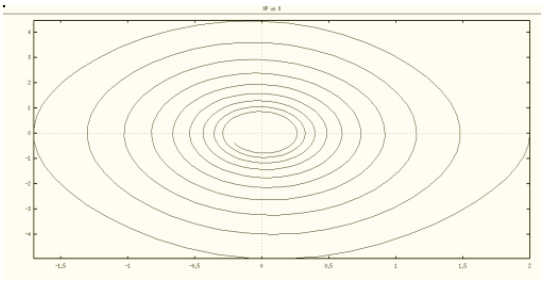

FIG. 5. SOLUTION CURVES OF SIMPLE PENDULUM

The direction field establishes a meaningful relation between the previous behaviors to the future response. The differential equation does not require analytical solution of the differential equations prior to generation of direction field. In Fig. 5 the small lines specify the flow direction to see the long term behavior of generic trajectories of an exact ODE [3].

5. CONCLUSION

The solution of ODEs has never been so easy. It requires analytical treatment of ODEs. Simulations need syntax familiarity and list of commands to execute a task. The main goal of the current study was to explore a simulator for dynamical systems. The mathematical treatment of differential equations with XPPAUT is found really straight forward. This software was explored, learned and found a powerful simulating tool for technical computing. Its user friendly, command oriented interface is easy to use. It does not require any proficiency in programming languages. The closed-form generic solutions are obtained with limited accuracy by employing methods named as direction field and isoclines. The same pair of differential equations has been simulated with said methods using MATLAB and XPPAUT. Null-Clines and Direction Filed has been plotted just by a click on null-cline and direction field options which are readily available on the main XPP window of XPPAUT. On contrast the plot of direction field in MATLAB needs a set of programming instructions i.e. “meshgrid” and “quiver” for every problem involving differential equations. System involving linear, non-linear ordinary differential equations and BVPs has been studied and solution curves have been discussed.

ACKNOWLEDGEMENT

The research work is supported by University of Engineering and Technology Lahore, Lahore, Pakistan. Authors are also thankful to our reviewers for their time and effort.

REFERENCE

[1] Ermentrout, B., "Xppaut", Scholarpedia, Volume 2, pp. 1399, 2007.

[2] Ermentrout, B., "Simulating, Analyzing, and Animating Dynamical Systems: A Guide to XPPAUT for Researchers and Students, Society of Indian Automobile Manufacturers, Volume 14, 2002.

[3] Ermentrout, B., "XPPAUT 5.0 - The Differential Equations Tool", Ph.D., Thesis, University of Pittsburgh, Pittsburgh, USA, 2001.

[4] Kreyszig, E., "Advanced Engineering Mathematics" 10th Edition, Wiley, 2010.

[5] Burkard, E., "Introduction to Ordinary Differential Equations and Some Applications", Create Space Independent Publishing Platform, 2014.

[6] Wasow, W., Asymptotic Expansions for Ordinary Differential

Equations", Courier Dover Publications, 2018.

[7] Grimshaw, R., "Nonlinear Ordinary Differential Equations", Routledge, 2017.

[8] Chonacky, N., and Winch, D., "Maple, Mathematica, and Matlab: The 3M's Without the Tape", IEEE Computer Society, 2005.

[9] Moore, H., "MATLAB for Engineers", Pearson, 2017.

[10] Abbena, E., Salamon, S., and Gray, A., "Modern Differential Geometry of Curves and Surfaces with Mathematica", Chapman and Hall/CRC, 2017.

[11] Gander, W., and Hrebicek, J., "Solving Problems in Scientific Computing Using Maple and Matlab®", Springer Science & Business Media, 2011.

[12] Iqbal, S., Sher, H.A., and Qureshi, S., "Pspice in Undergraduate and Graduate Electrical Engineering Courses", New Horizons, Journal of the Institution of Electrical and Electronics Engineers Pakistan, Volume 57, pp. 18-20, 2007.

[13] Rashid, M.H., "Introduction to PSpice Using OrCAD for Circuits and Electronics", Prentice-Hall Inc, 2003.

[14] Doedel, E., "AUTO: Software for Continuation and Bifurcation Problems in Ordinary Differential Equations; Including the AUTO 86 User Manual", California Institute of Technology, 1986.

[15] Doedel, E.J., Paffenroth, R.C., Champneys, A.R., Fairgrieve, T.F., Kuznetsov, Y.A., Oldeman, B.E., Sandstede, B.J., and Wang, X., "AUTO 2000: Continuation and Bifurcation Software", Concordia University, Montreal, Canada, 2002.

[16] Cai, L.-W., "Using Matlab to Enhance Engineering Students' Analytical Problem-Solving Skills", ASME International Mechanical Engineering Congress and Exposition, pp. 503-512, 2007.

[17] Iqbal, S., Qureshi, S.A., Rizvi, T.H., Abbas, G., and Gulzar, M.M., "Concept Building through Block Diagram Using Matlab/Simulink," New Horizons, Journal of the Institution of Electrical and Electronics Engineers Pakistan, Volume 66, pp. 4-7, 2010.

[18] Semwal, V.B., and Nandi, G.C., "Toward Developing a Computational Model for Bipedal Push Recovery - A Brief", IEEE Sensors Journal, Volume 15, pp. 2021-2022, 2015.

[19] Wornle, F., Harrison, D.K., and Zhou, C., "Analysis of a Ferroresonant Circuit Using Bifurcation Theory and Continuation Techniques", IEEE Transactions on Power Delivery, Volume 20, pp. 191-196, 2005.

[20] Omaiye, O.J., and Mohd, M.H., "Computational Dynamical Systems Using XPPAUT", SEAMS School on Dynamical Systems and Bifurcation Analysis, pp. 175-203, 2018.

[21] Weiwang, K., and Qizhi, Y., "The Application of XPPAUT in Systems Biology", Computers and Applied Chemistry, pp. 9, 2015

Subspace Aided Parity-Based Robust Data-Driven Fault Detection in Pakistan Research Reactor-2

Muhammad Asim Abbasi*, Abdul Qayyum Khan*, Muhammad Abid*, and Aadil Sarwar Khan*
* Pakistan Institute of Engineering & Applied Sciences, Islamabad, Pakistan.
engrasimabbasi@gmail.com, aqkhan@pieas.edu.pk ,mabid@pieas.edu.pk, adilsarwar20@gmail.com

ABSTRACT

This article is concerned with FD (Fault Detection) in PARR-2 (Pakistan Research Reactor-2) using a subspace aided parity-based FD scheme. The safety is of vital importance for nuclear reactors and in time fault diagnosis is necessary for safe operation. Conventional model-based FD approaches required the mathematical model of the process. For complex systems like nuclear reactors, the modeling of the system is too much complicated. Due to the availability of huge process data of the reactor and largely inaccessibility moreover as the complexity of the process model, data-driven approaches are effective fault diagnosis techniques for reactors. Subspace aided parity-based data-driven FD approach is a simple, efficient FD approach and has required less online computations. By using a subspace-aided approach, an optimized parity vector is identified directly from the process data instead of the identification of the system model. The identified parity vector is utilized to compute residual generator that ensures robustness against system noises and disturbances and sensitivity to faults. The parity-based FD scheme is successfully implemented for PARR-2. Two possible faults in PARR-2 that are external reactivity insertion fault and control rod withdrawal fault are considered and detected successfully. GLR (Generalized Likelihood Ratio) based threshold setting is used for efficient FD and reduce false fault detection rate.

Key Words: Fault Detection, Data-Driven, Pakistan Research Reactor-2.

1. INTRODUCTION

Nuclear power plants have become predominant supporters of the energy resources of the world. They are generating about 11% of world energy IEA (International Energy Agency) [1]. Presently, almost 450 nuclear power plants are in operation and these numbers are increasing. Nuclear energy is clean, competitive, safe and reliable among other resources [2].

It is of vital importance to decrease and prevent the hazards of faults occurring within a nuclear reactor. The improvement in safety and capacity factor of a nuclear reactor is of central importance. Some certain preventive measure must be there to deal with critical issues in nuclear reactors. Three Mile Island accident [3] drew the attention of researchers towards the application of FD methods for consistent and safe operation of nuclear reactors. In that accident, the recovery procedure became complicated because of the complex alarm and indicator system. This complex system confused the reactor operational crew and they failed in recognizing the alarms and indications properly.

Model-based FD techniques are well-established and effective techniques in fault diagnosis [4-6]. These approaches depend vigorously upon accessible system model. The residual signal is constructed by comparing the output of the process and the estimated output of the analytical process model, which shows the information of fault. Model-based techniques are effective for those systems whose mathematical model is available. It is noticed that for majority of the industrial processes, modeling demands considerable engineering efforts and in some cases becomes impractical. For industrial processes, the data-driven FD approaches have been developed which do not oblige the process models a priori for developing FD systems. Over the previous decade, momentous advancement has been done in the domain of data-driven fault diagnosis [7-12]. Data-driven schemes are most appropriate for fault diagnosis of nuclear reactors, as most of the times model is unavailable and complex, meanwhile, the huge amount of input and sensor output data is available during the operation that can be used to design fault diagnosis strategy.

Among data-based FD schemes, PCA (Principal Component Analysis), FDA (Fisher Discriminant Analysis) and KFDA (Kernel Fisher Discriminant Analysis) have been successfully practiced in PARR-2 [10-11]. But these techniques involve huge online computation and also mostly faulty data is unavailable while for FDA and KFDA both healthy and faulty data are required. Remarkable work has been made by Ding et. al. [13], Wang et. al. [14], Hussain et. al. [15] and Tariq et. al. [16] in parity-based data driven approach. Nuclear reactors have a complex model and access to model is not available. Due to inaccessibility and complexity of the model, the data-driven FD schemes are well suited for nuclear reactors. Among data-driven FD schemes, parity-based data-driven FD approach is easy and simple for implementation; it also required only fault-free data for processing and less online computation that is why this approach is most suitable for FD in PARR-2.

In this article, a subspace-aided parity-based data-driven FD strategy is implemented for FD in PARR-2. The data samples are collected in fault-free conditions and under two faults i.e. external reactivity insertion and control rod withdrawal faults due to safety limitations. This fault detection approach is effective, simple and involves least online computations. It also shows robustness against

disturbances and sensor noises. Generalized likelihood ratio based threshold setting is used for FD decision that also reduces the false alarm rate.

The forthcoming discussion in this article is classified as: In Section-2 review of subspace aided parity based data-driven technique is discussed then PARR-2is briefly explained in Section-3. Section-4 justifies the application of FD scheme employed in PARR-2 and its simulation results. At last, the conclusion is presented in Section-5.

2. REVIEW OF SUBSPACE AIDED DATA DRIVEN BASED FAULT DETECTION TECHNIQUE

Ding et. al. [13] proposed data-based parity space algorithm, then remarkable progress has been done in this direction by Wang et. al. [14], Hussain et. al. [15] and Tariq et. al. [16].

Consider a discrete LTI system given as:

$$\mathrm{x(k+1)} = \tilde{\mathrm{G}}\mathrm{x(k)} + \tilde{\mathrm{H}}(\mathrm{u(k)} + \mathrm{f_a(k)}) + \mathrm{w(k)}$$
$$\tilde{\mathrm{y}}\mathrm{(k)} = \tilde{\mathrm{C}}\mathrm{x(k)} + \tilde{\mathrm{D}}(\mathrm{u(k)} + \mathrm{f_a(k)}) + \mathrm{v(k)} + \mathrm{f_s(k)} \quad (1)$$

Here, $\tilde{G} \in R^{n\times p}, \tilde{H} \in R^{n\times \ell}, \tilde{C} \in R^{m\times n}, \tilde{D} \in R^{m\times \ell}. x(k) \in R^{n\times 1}$ is state vector, $u(k) \in R^{\ell\times 1}$,is input vector, $f_a(k)$, $f_s(k)$ are actuator and sensor fault vectors respectively and w(k), v(k) are disturbance and noise respectively.

As from (1)

$$\tilde{\mathrm{y}}\mathrm{(k-1)} = \tilde{\mathrm{C}}\mathrm{x(k-q)} + \tilde{\mathrm{D}}(\mathrm{u(k-q)} + \mathrm{f_a(k-q)}) + \mathrm{v(k-q)} + \mathrm{f_s(k-q)} \quad (2)$$

whereq ≥ 0. Similarly

$$\tilde{\mathrm{y}}\mathrm{(k-q+1)} = \tilde{\mathrm{C}}\mathrm{x(k-q+1)} + \tilde{\mathrm{D}}(\mathrm{u(k-q+1)} + \mathrm{f_a(k-q+1)}) + \mathrm{v(k-q+1)} + \mathrm{f_s(k-q+1)} \quad (3)$$

$$= \tilde{\mathrm{C}}\mathrm{x(k-q)} + \tilde{C}\tilde{B}u(k-q) + \tilde{C}\tilde{B}f_a(k-q) + \tilde{C}w(k-q) + \tilde{D}(u(k-q+1) + f_a(k-q+1)) + v(k-q+1) + f_s(k-q+1) \quad (4)$$

$$\vdots$$

$$\tilde{y}(k) = \tilde{C}\tilde{G}x(k-q) + \tilde{C}\tilde{G}^{q-1}\tilde{H}u(k-q) + \tilde{C}\tilde{G}^{q-2}\tilde{H}u(k-q+1)\ldots.$$
$$+ \tilde{C}\tilde{H}u(k-1) + \tilde{C}\tilde{G}^{q-1}\tilde{H}f_a(k-q) + \tilde{C}\tilde{H}^{q-2}(k-q+1)\ldots.$$
$$+ \tilde{C}\tilde{H}f_a(k-1) + \tilde{C}\tilde{H}^{q-1}w(k-q) + \tilde{C}\tilde{G}^{q-2}w(k-q+1)\ldots$$
$$+ \tilde{C}\tilde{H}f_a(k-q+1) + \tilde{C}\tilde{G}w(k-q) + \tilde{C}w(k-1) + \tilde{D}(u(k) + f_a(k)) + f_s(k)$$

From above expression it can be combined as:

$$\tilde{y}(k) = \Gamma_s x(k-q) + T_{uq}\left(u_q(k) f_{aq}(k)\right) + .T_{dq} w_q(k) + v_q(k) \quad (5)$$

where

$$\Gamma_q = \begin{bmatrix} \tilde{C} \\ \tilde{C}\tilde{G} \\ \vdots \\ \tilde{C}\tilde{G}^q \end{bmatrix}, u_q(k) = \begin{bmatrix} u(k-q) \\ u(k-q+1) \\ \vdots \\ u(k) \end{bmatrix}, f_{aq}(k) = \begin{bmatrix} f_a(k-q) \\ f_a(k-q+1) \\ \vdots \\ f_a(k) \end{bmatrix}$$

$$, w_q(k) \begin{bmatrix} w(k-q) \\ w(k-q+1) \\ \vdots \\ w(k) \end{bmatrix} \quad (6)$$

$$\tilde{y}_q(k) = \left[\tilde{y}(k-q)\tilde{y}(k-q+1)\ldots\tilde{y}(k)\right]^T$$

$$T_{uq} = \begin{bmatrix} \tilde{D} & 0 & \cdots & 0 \\ \tilde{C}\tilde{H} & \tilde{D} & \ddots & 0 \\ \vdots & \ddots & \ddots & 0 \\ \tilde{C}\tilde{G}^{q-1}\tilde{H} & \cdots & \tilde{C}\tilde{H} & \tilde{D} \end{bmatrix}, T_{dq} = \begin{bmatrix} 0 & 0 & \cdots & 0 \\ \tilde{C} & 0 & \ddots & 0 \\ \vdots & \ddots & \ddots & 0 \\ \tilde{C}\tilde{G}^{q-1}\tilde{H} & \cdots & \tilde{C} & 0 \end{bmatrix} \quad (7)$$

For subspace based data driven technique (5) could be modified as:

$$\tilde{Y}_f = \Gamma_q \tilde{X}_i + T_{uq}^i \tilde{U}_f + T_{dq}^i W_f + N_f \quad (8)$$

where, T_{uq}^i, T_{dq}^i are lower block Toeplitz deterministic and stochastic matrices respectively. W_f and N_f are disturbance and noise block hankel matrices respectively.

Equation (8) can also be expressed in the form

$$\tilde{Z}_f = \begin{bmatrix} \tilde{Y}_f \\ \tilde{U}_f \end{bmatrix} = \begin{bmatrix} \Gamma_q & T_{uq}^i \\ 0 & I \end{bmatrix} \begin{bmatrix} \tilde{X}_i \\ \tilde{U}_f \end{bmatrix} + \begin{bmatrix} T_{dq}^i W_f + N_f \\ 0 \end{bmatrix}$$

By post multiplying with $\tilde{Z}_p^T$ on both sides and dividing by N, above equation will becomes:

$$\frac{1}{N}\tilde{Z}_f\tilde{Z}_p^T = \frac{1}{N}\begin{bmatrix} \Gamma_q & T_{uq}^i \\ 0 & I \end{bmatrix} \begin{bmatrix} \tilde{X}_i \\ \tilde{U}_f \end{bmatrix} \tilde{Z}_p^T = \frac{1}{N}\Theta\tilde{Z}_p^T, \Theta = \begin{bmatrix} T_{dq}^i W_f + N_f \\ 0 \end{bmatrix}$$

Singular value decomposition of $\frac{1}{N}\tilde{Z}_f\tilde{Z}_p^T$ will be used to extract parity space $\alpha_q = \Gamma_q$ and $\Gamma_q T^i{}_{uq}$..

$$\frac{1}{N}\tilde{Z}_f\tilde{Z}_p^T = \tilde{U}_z E_z \tilde{V}_z, \tilde{U}_z = \begin{bmatrix} \tilde{U}_{z11} & \tilde{U}_{z12} \\ \tilde{U}_{z21} & \tilde{U}_{z22} \end{bmatrix}, \quad (9)$$

$$\Gamma_q^\perp + \tilde{U}_{z12}^T, \Gamma_q^\perp + \tilde{U}_{uq}^i = \tilde{U}_{z22}^T$$

$$I = \frac{\Gamma_q^\perp T_{uq}^i T_q^{iT} \Gamma_q^\perp}{\Gamma_q^\perp T_{dq}^i T_{dq}^{i\,T} \Gamma_q^\perp} \quad (10)$$

As an Eigen value problem, the solution of Equation (10) will be:

$$\ell_{q,\min}\left(\Gamma_q^\perp T_{dq}^i T_{dq}^{i\,T} \Gamma_q^\perp - \lambda_{q,\min}\Gamma_q^\perp T_{uq}^i T_{uq}^{i\,T} \Gamma_q^\perp\right) \quad (11)$$

where, $\ell_{q,\min}$ is minimum Eigen vector, $\lambda_{q,\min}$ is minimum Eigen value, and $\alpha_q = \ell_{q,\min}\Gamma_q^\perp$ is optimal robust \parity vector.

The core element of FDI is the generation of residualsγ(k).

$$\gamma(k) \neq 0 \text{ if } f(t) \neq 0 \quad (12)$$

Residual is computed by the following relation.

$$\gamma(k) = \alpha_k \left(\tilde{y}_q(k) - T_{uq} u_q \right) \quad (13)$$

Where α_q is optimal robust parity vector. From Equations (5) and Equation (13) the residual generator in the existence of disturbances and noises can be composed as:

$$\gamma(k) = \alpha_q \left(T_{uq} f_{aq}(k) + T_{dq} w_q(k) + v_q(k) + f_s(k) \right) \quad (14)$$

ALGORITHM-1 SUBSPACE AIDED PARITY SPACE FAULT DETECTION

Step-1: Store n fault free input-output samples.

Step-2: Construct past and future input-output block hankel matrices and build $\tilde{Z}_p$ and $\tilde{Z}_f$.

Step-3: Perform SVD on $\frac{1}{N} \tilde{Z}_f \tilde{Z}_p^T$.

Step-4: Extract the terms $\Gamma_q^{\perp}$ and $\Gamma_{quq}^{\perp} T_{uq}^{i}$ using Equation (9).

Step-5: Find optimal robust parity vector using Equations (10-11).

Step-6: Compute residual using Equation (13).

3. PAKISTAN RESEARCH REACTOR-2

PARR-2 an indigenously developed tank in pool type reactor capacity of 27-30 kW. The reactor is operating since 1991. It is a miniature neutron source reactor which operating with a 90% enriched fuel based on U-235. The fuel material consists of U-Al Alloy (UAl_4 – Al). Light water used for both cooling and neutron moderation purpose. Whereas heavy water, beryllium and graphite are used as neutron reflectors. The maximum thermal flux and maximum fast flux are rated as $10e^{+13}$ and $107e^{+14}$ n/cm^2s. It has a total number of 344 fuel rods along with control rods, 6 tie rods and 4 other dummy rods. The control rods are developed with Cd (Cadmium). The PARR-2 has been used to produce radio isotopes [17].

PARR-2 has a negative temperature coefficient due to its under- moderated core array. Therefore, the reactivity diminishes with increase in temperature, which damps the power excursions. Another salient feature of the reactor is its lower overabundance reactivity. The lower excess reactivity of core eliminates the danger of any critical incident. Thus provides additional benefits of safety. During exchange of heat between coolant and fuel an expansion in the coolant temperature is observed because the negative arbitrator coefficient of reactor minimizes the undue reactivity.

The most widely recognized faults that may happen amid the operations are control rod withdrawal and coincidental external reactivity insertion. Movement of control rod controlled the reactivity in core. Control rod withdrawal causes the insertion of positive reactivity that upgrade the power and fuel temperature. Because of inalienable safe attributes, this power outing will confine itself to 87 kW, fuel and clad temperature are beneath the immersion temperature of water. The examples are normally illuminated in the light locales amid tests. In these tests, if a fissile material case is implanted fortuitously in one among the brightening goals then reactivity is introduced in the core, state of flux can increase and power outgoing can happen that can increase the fuel and clad temperature.

4. APPLICATION OF FAULT DETECTION SCHEME IN PARR-2

The input-output data is acquired from accessible sensors of PARR-2 in both fault free and faulty case. Control rod withdrawal and external reactivity faults are introduced in PARR-2 and 120 measurements are recorded in presence of each fault. The inlet, outlet, pool temperatures and pool conductivity data collected from sensors. Reactivity and neutron flux are considered as actuators inputs. Observations were recorded under normal conditions in steady state with sampling time of 1 sec. The control rod was up to 15% to introduce control rod withdrawal fault and external reactivity was inserted for addition of external reactivity fault. Under each fault condition 120

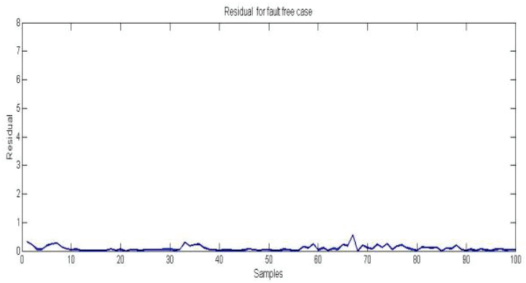

FIG. 1. RESIDUAL FOR NON-FAULTY CASE

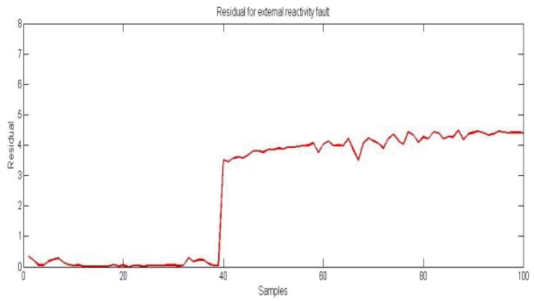

FIG. 2. RESIDUAL FOR EXTERNAL REACTIVITY FAULT

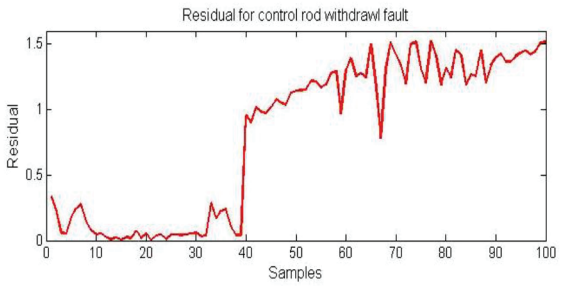

FIG. 3. RESIDUAL FOR CONTROL ROD WITHDRAWAL FAULT

measurements were recorded. The data of PARR-2 is taken from our references [10,17].

$$\tilde{Y} \in R^{4\times120}, \tilde{U} \in R^{2\times120}, \tilde{Y}_p, \tilde{Y}_f \in R^{24\times109} \text{ and } \tilde{U}_p \tilde{U}_f \in R^{12\times109}$$

Fig. 1 indicates the residual in non-faulty case. Then external reactivity fault is inserted from sample 40 to onward, Fig. 2 indicates the presence of external reactivity fault at sample 40. Fig. 3 shows the residual when control rod withdrawal fault is introduced at sample 40.

For successful FD and reduced false FD rate threshold is used. Residual is also effected by noise and disturbances that's why threshold setting is important for successful FD. Fault will occur if residual exceed the threshold level. GLRbased threshold setting is utilized here. GLR is explained in [4,18]. Steps for GLR based threshold setting for false detection rate<α and noise is assumed to be normal distributed $N(0,\sigma^2_r)$ is mentioned in Algorithm-2.

ALGORITHM-2 GLR BASED THRESHOLD SETTING [4]

Step-1: Find X_a .e. $P[X^2>X_a] = \alpha$ using chi-square distribution.

Step-2: Set threshold as: $J_{TH} = H_a/2$..

Step-3: The testing statistic is computed as: $J = \frac{1}{2\sigma_e^2 N}\left(\sum_{i=1}^{N}\gamma(i)^2\right)$ where, $\gamma(i)$is residual of i^{th} sample.

Step-4: Fault will be occurred if $J > J_{TH}$..

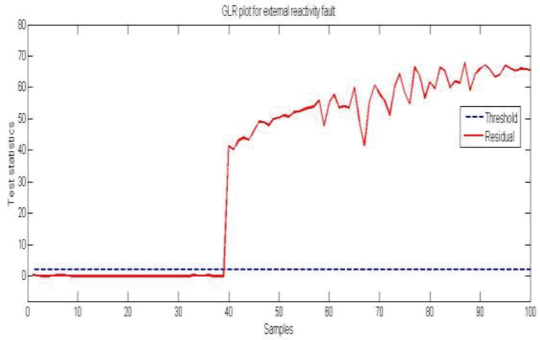

FIG. 4. GLR PLOT FOR EXTERNAL REACTIVITY FAULT

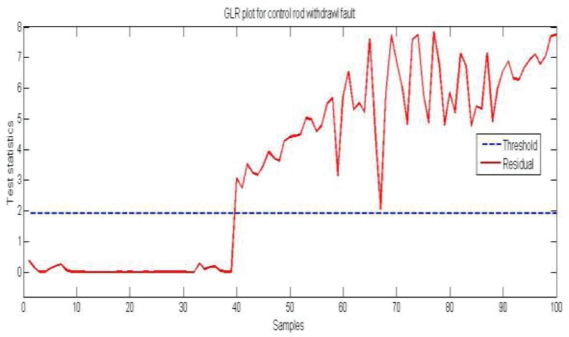

FIG. 5. GLR PLOT FOR CONTROL ROD WITHDRAWAL FAULT

GLR plots are presented in Figs. 4-5. Fig.4 indicates the residual plot in the presence of external reactivity fault and Fig.5 indicates the residual in the presence of control rod withdrawal fault. In the case of both faults, it indicates that when a fault occurs at sample 40 the residual across the threshold level. External reactivity and control rod withdrawal faults both are successfully detected. There are no false fault detection or miss fault detection as shown in Fig. 4-5.

Compared with the results of [10] the false alarm rate using this technique is reduced. The main advantage of using parity-based approach is it reduces online computation. For preprocessing faulty data is not mandatory as required in FDA, and KFDA. Performance index used to diminish the influences of disturbances and sensor noises on residual that increases the effectiveness of algorithm and becomes robust against disturbances.

5. CONCLUSION

In this article, the subspace-aided data-driven FD technique is successfully applied in PARR-2. The more possible faults i.e. external reactivity and control rod withdrawal faults are introduced and tested using this FD approach. Subspace aided parity-based FD technique is effective and simple in implementation for FD in PARR-2. It reduces the online computations as compared to PCA, FDA, and KFDA. It depends only on fault-free process data and information about the system model is not required. To address the issue of disturbances and sensor noise, an optimal parity vector is identified that minimizes the effect of disturbances and enhances faults effects on residual. The results demonstrate the effectiveness of the technique for PAAR-2.

6. FUTURE WORK

In future, the work can be extended to identify the level of fault so that it can be tolerated as much as it is possible.

ACKNOWLEDGEMENT

The research work is supported by Pakistan Institute of Engineering & Applied Sciences, and Higher Education Commission, Islamabad, Pakistan.

REFERENCES

[1] Energy Information Administration (US) and Government Publications Office, International Energy Outlook 2016: With Projections to 2040, Government Printing Office, 2016.

[2] Hashemian, H.M., "On-Line Monitoring Applications in Nuclear Plants", Progress in Nuclear Energy, Volume 53, No. 2, pp. 167-181, 2011.

[3] Zhao, K., "An Integrated Approach to Performance Monitoring and Fault Diagnosis of Nuclear Power Systems", Ph.D. Thesis, University of Tennessee, 2005.

[4] Ding, S.X., "Model-Based Fault Diagnosis Techniques: Design Schemes, Algorithms, and Tools", Springer Science & Business Media, 2008.

[5] Isermann, R., "Model-Based Fault-Detection and Diagnosis–Status and Applications", Annual Reviews in Control, Volume 29, No. 1, pp. 71–85, 2005.

[6] Abid, M., Chen, M., Ding, S.X., and Khan, A.Q., "Optimal Residual Evaluation for Nonlinear Systems Using Post-Filter and Threshold", International Journal of Control, Volume 84, No. 3, pp. 526–539, 2011.

[7] Chiang, L.H., Russell, E. L., and Braatz, R.D., "Fault Detection and Diagnosis in Industrial Systems", Springer Science & Business Media, 2000.

[8] Yin, S., Yang, X., and Karimi, H.R., "Data-Driven Adaptive Observer for Fault Diagnosis", Mathematical Problems in Engineering, 2012.

[9] Yin, S., Ding, S.X., Abandan, S.A.H., and Hao, H., "Data-Driven Monitoring for Stochastic Systems and Its Application on Batch Process", International Journal of Systems Science, Volume 44, No. 7, pp. 1366–1376, 2013.

[10] Jamil, F., Abid, M., Haq, I., Khan, A.Q., and Iqbal, M., "Fault Diagnosis of Pakistan Research Reactor-2 with Data-Driven Techniques", Annals of Nuclear Energy, Volume 90, pp. 433–440, 2016.

[11] Jamil, F., Abid, M., Adil, M., Haq, I., Khan, A.Q., and Khan, S., "Kernel Approaches for Fault Detection and Classification in PARR-2", Journal of Process Control, Volume 64, pp. 1–6, 2018.

[12] Yin, S., Ding, S.X., Haghani, A., Hao, H., and Zhang, P., "A Comparison Study of Basic Data-Driven Fault Diagnosis and Process Monitoring Methods on the Benchmark Tennessee Eastman Process", Journal of Process Control, Volume 22, No. 9, pp. 1567–1581, 2012.

[13] Ding, S.X., Zhang, P., Naik, A., and Huang, B., "Subspace Method Aided Data-Driven Design of Fault Detection and Isolation Systems", Journal of Process Control, Volume 19, No. 9, pp. 1496–1510, 2009.

[14] Wang, Y., Ma, G., Ding, S.X., and Li, C., "Subspace Aided Data-Driven Design of Robust Fault Detection and Isolation Systems", Automatica, Volume 47, No. 11, pp. 2474–2480, 2011.

[15] Hussain, A., Khan, A.Q., and Abid, M., "Robust Fault Detection Using Subspace Aided Data Driven Design", Asian Journal of Control, Volume 18, No. 2, pp. 709–720, 2016.

[16] Tariq, F., Khan, A.Q., Abid, M., and Mustafa, G., "Data-Driven Robust Fault Detection and Isolation of Three Phase Induction Motor", IEEE Transactions on Industrial Electronics, Volume 66, No. 6, pp. 4707–4715, 2018.

[17] Iqbal, M., Abdullah, M., and Pervez, S., "Parametric Tests and Measurements After Shimming of a Beryllium Reflector in a Miniature Neutron Source Reactor (MNSR)", Annals of Nuclear Energy, Volume 29, No. 13, pp. 1609–1624, 2002.

[18] Qin, S.J., and Li, W., "Detection and Identification of Faulty Sensors in Dynamic Processes", AIChE Journal, Volume 47, No. 7, pp. 1581–1593, 2001.

Mixed Sensitivity H∞Controller Design for Force Tracking Control of Electro-Hydraulic Servo System

Umair Javaid*, Syed Abdul Rahman Kashif*, Ali Ahmad, Noor-ul-ain, And Salman Fakhar***
*Department of Electrical Engineering, University of Engineering &Technology, Lahore, Pakistan.
**Department of Electrical Engineering, University of Central Punjab, Lahore, Pakistan.
engr_umair16@hotmail.com, abdulrahman@uet.edu.pk, a.ahmad@ucp.edu.pk, noorulain0412@gmail.com, salmanfakhar.uet@gmail.com

ABSTRACT

The paper presents the mixed sensitivity H∞ controller design for force tracking control of EHSS (Electro-Hydraulic Servo System). The system is inherently nonlinear and includes hard non linearity like relationship between pressure and flow rate that effect system dynamics and deteriorate the nominal behavior of the system. To cope with such nonlinear function and improve the system performances, a mixed sensitivity H∞controller is designed using MIXSYN tool in MATLAB. The nonlinear model of EHSS is first linearized into 2nd order LTI (Linear Time Invariant) model and H∞ controller is designed. The weighting filters are included to improve the performance of system. The MATLAB function MAGSHAPE is used to tune the weight functions so that desirable gain and phase margin could be achieved. Simulation results on linear and nonlinear system show the better force tracking as compared to other robust control techniques. The proposed technique is found robust in the presence of disturbance.

Key Words: Electro-Hydraulic Servo System, Linear Time Invariant, Weighting Function, H∞ Controller.

1. INTRODUCTION

EHSS is being used worldwide in several fields of engineering for position or force servo applications due to the fact that it has small volume, swift response, controlling signals flexibly, high arduousness and huge output power [1]. Due to growing demand of EHSS, the researchers paid special attention to achieve precise level in control of such system. Although, in designing the governor of EHSS several challenges appear which makes the task quite difficult. For instance, there are extremely unpredictable reasons like the flow-pressure and the dead band caused by internal outflow, hysteresis, and many more unpredictable behaviors due to linearization [2]. Hence, to the EHSM, a precise mathematical model is very tough to develop hypothetically and it is challenging for conventional PID (Proportional Integral Derivative)to provide effective control for servomechanism [3].

Enormous control techniques have been applied for position, velocity and forces/torques tracking control of EHSS.A brief review of force tracking control technique is presented in this section. The difficulties with EHSS drives are their nonlinear behavior and low damping; so the accurate control of these systems for particular applications is a difficult task to achieve [4].A layapunov based adaption scheme for force tracking control of EHSS is presented in [5-7] show worthwhile results. The proposed scheme found robust in the presence of parameter uncertainty and external disturbance.

Robust controller resides to the class of LTI system and has been studied intensively for the last two decades for position/force tracking control of EHSS [8-10]. Robust controller design preserves assurance of system performance regardless of the model inaccuracies and parameter variations. Robust controller, because of the independence on linear model of plant, guaranteed local stability.

The paper focused on special class of robust control technique in which H∞ controller is designed using mixed sensitivity approach. The proposed approach accounts non-linearity and model uncertainties in the presence of disturbance. Since the proposed approach is based upon LTI model of the system so the model is first linearized at operating point and then led for controller design.

The paper is structured as follows; Section 2 includes the calculated model for the system. Section 3 consists of the LTI model of EHSS. Section 4 discussed the design consideration of mixed sensitivity H∞ controller. Section 5 includes simulations results and finally the concluded remarks are given in section 6.

2. EHSM DISCRIPTION

The EHSM module consists of electronic drives, hydraulic actuators, and position transducers. The association between the piston position (X_p) and input voltage (u) for the servo valve is used for the development of an accurate mathematical model of EHSM servo valve [11]. The proportional valve, the asymmetric piston, controller and sensor are the main parts of control scheme. A force control servo mechanism of EHA (Electro Hydraulic Actuator) is shown in Fig. 1. The basic components of this EHSS include hydraulic supply, EHSM valve hydraulic piston, and a robust controller.

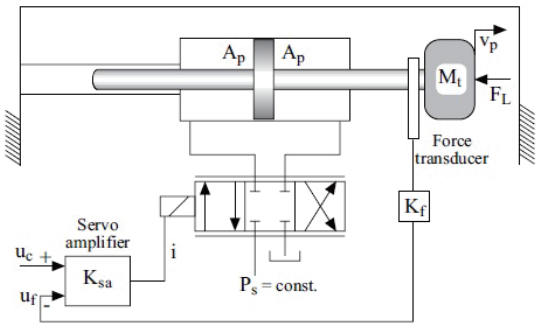

FIG. 1. EHSSFORCE TRACKING CONTROL SCHEME

2.1 System Modeling

The actual setup consists of double acting hydraulic cylinder and is connected to pressure supply thorough proportional valve. The motion of piston is due to the inflow of oil into the chamber and by controlling the oil flow in and out of the cylinder compartments its motion can be controlled. A proportional valve configuration is shown in Fig. 2. By regulating flow Q_1 and Q_2, the pressure delivered to the load can be controlled. However, the piston displacement (X_p), and the stream rates relationship rest on the changing aspects of the load applied on the piston [11].

The nonlinear mathematical representation of EHSS is model of hydraulic flow through orifice and is represented by Equation (1) as:

$$\frac{V_t}{4\beta_e}\dot{P}_L = -\dot{A}x - C_t P_L - Q_L \quad (1)$$

Where V_t is Actuator volume β_e is Effective Bulk Modulus, P_L is Load Pressure, x_p is Piston Position, C_t is Total Coefficient Leakage and Q_L is Load Pressure

For an ideal servo valve, the major non linearity exists between load pressure P_L and load flow Q_L, described by the relationship given in Equation (2) as:

$$Q_L = C_d w x_v \sqrt{\frac{P_s - \text{sign}(x_v)P_L}{\rho}} \quad (2)$$

Where C_d is Discharge Coefficient w is Gradient Area of spool, x_v is Spool Displacement.

The spool displacement x_v is actuated through some input signal u(s) and is described by 2nd order Equation (3).

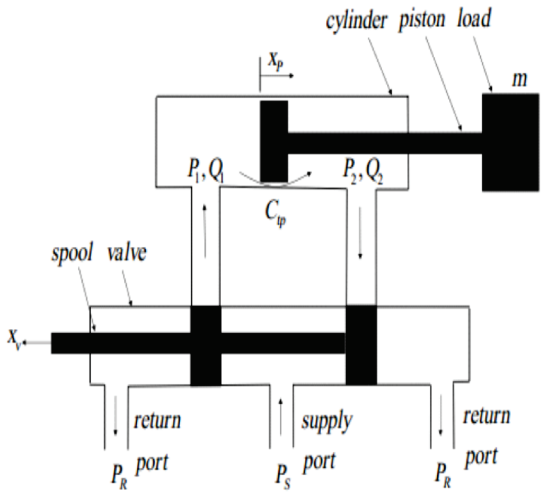

FIG. 2. EHSM FOUR-WAY VALVE CONFIGURATION

$$x_V(s)s^2 + 2\zeta\zeta_e x_v + x_v(s)\omega_e^2 = k_v u(s) \quad (3)$$

The relationship between spool displacements x_v to the input current i is also approximated to 1st order differential equation described in reference [1].

$$\tau_v \dot{x}_v = -X_v + K_v i \quad (4)$$

Where K_v and τ are gain and time constant of servo valve.

The force acting on the piston is derived by 2nd order equation,

$$F = P_L A = ms^2x(s) + Bsx(s) + K_v x(s) + F_f \quad (5)$$

P_L is the pressure delivered to the load, A is the area of cylinder, m is the mass attached to the piston and B is the damping coefficient, F_f is external disturbance load. From Equations (1-5) the system can be written in state space form as described in reference [9].

$$\dot{x}_1 = \dot{x}_2$$

$$\dot{x}_2 = \frac{1}{m}(-kx_1 - bx_2 + Ax_3)$$

$$\dot{x}_3 = \alpha x_2 - \beta x_3 + \gamma\sqrt{P_s - \text{sgn}(x_4)x_3}x_4 \quad (6)\quad \dot{x}_4 = -\frac{1}{\tau}x_4 + \frac{K}{\tau}u$$

Where states and inputs are; x_1 is Actuator Piston position, x_2 is Actuator Piston Velocity, x_3 is Load Pressure, x_4 is Valve Position, u is Input Current to Servo Valve, and Flow rate constants are:

$$\alpha = \frac{4\beta_e A}{V_t}$$

$$\beta = \frac{4C_{tm}\beta_e}{V_t}$$

$$\gamma = \frac{4C_d\beta_e w}{V_t\sqrt{\rho}}$$

System parameters are; m is Mass of actuator, k is Spring Constant, b is Damping Constant, K is DC Gain of Servo Valve

In order to capture the key component of system dynamics, a nonlinear model of system is designed in SIMULINK/MATLAB using s-function. That model is used for validation of mixed sensitivity controller.

3. LINEAR TIME INVARIANT MODEL OF EHSS

The LTI model of the system is presented in this section prior to design of controller. As discussed earlier that nonlinear model of EHSS contained some hard non linearity that contained function sgn(x) that is not differentiable at x=0. This would make the use of any feedback linearization approach impossible.

In practice, this is equivalent to designing two controllers for the two basic models corresponding to sgn(x) = 1 and sgn(x) = -1 and switching between them according to the sgn function. This leads to a variable structure controller, and it is seldom possible to prove that, in general, the corresponding closed-loop system will not chatter [12].
In practice, this approach has been found to work correctly. It must be noted, by the way, that the same dilemma is typical of most real-life applications: the design is made under assumptions which will never be met by the implementation. For instance, feedback linearization is mostly designed assuming a continuous controller; in practice, a digital controller will be used.

In the non-reduced model (2), the variable P_L is a state variable of a subsystem with input x_v. Therefore, replacement of the nonlinear term is given as:

$$\left(\sqrt{P_s} - \text{sgn}(x)x_3\right)x_4 \tag{7}$$

By applying the bilinear transformation the approximate expression becomes

$$x_4\left(P_s \frac{x_3}{2}\right) \tag{8}$$

3.1 Linear Approximation

One of the main limitations of this approximation is that the dominant hard nonlinearity of the system, which appears in the proportional valve flow Equation (2), is totally neglected. Using the above transformation, the nonlinear model, in fact, Equation (2) is approximated as:

$$\left(\sqrt{P_s} - \text{sgn}(x)x_3\right)x_4 = x_4 \tag{9}$$

The state space representation of the system is then given by the following equation.

$$\begin{bmatrix}\dot{x}_1\\ \dot{x}_2\\ \dot{x}_3\\ \dot{x}_4\end{bmatrix} = \begin{bmatrix}0 & 1 & 0 & 0\\ -\frac{k}{m} & -\frac{b}{m} & \frac{A}{m} & 0\\ 0 & -\alpha & -\beta & 0\\ 0 & 0 & 0 & -\frac{1}{\tau yy}\end{bmatrix}\begin{bmatrix}x_1\\ x_2\\ x_3\\ x_4\end{bmatrix} + \begin{bmatrix}0\\ 0\\ 0\\ \frac{K}{\tau}\end{bmatrix}u \tag{10}$$

$$y = \begin{bmatrix}1 & 0 & 1 & 0\end{bmatrix}\begin{bmatrix}x_1\\ x_2\\ x_3\\ x_4\end{bmatrix}$$

Where

$$\alpha = \frac{4A\beta_e}{V_t} = 3.6\times10^{-11}$$

$$\beta = \frac{4C_{tm}\beta_e}{V_t} = 7.6\times10^{8}$$

$$\gamma = \frac{4C_d\beta_e\omega}{V_t\sqrt{P}} = 2.917\times10^{9}$$

A 2nd transfer function of the EHSS with the current u(s) input to the system and force F(s) act as an output:

$$\frac{F(s)}{u} = \frac{0.0119}{S^2 + 563.33s + 1.809} \tag{11}$$

4. CONTROLLER DESING

4.1 Mixed Sensitivity H∞ Controller

This section presents the design procedure for H∞ controller using mixed sensitivity technique. Since the LTI model of the system is 2nd order so the proposed controller is the sum of order of plant and weighting functions [12]. Weighting function W_1, W_2 and W_3 are introduced in the system in order to improve the stability margin and robust performance of system in the presence of parametric uncertainty [13]. The design procedure is discussed in coming sections.

4.2 Norms

H_∞ Norm for continuous time stable LTI system "G(s)"are defined using singular values of G(jw) as:

$$H_\infty \text{norm} : \|G\|_\infty = \text{Sup}\,\sigma_{i,\max}\left[G(j\omega)\right]$$

For controller design, consider a CL (Closed-Loop) system shown in Fig. 3. Where r(t) is reference input, d(t) is the disturbance signal and n(t) is the measurement noise. The controlled output is define as:

$$y = Gu + d \tag{12}$$

Where

$$u = K(r-y) \tag{13}$$

Using Equation (3) in Equation (2), we can write as:

$y = GK(r-y) + d$

Or we have:

$(1+GK)y = GK_r + d$

So controlled output

$y = (I+GK)^{-1}GKr + (I+GK)^{-1}d$

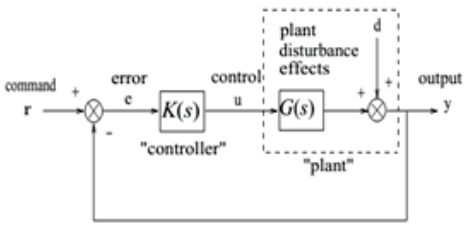

FIG.3. BLOCK DIAGRAM OF FEEDBACK CONTROL OF SISO SYSTEM

Stability performance and margins of feedback control of system given in Fig. 3, can be quantified using singular values of transfer function from "r" to outputs e, u and y that is represented by following expressions:

$$S(s) = (I + G(s) * K(s))^{-1}$$
$$R(s) = K(s)(I + G(s) * K(s))^{-1}$$
$$T(s)\, G(s) * K(s)(I + G(s) * K(s))^{-1}$$
$$T(s) + I - S(s)$$

Where S(s) is sensitivity function and T(s) is complement sensitivity function where as R(s) has no common name. S(s), T(s) and R(s) are very important for stable control system design.

4.3 Disturbance Rejection Performance

Disturbance rejection performance is determined by singular value of S(jω). Where S(jω) is transfer function of close loop from disturbance d to output y. Disturbance rejection performance is:

$$\sigma_{i,max}\left[S(jw)\right] \le \left|W_1^{-1}(jw)\right| \quad (14)$$

$\left|W_1^{-1}(jw)\right|$ is required disturbance rejection factor

4.4 Additive and Multiplicative Robustness

Singular value bode plots for T(s) and R(s) gives measure of stability margins for feedback design of additive and multiplicative uncertainties of plants [14]. Multiplicative stability margin can be defined as the smallest stable $\Delta_m(s)$ that stabilizes system for Δ_4. System with perturbation is shown in Fig. 4.

Taking $\sigma_{i,max}\left[\Delta_m(jw)\right]$ then multiplicative robust stability margins of system can be defined by following Equation (15) as:

$$\sigma_{i,max}\left[\Delta_m(j\omega)\right] = \frac{1}{\sigma_{i,max}\left[T(jw)\right]} \quad (15)$$

Lower value of $\sigma_{i,max}\left[T(jw)\right]$ will result large $\sigma_{i,max}\left[\Delta_m(j\omega)\right]$ i.e. large stability margins. Similarly additive robust stability margins of system can be defined as:

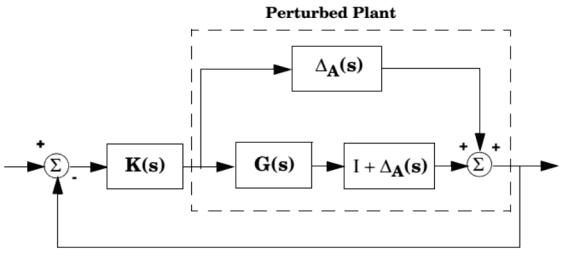

FIG. 4. UNCERTAINTIES IN SYSTEM

$$\sigma_{i,max}\left[\Delta_A(j\omega)\right] = \frac{1}{\sigma_{i,max}\left[R(jw)\right]} \quad (16)$$

From Equations (2-3) singular values based stability margin of feedback control are given as:

$$\sigma_{i,max}\left[R(jw)\right] \le \left|W_2^{-1}(jw)\right| \quad (17)$$

$$\sigma_{i,max}\left[T(jw)\right] \le \left|W_3^{-1}(jw)\right| \quad (18)$$

Where $\left|W_2^{-1}(jw)\right|$ and $\left|W_3^{-1}(jw)\right|$ is size of largest possible additive and multiplicative plant perturbation. The effects of all perturbations are combined into multiplicative perturbation. Performance specification given in Equation (14) and stability robustness specification given in Equation (17-18) are combined to get single infinity norm as:

$$\left\|T_{y1u1}\right\|_\infty \le 1$$

T_{y1u1} is mixed-sensitivity cost function which can be written as:

$$T_{y1u1} = \begin{bmatrix} W_1 S \\ W_2 R \\ W_3 T \end{bmatrix}$$

Loop shaping is obtained for frequencies $\omega < \omega_c$ by appropriately choosing W_1 whereas $1/W_3$ targets loop shaping of frequencies $\omega > \omega_c$. Plant with weight function is shown in Fig. 5. The weighting function, according to design criteria discussed above, are tuned using MAGSHAPE command in MATLAB. A particular limitation in selection of weighting function is that it must be proper and stable.

$$W_1 = \frac{0.09s + 1}{s + 0.2}$$

$$W_2 = 0.1$$

$$W_3 = \frac{2.522}{s + 0.23}$$

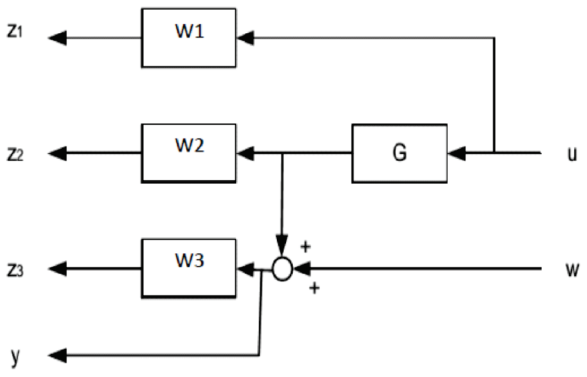

FIG. 5. AUGMENTED PLANT WITH WEIGHTS

5. SIMULATION AND RESULTS

This section includes the simulation results for force tracking control of EHSS. The designed controller satisfied the H∞ norm and quadratic H∞ performance criteria. The block diagram representation of controller implementation is shown in Fig. 6. Our design objective is fast tracking of step changes for reference inputs, with little or no overshoot. The simulation results are compared with conventional PID controller.

5.1 Simulation Results Based Upon LT1 Model of the System

Figs. 7-9 shows the simulation results based upon the LTI model of system under the step, saw tooth and sinusoidal reference inputs. It is clearly seen the performance of H∞ controller is dominant as compared to the conventional techniques of control system like PID. The performance criterion as mentioned above is the fast tracking performance under the different frequency input signals.

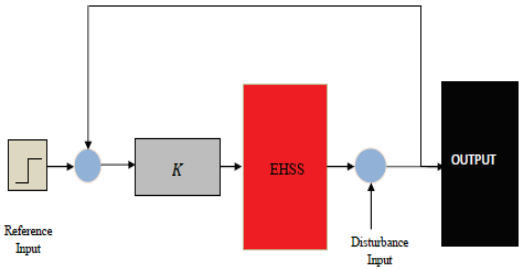

FIG. 6. BLOCK DIAGRAM OF MIX-SENSITIVITY H∞ CONTROLLER

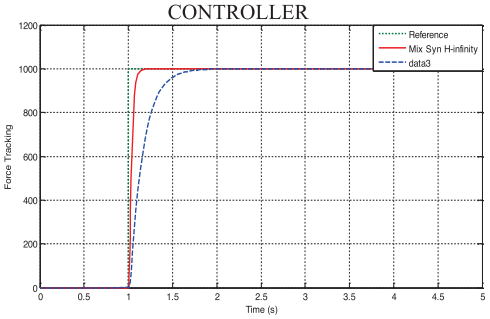

FIG. 7. FORCE TRACKING CONTROL UNDER THE STEP INPUT

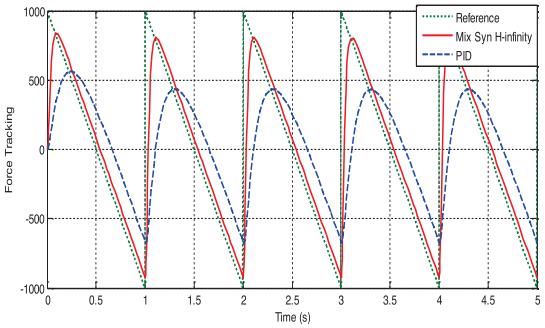

FIG. 8. FORCE TRACKING CONTROL UNDER THE SAW TOOTH INPUT

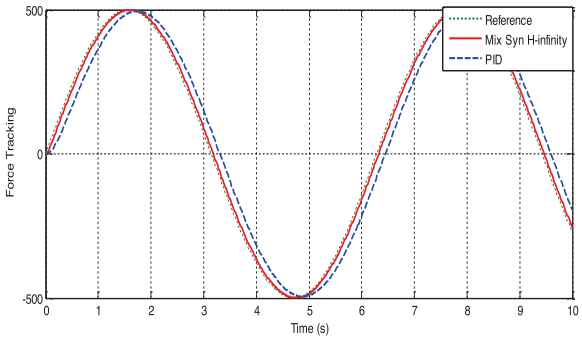

FIG. 9. FORCE TRACKING CONTROL UNDER THE SINE INPUT

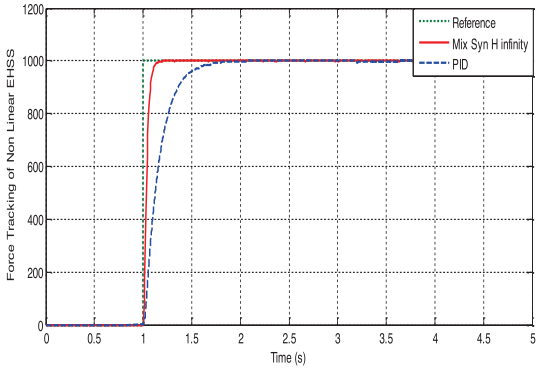

FIG. 10. FORCE TRACKING CONTROL UNDER THE STEP INPUT FOR NONLINEAR EHSS

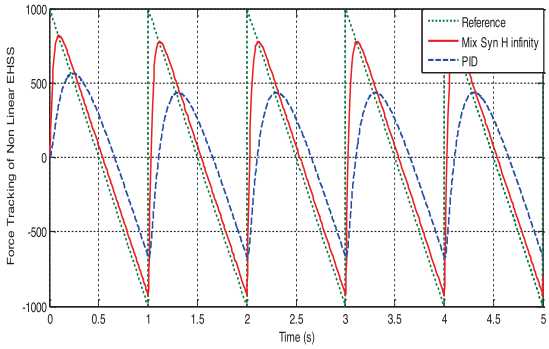

FIG 11. FORCE TRACKING CONTROL UNDER THE SAW TOOTH INPUT FOR NONLINEAR EHSS

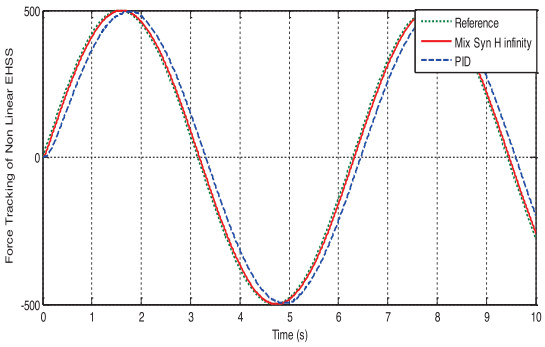

FIG. 12. FORCE TRACKING CONTROL UNDER THE SINUSOIDAL INPUT FOR NONLINEAR EHSS

5.2 Simulation Results on Non-Linear System

Figs. 10-12 shows the simulation result of force tracking control based upon the nonlinear model of the system. Simulation results on nonlinear system validate the performance of controller. Also the PID is applied on nonlinear system for comparison.

5.3 Simulation Results in the Presence of Step Disturbance

To check the robustness of the controller, a disturbance signal that is the function of state of the system is applied at the input of the nonlinear EHSS. The simulation results show the better tracking performance of mixed sensitivity Hcontroller than PID even in the presence of disturbance. Simulation result under the square and sinusoidal inputs are shown in Figs. 13-14.

6. CONCLUSION

The paper focused on mixed sensitivity H∞ pe controller design for force tracking control of EHSS. The control task is to achieve precise force tracking electro-hydraulic actuator under varying load conditions. The nonlinear system is first linearized and then H∞ controller is designed. The controller is evaluated both on linear and nonlinear model of system. Simulation results demonstrate the dominant performance of controller as compared to PID controller. Further the proposed controller is found robust in the presence of parametric uncertainty and external disturbances. The controller is simpler in design and implementation. Moreover, it also satisfied performance criteria of quadratic stability.

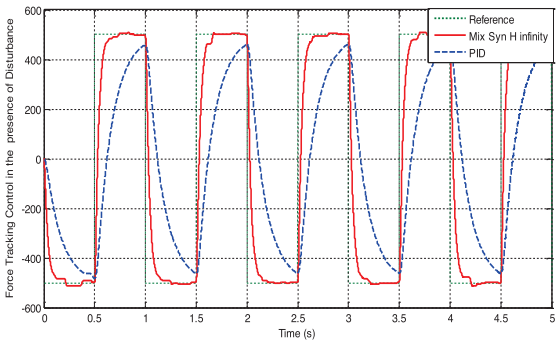

FIG 13. FORCE TRACKING CONTROL UNDER THE SQUARE INPUT FOR NONLINEAR EHSS IN THE PRESENCE OF DISTURBANCE

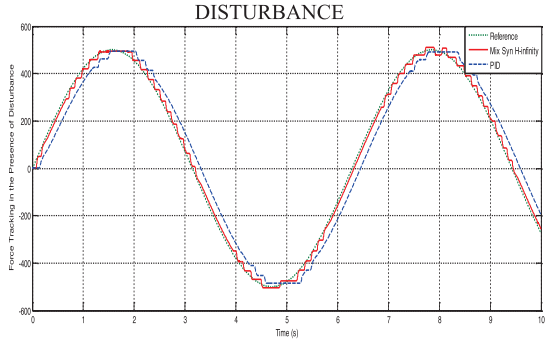

IG. 14. FORCE TRACKING CONTROL UNDER THE SINUSOIDAL INPUT FOR NONLINEAR EHSS IN THE PRESENCE OF DISTURBANCE

REFERENCES

[1] Alleyne, A., Liuand, R., "Systematic Control of a Class of Nonlinear Systems with Application to Electro-Hydraulic Cylinder Pressure Control", IEEE Transactions on Control Systems Technology, Volume 8, No. 4, pp. 623–634, 2000

[2] Zhao, P., Wang, S., Li, X., and Zhang, B., "A Novel Method of Parameter Identification of Nonlinear Electro-Hydraulic Servo Systems", Proceedings of International Conference on Fluid Power and Mechatronics, pp. 547-551, August, 2011.

[3] Garagic, D., and Srinivasan, K., "Application of Nonlinear Adaptive Control Techniques to an Electro-Hydraulic Velocity Servomechanism", Control Systems Technology, Volume 12, No. 2, pp. 303- 314, March, 2004.

[4] Ferreira, J., Sun, P., and Gracio, J., "Close Loop Control of a Hydraulic Press for Spring Back Analysis", Journal of Materials Processing Technology, pp. 377–381, 2006.

[5] Alleyne, A., and Liu, R., "Nonlinear Force/Pressure Tracking of an Electro-Hydraulic Actuator" *IFAC World Congress*, Beijing, PR China, July, 2009.

[6] Alleyne, A., and Liu, R., "A Simplified Approach to Force Control for Electro-Hydraulic Systems",Control Engineering Practice, Volume 8, No. 12, pp. 1347–1356, December, 2000.

[7] Alleyne, A., "Nonlinear Force Control of an Electro-Hydraulic Actuator", Proceedings of Japan/USA Symposium on Flexible Automation, pp. 193-200, New York, NY, 1996.

[8] Yanada, H., and Furuta, K., "Robust Control of an Electro-Hydraulic Servo System Utilizing Online Estimate of its Natural Frequency", Proceedings of 6th JFPS International Symposium on Fluid Power, Tsukuba, 2005.

[9] Takariho, S., and Kenko, U., "Gain Scheduling Control for Electro-Hydraulic Servo System Considering Time-Delay Modeling Error", Proceedings of IEEE International Conference on Control Applications, Taipei, Taiwan, 2004.

[10] Takariho, S., and Uchida, K., "Gain Scheduling Velocity and Force Controllers for Electro-Hydraulic Servo System", Proceedings of American Control Conference, pp. 4433-4438.Anchorage, USA, 2002.

[11] Yuan, X., Fang, Z., and Li, H., "Research on Fuzzy Control for the Electro-Hydraulic Servo System", Proceedings of International Conference on Fuzzy Systems and Knowledge Discovery, pp. 918-921, 2010.

[12] Bonchis, A., Corke, P.I., Rye, D.C., and Ha, Q.P., "Variable Structure Methods in Hydraulic Servo Systems Control", Automatica, Volume 37, pp. 589-595, 2001.

[13] Formentin, S., and Karimi, A., "A Data-Driven Approach to Mixed-Sensitivity Control with Application to an Active Suspension System", IEEE Transaction on Industrial Informatics, Volume 9, No. 4, pp. 2293-2301, 2013.

[14] Galindo, R., Malabre, M., and Kucera, V., "Mixed Sensitivity H∞ Control for LTI Systems", Proceedings of IEEE 43rd Conference on Decision and Control, December, 2004.

[15] Fales, R., and Kelkar, A., "Robust Control Design for a Wheel Loader Using Mixed Sensitivity H∞ and Feedback Linearization Based Methods", Proceedings of American Control Conference, Portland or USA, June, 2005.

Simulation of Process Parameters for the Growth of Ba-Doped ZnO Nano-Rods Using Fuzzy Analysis

Mohammad Aqib*, Ghulam Muhiudin*, Maham Akhlaq*, Muhammad Waseem Ashraf*, and Shahzadi Tayyaba*
*Department of Physics, Government College University, Lahore, Pakistan.
**Department of Computer Sciences, University of Lahore, Lahore, Pakistan.
maham_9458@hotmail.com, muhammad.waseem.ashraf@gmail.com,maqib3781@gmail.com,
gmuhiudin786@gmail.com, shahzadi.tayyaba@hotmail.com

ABSTRACT

Advancement in technology and industrialization has made nano-technology a significant research area. Among the wider field of nano-technology, nano-materials are considered as the future of research and applications. Due to their unique properties, nano-materials are gaining enormous attention in the field of energy, medical, electronics and chemistry. These materials exhibits advanced properties and provide large surface area to volume ratio due to decrease in their rod dimeter. Between other nano-materials, ZnO (Zinc Oxide) nano-structures are extensively known due to their excellent piezo and pyro electric properties. Various materials are doped with ZnO to decrease its rod diameter for advanced application. In this work, we have fabricated, simulated and studied Barium doped ZnO nano-rods and their effect on the rod diameter using fuzzy analysis. The result depicts that the rod diameter decrease with increase in barium doping and process temperature for the growth of ZnO nano-rods. The simulated results are compared with the fabricated results and the calculated results, with less than 1% error in the value. The fabricated Ba (Barium)-doped ZnOnano-rods are highly symmetric and show hexagonal geometry. The size of the nano-rods is also similar to the Mamdani model simulated results. Ba-doped ZnO nano-rods are thus suitable for nano-scale applications including energy harvesting and bio-medical applications.

Key Words: Zinc Oxide, Nano-Rods, Fuzzy Analysis, Barium Doped ZnO.

1. INTRODUCTION

Nano technology has extensively added up to the work of research in almost every field of life directly or indirectly. The most important thing in nano materials is its novel properties which different nano material exhibits. The small size of nano materials is responsible for its every kind of practical use [1]. Specially nano materials of ZnO have attracted the scientists in this aspect because of its wide direct band gape(3.37ev) and excitation binding energy(60ev) and piezoelectric properties which make it vital for nano-electronics, optoelectronics and energy harvesting [2-3]. ZnO has remarkable specific capacitance, high chemical stability, good electrical conductivity, and fast redox kinetics [4]. It has a lot of practical applications, such as in optoelectronic devices (laser diodes, light emitting diodes, photodetectors), electronic devices (Transistors, ICs), catalysts, sensors, energy harvesting devices, active compounds in sunscreens, etc. [5-7]. A lot of research has been conducted on synthesizing one-dimensional ZnO nano-structures and on studying their morphologies according to their shape-related optical and electrical properties. Various types of ZnO nanostructures have been considered, such as, nano-rods, nano-wires, nano-tubes, nano-helixes, nano-belts, seamless nano-rings, nano-dots, mesoporous single-crystal nano-wires and polyhedral cages nano-wires and nano-rods. In all structures nano-rods and nano-wires are being studied widely because of the ease of their production and device applications [8-9]. They are used as both functional units and interlinks in the formation of optoelectronic, electronic, electrochemical and electromechanical nano-devices. ZnO is synthesized by various techniques such as thermal decomposition, laser ablation, chemical vapour deposition, precipitation, hydro-thermal, electrochemical depositions, combustion, ultrasound, thermal evaporation under vacuum ormechano-chemical-thermal synthesis. And to open up possibilities of new applications in photonics, photocatalytic, and light emitting diode devices, second group elements of periodic table are considered as good doping elements for conforming the structure and morphology of ZnO [10-12]. For example, the doping of Mg in ZnO produced significant changes in properties, it increased the photocatalytic activity [13]. Some groups synthesized Ba-doped ZnO expressing modifications in ferroelectric and catalyticproperties [14-15]. In the same way ZnO is doped by other second group elements as well. Despite, Ba has a greater ionic radius than that of ZnO, substitution is still difficult with the help of ordinary general doping rules. Among these second group elements, Ba doping is important because of its applications in varistors and liquid sensors' guiding layers [16]. But literature provides a very few reports on Ba-doped ZnO nano-rods.

Various simulations tools can be adopted which provides experimentalist the righteousness and efficiency of the design before it is actually built up. There are different ways for the simulation including ANYSY, TRANSYS and MATLAB for structural, mechanical, magnetic and parametric estimations of the material to be fabricated. Among these methods, FLC (Fuzzy Logic Controller) is highly efficient software providing a very valuable flexibility for reasoning. This is a good way to consider the inaccuracies and uncertainties of any experiment. It is a technique to impose human-like thinking into a controlled experiment.

In this paper we discuss the simulation and synthesis of growth of Ba-doped ZnO nano-rods ranged from 50-300nm rod diameter are presented according to the

doping percentage and temperature. Rods of this size will improve the energy harvesting capability and can be widely used for solar energy and bio-medical applications.

2. MATERIALAND METHODS

Ba-doped ZnO nano-rods are fabricated using self-designed chemical bath deposition temperature. Zinc acetate di-hydrate is used as a precursor of ZnO and ba-acetate is used for ba-doping. Glass substrate was initially cleaned using ultra-sonication bath with DI water and acetone. The cleaned glass substrate is then subjected to seeding. Seeding layer is a thin film of ZnO nano-particles that facilitates to growth of ZnO ano-rods. 5mM zinc acetate dehydrate is dissolved in 40 ml of 2-propanol. The substrate was dipped in the solution at a rate of 20 dips per minute for 2 minutes followed by drying at 80 ^{O}C for 15 minute to properly evaporate the solvents. Solution of 20mm of Zinc acetate di-hydrate, hexa-methylene tetra amine and 1.3% ba-acetate was stirred in DI water. This solution is inserted in the chemical bath deposition setup. The temperature was set at 95^{o}C for 3 hours. After 3 hours the film was annealed at 470^{o}C. The doping and annealing temperature was set on the basis of fuzzy analysis performed in section 3 for the validation of results.

The prepared Ba-doped nano-rods are then characterized using scanning electron microscopy for the structural analysis of the film

3. FUZZY SYSTEM DESIGN

With the help of fuzzy analysis we have shown up the input variables, 'Ba-doping concentration in ZnO' and 'the process temperature' along with the output 'rod diameter' on fuzzy inference editor shown in Fig. 1, Because fuzzy logic provides almost ideal conditions, it has numerous values between 0 and 1.

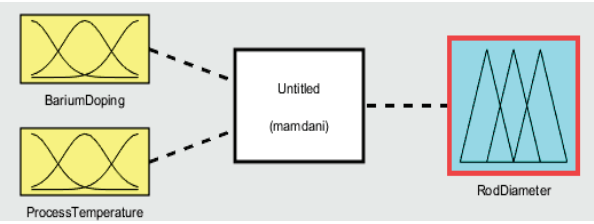

FIG. 1. FUZZY INFERENCE SYSTEM FOR THE ROD DIAMETER OF BA DOPED ZNONANO-RODS

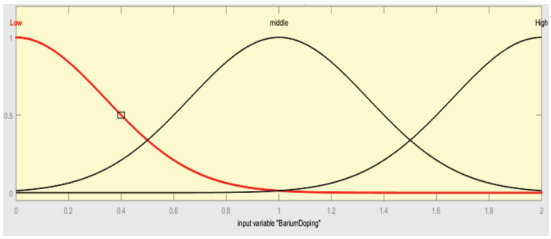

FIG. 2. MEMBERSHIP FUNCTION GRAPH SHOWING BARIUM DOPING(0-2%)

The graphs for the input and output variables have been drawn by MATLAB membership function. The graphs for the inputs, Ba-doping percentage and process temperature and output rod diameter are shown in Figs. 2-4 respectively. The input parameter of barium concentration was taken in the range of 0-2%. The range for process temperature was taken from 200-600^{o}C. The ranges for output parameter are 50-300 nm.

The rules are defined in the MATLAB rule editor using IF, AND, and THEN logic, based on the real life value. On the basis of the rules, the 2D and 3D graphs are studied. To show up the three values at a time in a graph 'two inputs and one output' we have three dimensional graph shown in Fig. 5.

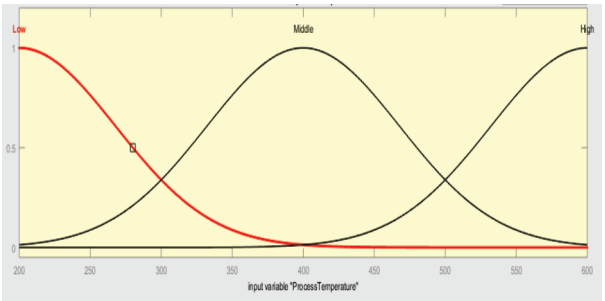

FIG. 3.MEMBERSHIP FUNCTION GRAPH SHOWING PROCESS TEMPERATURE (200-600^{0}C)

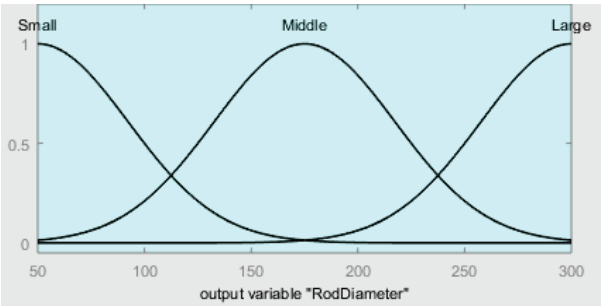

FIG. 4.MEMBERSHIP FUNCTION SHOWING ROD DIAMETER (50-300 nm)

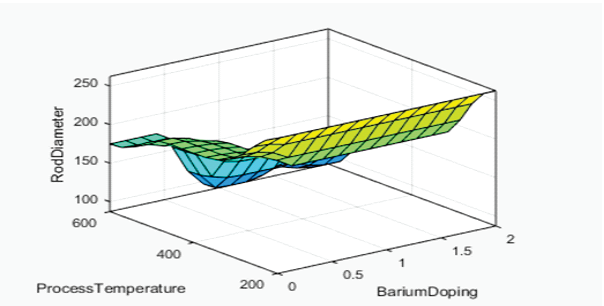

FIG. 5. THREE DIMENSIONAL GRAPH SHOWING ALL THE THREE VARIABLES

The Figs. 6-7 show the behavior of both the inputs with the output individually. Fig.6 shows the 2D graph of rod diameter and process temperature. The decrease in rod diameter with increase in temperature depicts the creation of crystals with small size. High annealing temperature will results in the change of phase of Ba-doped ZnO nano-rods which will result in decrease in diameter. These crystals can be more beneficial because they will occupy less surface area which will result in an increase in surface area to volume ratio. On the other hand shown in Fig. 7 shows the 2D graph of the two quantities rod diameter and percentage doping. Which increase in ba-doping rod diameter decrease which will result in an increase in surface area to volume ratio.

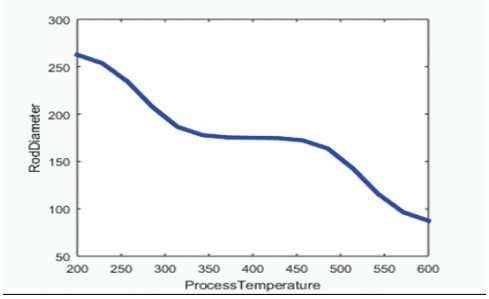

FIG. 6. 2D GRAPH BETWEEN ROD DIAMETER AND PROCESS TEMPERATURE

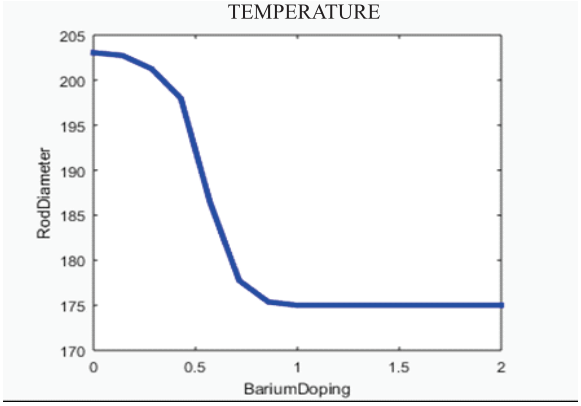

FIG. 7. 2D GRAPH OF BETWEEN ROD DIAMETER AND PERCENTAGE DOPING

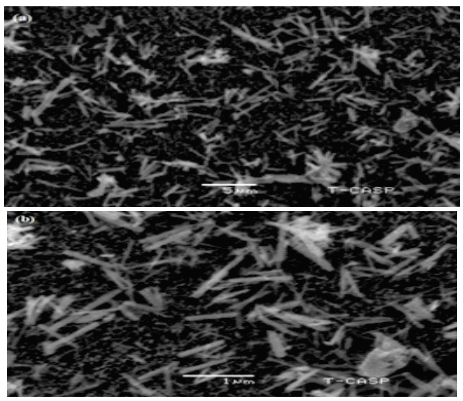

FIG. 8. SEM MICROGRAPHS OF BA-DOPED ZNO NANORODS

3. ANALYSIS AND RESULTS

The SEM (Scanning Electron Microscopy) graphs are shown in Fig. 8. These graphs show the growth of Ba-doped ZnO nano-rods. These rods are symmetric and shown in the micro-graphs and have hexagonal geometry. The average diameter of the prepared nano-rods is I range of 165-175 nm. From the rule viewer in fuzzy analysis, the crisp value of rod diameter is studied which is equal to 169 nm, which lies in the range of the average value of the rod diameter calculated using SEM. The rules defined by the rule editor are viewed in the rule viewer. For calculations, a crisp value of both inputs is selected. On the basis of these crisp values a comparison is carried out in between the simulated value of output and the calculated value (Fig. 9).

Calculation was performed for the crisp value of Ba-doping of 1.35% and process temperature of 471°C.For these corresponding crisp values the rod diameter is 169 nm. Both the input values lie in the membership function region "High". On the basis of these tow value 4 values of membership functions are calculated. These membership functions values are calculated from the selected crisp values as shown in Fig.9. These values depict the highest and the lowest value of the crisp value range. The membership function values are:

$b_1 = 2 - 1.35/2 = 0.325\%$
$b_2 = 1 - b_1 = 0.675\%$
$b_3 = 600 - 471/600 = 0.215^{o}C$
$b_4 = 1 - b_3 = 0.785^{o}C$

For the values of membership function 4 rules are selected out of 9 rules which are considered for this work. The minimum membership function value (Gi) and Singleton value (Vi) is calculated based on mamdani

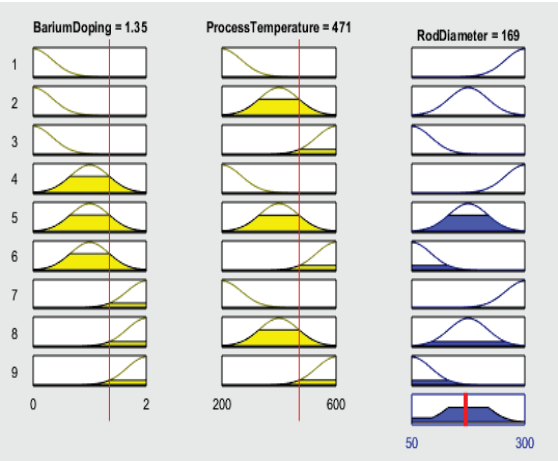

FIG. 9. RULE VIEWER' TO SHOW UP ONE OUTPUT FOR THE CORRESPONDING TWO INPUTS

formulae. The sum of all the minimum membership function values and singleton values are calculated which are furthermore used to calculate the crisp value of output using Mamdani model.

$\sum Gi = 1.43$
$\sum Gi \times Vi = 2.4$
Mamdani model = $[\Sigma(Gi \times Vi) / Gi] * 100$
Mamdani model = 168 nm

The Crisp value of the output from rule viewer is 169 and mamdani model calculated value is 138. The error between the simulated value and the calculated value is less than 1% which shows the accuracy of the results. These Ba-doped ZnO nano-rods based structures can be synthesized and can be used for various nano-rods diameter based nano-scale applications.

4. CONCLUSION

In this work, the effect of ba-doping on ZnO nano-rods was studied using fuzzy analysis. The results depicts that the rise in temperature and ba-doping will results a decrease in rod diameter. The decrease in rod diameter is directly attributed to the decrease in nano-rods size which will results in a large surface area to volume ratio. The fabricated ba-doped ZnO nano-rods and fuzzy analysis results show that the simulated and calculated values are similar to each other with less than 1% error in the value. The results show that barium doping will eventually results in a decrease in rods diameter which make is suitable for nano-scale applications.

ACKNOWLEDGEMENT

Authors would like to acknowledge Department of Physics (Electronics), Government College University, Lahore, Pakistan, for providing resources to carry out this research. Authors would also like to acknowledge Department of Computer Sciences, University of Lahore, Pakistan, for their support during the research work.

REFERENCES

[1] Abdulkareem, G.A., Mijan, N.,and HinTaufiq-Yap, Y., "Nanomaterials: An Overview of Nanorods Synthesis and Optimization", Nanorods and Nanocomposites, Intechopen, 2019.

[2] Ali, B., Ashraf, W.M., Tayyaba, S., Qureshi, M.Z., Sarwar, G., Wasim, M.F., and Afzulpurkar, N., "Fuzzy Logic Based Energy Harvesting with the Movement of Plants Branches and Leaves", Pakistan Journal of Agricultural Science, Volume 53, No. 2, pp. 449-454, 2016.

[3] Prasad, K., and Anal K. Jha. "Zno Nanoparticles: Synthesis And Adsorption Study". Natural Science, vol 01, no. 02, pp. 129-135, 2009.

[4] Karaköse, E.,and Çolak, H., "Structural and Optical Properties of ZnO Nanorods Prepared By Spray Pyrolysis Method", Energy, Volume 140, pp. 92-97, 2017.

[5] Bacaksiz, E., Parlak, M., Tomakin, M., Özçelik, A., Karakiz, M., and Altunbaş, M., "The Effects of Zinc Nitrate, Zinc Acetate and Zinc Chloride Precursors on Investigation of Structural and Optical Properties of ZnO Thin Films", Journal of Alloys and Compounds, Volume 466, No. 1-2, pp. 447-450, 2008.

[6] Son, D., Im, J., Kim, H.,and Park, N., "11% Efficient Perovskite Solar Cell Based on ZnONanorods: An Effective Charge Collection System", The Journal of Physical Chemistry-C, Volume 118, No. 30, pp. 16567-16573, 2014.

[7] Wang, X., Sun, F., Duan, Y., Yin, Z., Luo, W., Huang, Y.,and Chen, J., "Highly Sensitive, Temperature-Dependent Gas Sensor Based on Hierarchical ZnONanorod Arrays", Journal of Materials Chemistry-C, Volume 3, No. 43, pp. 11397-11405, 2015.

[8] Vasudevan, A., Jung, S.,andJi, T., "Synthesis and Characterization of Hydrolysis Grown Zinc Oxide Nanorods", International Scholarly Research NetworkNanotechnology, Volume 2011, pp. 1-7, 2011.

[9] Mushtaq, Z., Tayyaba, S., and Ashraf, M.W., "Liquid Level Controlling by Fuzzy Logic Technique", International Journal of Innovation and Scientific Research, Volume 12, No. 2, pp. 372-379, December, 2014.

[10] Wasim, M.F., Ashraf, M.F., Tayyaba, S., Ali, B., and Afzulpurkar, N., "Nano Generator Simulation Using Fuzzy Logic", Journal of Engineering Research and Technology, Volume 2, Issue 4, December, 2015.

[11] Iqbal, J., Jan, T., Ismail, M., Ahmad, N., Arif, A., Khan, M., Adil, M., Haq, S.U., and Arshad, A., "Influence of Mg Doping Level on Morphology, Optical, Electrical Properties and Antibacterial Activity of ZnO Nanostructures", Ceramics International, Volume 40, No. 5, pp. 7487-7493, 2014.

[12] Suwanboon, S., and Amornpitoksuk, P., "Preparation of Mg-Doped ZnO Nanoparticles by Mechanical Milling and their Optical Properties", Procedia Engineering, Volume 32, pp. 821-826, 2012.

[13] Yousefi, R., Jamali-Sheini, F., Cheraghizade, M., Khosravi-Gandomani, S., Sáaedi, A., Huang, N.M., Basirun, W.J.,and Azarang, M., "Enhanced Visible-Light Photocatalytic Activity of Strontium-Doped Zinc Oxide Nanoparticles", Materials Science in Semiconductor Processing, Volume 32, pp. 152-159,2015.

[14] Wenlei, X., and Yang, Z., "Ba-Zno Catalysts for Soybean Oil Transesterification", Catalysis Letters, Volume 117, No. 3-4, pp. 159-165, 2007.

[15] Ando, E., and Miyazaki, M., "Durability of Doped Zinc Oxide/Silver/Doped Zinc Oxide Low Emissivity Coatings in Humid Environment", Thin Solid Films, Volume 516, No. 14, pp. 4574-4577, 2008.

INFORMATION FOR AUTHORS

Before Submission

- Before Submission of an article, authors should carefully read the Publication Ethics, Open Access policy and Plagiarism Policy of the Journal.
- Authors should ensure that the work has not been published previously and it is not under consideration for publication elsewhere.
- Publication must be approved by all authors of the paper.
- Authors should carefully list and order their names on the first page of the article. An author's name will not be added or deleted after submission. One of the author should be nominated as Corresponding Author.
- An article should be written in good English.

Submission

- Authors may submit an article through our on line submission system or through an email as a MS Word file. In case of on line submission, author will be required to Sign up. On successful registration, author can upload the article. Alternatively, an artic le may be sent through email to the Editor-in-Chief, or Focal/Coordinating Person.
- Authors should note that all submitted articles are refereed through a double blind peer review process (National and International) which means that author's identities remain unknown to reviewers and vice versa throughout the reviewing process.
- Articles should be formatted in single or double spacing, preferably in Times New Roman size 12 font. Accepted articles will be correctly formatted by our publication team.
- The first page should contain the full title of the article and full names and affiliations of all authors including email address of the corresponding author.
- The format of the manuscript is Abstract of up to 200-300 words, Keywords, Introduction then main body of the paper ending with conclusion followed by acknowledgement and list of references.
- References should be cited in the text by number within square brackets. At the end of the paper, they should be listed in the order in which they appear in the text.

After Acceptance

- Authors will be notified about the acceptance/rejection of the paper through email.
- Upon acceptance of an article, authors will sign copy right and Authorship form.
- Accepted manuscript will be sent to the corresponding author for proof reading. No editing or proofreading will be allowed after publication of an article.
- Authors to give Undertaking/Copy Right that this Research Paper is their original work/contribution and not published before in any Journal or in any Conference and contribution of individual authors regarding submitted research paper